EVALUATION OF THERAPEUTIC STRATEGIES FOR OSTEOARTHRITIS USING CONTRAST BASED CT IMAGING

A Dissertation
Presented to
The Academic Faculty

by

TanushreeThote

In Partial Fulfillment
of the Requirements for the Degree
Doctor of Philosophy in Biomedical Engineering

Georgia Institute of Technology
August 2014

EVALUATION OF THERAPEUTIC STRATEGIES FOR OSTEOARTHRITIS USING CONTRAST BASED CT IMAGING

Approved by:

Dr. Robert E. Guldberg, Advisor
School of Mechanical Engineering
Georgia Institute of Technology

Dr. Zigang Ge
Department of Biomedical Engineering
Peking University

Dr. Andrés García
School of Mechanical Engineering
Georgia Institute of Technology

Dr. Johnna S. Temenoff
Department of Biomedical Engineering
Georgia Institute of Technology

Dr. Rajesh V. Kamath
AbbVie Laboratories

Date Approved: June 17, 2014

To my friends & family

ACKNOWLEDGEMENTS

A PhD is a long path and I certainly wouldn't have finished the journey alone. Bob has been a great advisor who has provided support and critical input throughout my PhD. He has at times shown more confidence in my data than I had, which helped me to keep going. I joined the lab with no experience in the particular area and since then, have learned a lot along the way.

I would also like to thank my committee members who have provided invaluable advice through the course of my PhD. Dr Ge helped me carve out a project when I was in Beijing and also helped me assimilate with Chinese culture through lab dinners and trips.Dr. Johnna Temenoff helped me design experiments and challenged me to think about the science behind it. Andres's comments have been extremely useful and more so, his confidence in my thesis especially towards the end of my PhD has been a much needed morale boost. Raj, at AbbVie has collaborated on this project since the beginning and his expertise on OA and viewpoints from an industry perspective really helped bring my thesis together. I have also had the opportunity to work with MiMedx and everyone on their team including Tom, Rebeccah and Michelle have been great collaborators. Michelle especially helped me with some of the nitty-gritty in vitro experiments for which I am very grateful.

I could not have finished my PhD without the amazing people in the Guldberg Lab. Angela and Hazel were the first two members who interviewed me as a grad student, and I am so very glad that they deemed I was worthy to join the ranks of Guldberg Lab. Thank you for that, I can't imagine being a part of any other lab. Angela taught me everything CT related without which my thesis would not have happened. She

also helped correct quite a few of my beginner errors for my first ORS poster, preventing me from committing scientific damage. Nick helped oversee the OA project and has helped me from surgeries, dissections, troubleshooting data, all the way to manuscript writing. He has always had new ideas which helped me structure my thesis better. Hazel has been the voice of reason and has even been patient with my rants about grad school at times. Vivian has helped me to get onto Bob's calendars when he is busy and made paperwork, conference travel etc. an easier process. Brent, Joel and Dosier always had words of wisdom as the then senior grad students. I would not have passed my qualifying exams without Joel giving me a crash course on mechanics. Inheriting Dosier's desk has been a huge responsibility and while I can't live up to his legend I did manage to save his post-it notes of wisdom. Brent, thank you for your advice on the final legs of the PhD. David is successfully leading the OA project into exciting areas and I'd like to thank him for his help on experiments that led to some pretty "spiffy" data, as he'd say. Giuli has also helped me with surgeries and the like, and I still think she has the magic touch as sterile assist! Jason, Marian, Albert and Brennan have helped with surgeries in the PRL and also with feedback during lab meetings that helped me become a better researcher. Without my undergrads – Shamus, Sanjay and Boao, I would not be graduating. Shamus was there at the start of the OA project, learning techniques and helping out with the data analysis. Though Shamus set a high bar, Sanjay took over and did some great work. Boao, while being one of the newest undergrads took to research really quickly and helped me finish in time. Ashley is not only an office-mate but also a great friend. Her infectious laughter and fun personality make the lab a more fun place to be. Lauren and Alice as back row-mates were always there to listen to long winded rants. Lauren has

been a great co-chair, a great friend and I can totally picture her as a professor in a few years. Alice, has been one of my first friends in Atlanta. From morning classes at Emory to walking across campus for Applied Phys and to numerous food outings, Alice has been there. I do blame her for making me hungry every time I walked by to see delicious food on her computer screen. Alice has been the best of friends and a pretty hard-core workout partner that I could have asked for and I am going to keep trying to convince her to find a job in Minneapolis!

Speaking of friends, I have met some great people at Tech and believe that these are the kind of friendships which last forever. The BME 2009 cohort and other folks along the way have been an awesome bunch who were always up for doing new things . Inthu, Akhil, Warren, Brian, Kristin, Saujan, Patricia, Arthur, Eric, Marilyn, Mei and Stacie have been around to celebrate birthdays and Thanksgivings and other no reason outings. I'd like to thank Patricia for all her baking and food and cheerful laughter that echoes through IBB. Mei and Inthu have not only been great friends but also awesome roommates to live with, sharing grad school woes and successes over dinner. I'd also like to thank Nitesh, Rohan, Bhai, Pradnya, Paras and Gautami for keeping me in the loop for Diwali functions and Bollywood movie nights. I must say that the trip to Florida was one of the entertaining beach holidays !

An integral part of my life in Atlanta is my boyfriend, Ambar. For his unconditional love and support, I am so very grateful. He put up with my bad days and celebrated the good days. Also, he never judged me for sleeping for 10+ hours on the weekends! For all the times he cooked for me, took care of me when I was sick, gave me rides, was my carpool to avoid traffic and for the random cakes from Sweet Hut, thank

you. I cannot imagine grad school at Tech without him in the picture. I can only hope that I can provide him the same support that he provided me, as he makes his journey to becoming a professor.

Finally, I would like to thank my family. Growing up in a joint family with parents, uncles & aunts and cousins, everyone has been part of my PhD journey. Trips to India were always fun and though the question – "When are you finishing?" came up more often than I liked, I am here because of their support. I'd like to thank my cousins – Saket, Yamini, Poonam, Aditya, Omkar and Dipti for the fun times since I was a kid. Last but not the least, my parents and my sister have been there for me, in every which way. My parents have certainly defied the "traditional Indian parents" role by allowing me to move to the US when I was 17 for my undergrad. They have stood by my decisions and have always got my back. I know that if I ever stumble, even if it is my fault, they will be there for me. My sister, Supriya, even though younger than me, has taught me a lot about life for which I am thankful.

Thank you all for being there and helping me get to the end !

TABLE OF CONTENTS

LIST OF TABLES

LIST OF FIGURES

LIST OF SYMBOLS AND ABBREVIATIONS

2D	two dimensional
3D	three dimensional
µCT	microcomputed tomography
µ-dHACM	micronized dehydrated human amnion/chorion membrane
AAALAC	Association for assessment and accreditation of laboratory animal care
ACLT	anterior cruciate ligament transection
ANOVA	analysis of variance
BMP	bone morphogenetic protein
CT	computed tomography
dGEMRIC	delayed gadolinium-enhanced MRI of cartilage
DMOAD	disease modifying OA drug
ECM	extracellular matrix
EGF	epithelial growth factor
ELISA	enzyme-linked immunosorbent assay
EPIC-µCT	equilibrium partitioning of an ionic contrast agent via micro-CT
FGF	fibroblast growth factor
FT-IRS	fourier-transform infrared spectroscopy
GAG	glycosaminoglycans
GI	gastrointestinal
IA	intra-articular
IACUC	institutional animal care and use committee
H&E	hematoxylin& eosin
IFN-γ	interferon gamma

IL	interleukin
MCL	medial collateral ligament
MCP-1	monocyte chemoattractant protein-1
MIA	monosodium iodoacetate
Micro-CT	microcomputed tomography
MMP	matrix metalloproteinase
MMPi	matrix metalloproteinase inhibitor
MMT	medial meniscal tear
MRI	magnetic resonance imaging
NBF	neutral buffered formalin
NSAID	non-steroidal anti-inflammatory drug
OA	osteoarthritis
OARSI	osteoarthritis research society international
OP	osteophyte
PBS	phosphate buffered saline
PDGF	platelet derived growth factor
PLGA	poly-lactic glycolic acid
RANKL	receptor activator of nuclear factor kappa-B ligand
ROI	region of interest
Saf-O	safranin-O
sCT	salmon calcitonin
SEM	standard error of the mean
sGAG	sulfated glycosaminoglycans
SLP-1	synaptotagmin-like protein 1
TGF-β	transforming growth factor beta

TNF-α	tumor necrosis factor alpha
VEGF	vascular endothelial growth factor
VOI	volume of interest

SUMMARY

Osteoarthritis (OA) is the leading cause of disability in the US and is characterized by cartilage degradation, subchondral bone changes and synovial inflammation. OA presents a unique challenge as there are no approved disease modifying OA drugs (DMOADs) and the current mode of treatment is palliative therapy and eventual total joint replacement. Thus, there is a pressing, unmet clinical need to test and develop novel DMOADs to improve outcomes. This includes development and characterization of suitable animal models to provide a test-bed for screening therapeutics.

Cartilage is an avascular tissue containing water which makes imaging cartilage difficult. In order to study pre-clinical models of OA and test therapeutics, an efficient technique with quantitative outcome measures is required. Accordingly, the goal of this thesis was to investigate contrast based CT imaging (EPIC-μCT – Equilibrium partitioning of an ionic contrast agent)as a tool to test therapeutic strategies in a pre-clinical rat OA model. First, we characterized two different models of joint degeneration, one induced by injection of monosodium iodoacetate (MIA) and a second, created surgically via medial meniscal transection (MMT). Our results indicated that the MIA model leads to global cartilage and bone degeneration whereas the MMT model produces focal defects, similar to human OA. Second, we tested the sensitivity of EPIC-μCT to detect effects of a broad spectrum matrix metalloproteinase inhibitor (MMPi) in the rat MMT model. Our results demonstrated that quantitative measures established by EPIC-μCT were able to detect damage in cartilage and subchondral bone in response to MMPi treatment with greater sensitivity than the gold standard of histopathology. Finally, we

investigated the effects of micronized dehydrated human amnion/chorion membrane (µ-dHACM) in the rat MMT model. Our results indicated a protective effect of a single intra-articular injection of µ-dHACM at 3 weeks. Treatment of an arthritic joint with a delayed injection also demonstrated a chondro-protective effect of µ-dHACM at a longer time point of 6 weeks. Denaturation of µ-dHACM led to loss of chondroprotective effect at 3 weeks.

Taken together, this thesis presents pioneering work on the use of EPIC-µCT as a quantitative technique to assess cartilage and also presents µ-dHACM as a novel DMOAD to be tested further. This work has provided new insights on the development of OA in the rat MMT model. It is also the first instance of using µ-dHACMas a therapeutic for OA which shows potential to be translated to large animal models and human clinical use. Going forward, EPIC-µCT can be used to screen other therapeutics efficiently and can be adapted to other diseasessuch as juvenile OA, rheumatoid arthritis and osteochondritis dissecans. Ultimately, this technique may enhance the drug testing phase for OA by enabling quicker screening, making the bench to clinic translation a faster process.

CHAPTER 1

SPECIFIC AIMS

Introduction

Osteoarthritis (OA) affects nearly 27 million people in the US and represents the leading cause of chronic disability (Cutler and Ghosh 2012). It primarily manifests as joint degeneration, characterized in part by a decrease in proteoglycan (PG) content, fibrillation of the cartilage surface, reduction of articular cartilage thickness and subchondral bone sclerosis. Current treatment methods target pain relief for OA via non-steroidal anti-inflammatory drugs (NSAIDs) since there are currently no clinically approved disease modifying OA drugs (DMOADs) demonstrating efficacy(Clouet, Vinatier et al. 2009). Despite multiple small animal model DMOAD experiments being conducted, the screening rate for drugs is severely limited by the lack of sensitivity of outcome measures and the time consuming process to achieve them. Equilibrium Partitioning of an Ionic Contrast agent via μCT (EPIC-μCT) is a recently developed technique that allows for evaluating articular cartilage changes with μCT(Palmer, Guldberg et al. 2006). It has been validated and was used to study joint degeneration induced by injecting a high dose of monosodium iodoacetate (MIA) into rat joints (Grogan, Miyaki et al. 2009). This MIA model, though commonly used, is not physiologically relevant to human OA. An alternative more relevant small animal model involves induction of OA via medial meniscal transection (MMT). However, the ability of EPIC-μCT imaging to analyze disease progression in the MMT model and detect the therapeutic efficacy of candidate DMOADs has not been previously evaluated.

DMOADs exist in various forms including broad spectrum agents that target inflammation and small molecule based therapeutics. Matrix metalloproteinase inhibitors (MMPis) are a class of small molecule based drugs which have previously shown efficacy when delivered systemically/orally in small animal models but have not yet been tested using EPIC-µCT (Clouet, Vinatier et al. 2009). Testing a drug that has previously been shown to have a therapeutic benefit will allow for assessing the sensitivity and applicability of EPIC-µCT as a tool to screen for DMOADs. Extracellular matrix (ECM) based materials are another class of therapeutics that are being tested for a variety of applications. Amniotic membrane, by virtue of its anti-inflammatory and anti-fibrotic qualities, may prove useful as an extracellular matrix based intervention for OA (Jin, Park et al. 2007, Diaz-Prado, Rendal-Vazquez et al. 2010). The objective of this proposal was to examine two distinct treatment strategies for OA in a rat joint degeneration model using EPIC-µCT. The central hypothesis of this work was that EPIC-µCT could be used to establish quantitative outcome measures which would be sensitive to detect effects of therapeutics in the rat OA model. We approached this objective through the following specific aims:

Specific Aim I

Utilize EPIC-µCT for localized 3D analysis of cartilage composition & morphology in rat joint degeneration models

There is a need to develop faster, less destructive yet quantitative metrics to examine articular cartilage changes in preclinical OA models other than the current histological techniques. Our *hypothesis* was that EPIC-µCT could quantitatively detect

degenerative cartilage changes in the MIA and MMT model. To test this hypothesis, we utilized a low dose of MIA (0.3mg) injected intra-articularly or induced joint degeneration surgically in the MMT model. We defined localized regions of interest to facilitate detection of cartilage changes and compared the results to contralateral joints. We characterized the models by evaluating quantitative parameters such as cartilage thickness, volume, attenuation as well as measurement of focal defects via EPIC-µCT. Histology was performed to compare results with EPIC-µCT analyses. The outcomes of this aim are discussed in Chapter 3.

Specific Aim II

Examine sensitivity of EPIC-µCT analysis and quantify effects of broad spectrum MMP inhibitor in selected rat OA model

Testing new therapeutics for OA in pre-clinical animal models requires a sensitive diagnostic tool to assess the effects of the selected therapeutic on the articular cartilage. Based on Aim 1, our hypothesis was that EPIC-µCT would be a more sensitive metric to characterize the rat MMT model compared to histopathology and could be used successfully to analyze effects of a MMPi in the rat MMT model at 3 weeks. Initially, EPIC-µCT was used to analyze the MMT model at 1, 2 and 3 weeks and the results compared with histopathology data. Next, an MMPi was orally delivered and tested in the rat OA model at 3 weeks. The joints were analyzed via both EPIC-µCT and histopathology. Additional analyses such as osteophyte characterization and subchondral bone analysis were also performed. The outcomes of this aim are discussed in Chapter 4.

Specific Aim III

Quantify effects of micronized dehydrated human amnion/chorion membrane (µ-dHACM) on the progression of joint degradation in an established rat OA model

A variety of DMOADs are currently being researched and tested. ECM based therapeutics have been shown to have improved wound healing outcomes. µ-dHACM is an ECM derived material which has been used for regenerative therapy applications such as corneal defects and tendon repair. However, its effects on articular cartilage degeneration have not been determined. Our hypothesis was that intra-articular delivery of micronized dHACM (EpiFix Injectable™) will ameliorate the progression and extent of joint degeneration in the rat MMT model and based on our results from Aim II, EPIC-µCT would be able to assess changes in the articular cartilage in response to µ-dHACM. First, we tested the effects of dHACM in naïve rats followed by delivering it intra-articularly in the OA model. Short-term effects were analyzed using EPIC-µCT at 3 weeks. Longer term effects including treatment of a pre-arthritic joint via a delayed injection, were examined at 6 weeks. Denatured µ-dHACM was also tested both in vitro and in vivo. Outcome measures included EPIC-µCT analysis and histology. The results of this aim are discussed in Chapter 5.

Significance

The burden of joint diseases is enormous and is continually increasing, with only limited intervention options available. The incidence of OA is expected to rise with a growing ageing population as well as with an increase in the rate of obesity. The lack of effective DMOADs leads to only temporary pain relief options available to OA patients.

This leads to a loss of patient's quality of life while creating an economic burden on the healthcare sector as well.

Development and testing of new therapies requires suitable animal models for OA combined with efficient diagnostic tools. There is considerable ongoing research exploring DMOADs and testing them in vitro and in pre-clinical animal models; however, the testing process in animal models remains inefficient and subjective. This makes the therapeutic testing process challenging, as extensive resources are required to screen potential DMOADs. Developing effective DMOADs and translating these to the clinic would require a suitable, well characterized pre-clinical model of OA with quantitative, objective outcome measures to use as a test-bed for evaluating potential DMOAD candidates. Accordingly, there exists a need to quantitatively characterize a rat OA model and assess the efficacy of this model using a suitable diagnostic tool to test therapeutics. In this project, we used EPIC-μCT as a high throughput screening technique to test DMOADs in the widely accepted rat MMT model for OA.

The work described in this thesis is *significant* because it presents innovative research on characterizing a well-accepted rat OA model using a quantitative contrast based imaging technique, followed by assessing the sensitivity of the technique and then utilizing it to test a novel tissue engineering based therapeutic strategy. No previous studies have demonstrated the use of EPIC-μCT as a tool to study disease modifying drugs for joint diseases. 3D quantitative analysis using EPIC-μCT provides a more complete picture of disease progression in the tissue as a whole with higher sensitivity of therapeutic efficacy than current 2D histopathology. EPIC-μCT is non-destructive

allowing for additional histology analysis on the same samples, which could additionally be beneficial as some outcomes, such as cellularity, cannot be observed with CT. Overall this technique can provide a powerful tool moving forward for enabling higher throughput, fewer samples, and more sensitivity when screening new therapies for joint diseases.We have successfully established EPIC-μCT as a high throughput screening technique to test DMOADs in small animal models and evaluated the efficacy of two different therapeutics to slow the progression of joint degeneration. Additionally, this research has advanced our understanding of the progression of OA in the rat MMT model and presents results of an ECM based therapeutic as a potential DMOAD candidate. Ultimately, testing novel therapeutics in an efficient, quantitative manner will result in faster screening and improve the process of translating a new therapy through the pre-clinical development stage to clinical trials.

CHAPTER 2

LITERATURE REVIEW[a]

Articular Cartilage

Articular cartilage is a smooth, white tissue which covers the ends of bones in various joints. The joints themselves contain various components such as ligaments, supporting muscles and synovial membrane (Clouet, Vinatier et al. 2009). Hyaline articular cartilage is found on the ends of the bones in a joint where it provides a low friction surface allowing for joint movement (Athanasiou, Shah et al. 2001).

Structure and Composition

Cartilage possesses a unique structure and composition that allows articulating surfaces to glide over each other with minimal friction (Forster and Fisher 1996). Additionally, cartilage assists in biomechanical activity of the joint by distributing forces and absorbing energy in combination with other tissues such as the meniscus in the knee joint (Ahmed and Burke 1983).

Cartilage is unique because it is avascular and has minimal innervation. This leads to minimal regenerative capacity of the tissue. A major component of cartilage tissue volume is composed of the ECM as opposed to chondrocytes. The ECM is mainly constituted of proteoglycans (PGs) and collagen (Huber, Trattnig et al. 2000, Hunziker 2002).

---

[a] Parts of this chapter have been adapted from Thote T, Moran S, Lin ASP, Willett NJ, Neu C, Guldberg RE. "Methods for Detection of Joint Degradation" in Morris P. (Editor), Biomedical Imaging: Applications and Advances. 2014 (In press).

PGs are macromolecules with a basic PG unit consisting of a core protein with glycosaminoglycan (GAG) chains covalently bound to this core. The GAG chains are negatively charged which causes them to repel each other. This creates an osmotic imbalance that is partially balanced by influx of water into the tissue as well as due to cations in the surrounding area (Huber, Trattnig et al. 2000).

The major protein in cartilage is collagen. Collagen type II is most predominant though other types of collagen such as Type III, IX,X and XI have been identified in small amounts(Eyre, Weis et al. 2006). These different collagen types play different roles while creating the fibrillar structure of cartilage (Eyre 2004). Tightly packed collagen fibers allow for high tensile strength and dynamic compressive modulus of cartilage with collagen type II being predominant in its composition (Bader and Kempson 1994).

Articular cartilage is divided into three layers – superficial zone, transitional zone and deep zone (Fig 1). Collagen fibers are tightly packed in the superficial zone. These fibers display transition in their alignment in the transitional zone. In the deep zone, the collagen fibers are aligned perpendicular to the surface. The tidemark is the interface between the deep cartilage and the calcified cartilage. Below the calcified cartilage, lies the subchondral bone which eventually transforms into trabecular bone.

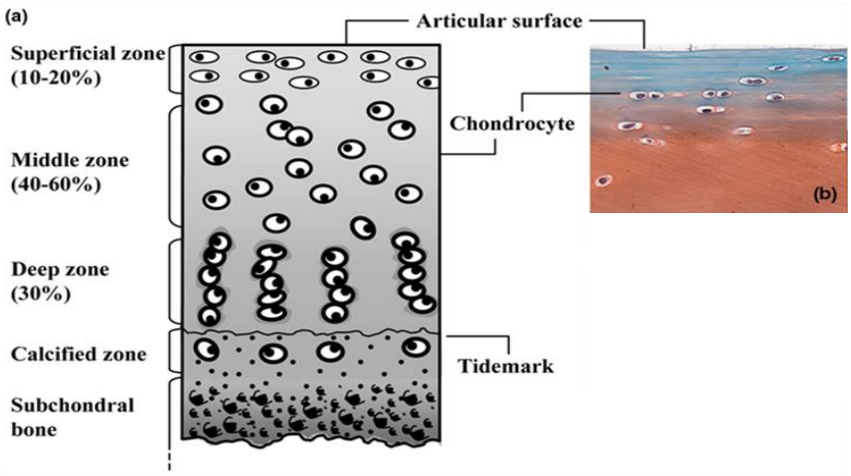

Figure 1. Articular cartilage structure a) Zonal architecture of cartilage b) Safranin O micrograph of chondrocytes in the superficial zone. (Adapted from Grogan, Miyaki et al. 2009Creative Commons License doi:10.1186/ar2719)

During loading of the joint, the internal pressure on cartilage increases. The collagen fibrils prevent the cartilage from deforming under load. In the presence of persistent loading, an increase in pressure causes an outflux of water from the cartilage until equilibrium is reached. PG control the balance during static loading and loss of PGs leads to decreasing the compressive modulus of the tissue(Herzog and Federico 2006) . This same effect is observed when the collagen network is disrupted. Changes in mechanical properties of the cartilage affect the functional capacity of cartilage to withstand normal loading. Thus, alteration of biomechanical properties makes the cartilage susceptible to further injuries.

Osteoarthritis

OA is a debilitating joint disease that causes damage to the cartilage and underlying subchondral bone in synovial joints.

Pathophysiology & Etiology

OA is the leading cause of disability in the US and affects nearly 27 million people. The most prevalent joints affected are knee, hip, hand, foot and the spine with knee OA being the most common(Martel-Pelletier, Wildi et al. 2012).

The pathophysiology of OA is complex and involves changes at the molecular, cellular, and tissue levels. At the initial stage, OA is characterized by subchondral bone alterations, loss of cartilage thickness, and fibrillation of the surface layers, which leads to a loss of cartilage integrity (Clouet, Vinatier et al. 2009). During this stage, there is an upregulation of chondrocyte metabolism followed by eventual apoptosis of chondrocytes and a decrease in osteoblast activity that causes thinning of adjacent trabecular bone. PG and collagen synthesis is also increased at the initial stage of the disease. As the disease advances, there is a progressive loss of chondrocytes at all levels of cartilage with pronounced thinning of the cartilage matrix possibly leading to lesions and excessive bone remodeling where cartilage has degraded (Kim and Blanco 2007, Clouet, Vinatier et al. 2009). Greater stress on the collagen network may occur at this stage which exposes the cartilage to further damage, first in the transitional zone which may progress into the radial zone. As collagen and PG are integral for maintaining articular cartilage function, the mechanical properties of cartilage are also typically impaired at this stage(Aigner and Stove 2003).

Various enzymes that degrade articular cartilage and the surrounding ECM have been characterized. The levels of anabolic factors such as fibroblast growth factors (FGFs) and bone morphogenetic proteins (BMPs) have been shown to decline as OA progresses. Cytokines such as tumor necrosis factor (TNF) and interleukin-1(IL-1) have

been implicated in the increase in catabolic enzymes (Goldring and Goldring 2007). Matrix metalloproteinases (MMPs) are an important group of enzymes implicated in OA and often observed to be upregulated during OA progression. Other degrading enzymes, such as aggrecanases, have also been detected and their role in the development of OA is being studied (Burrage and Brinckerhoff 2007).

Advanced OA is associated with inflammation of the synovium, which leads to release of pro-inflammatory cytokines that cycle back and play a role in further cartilage degradation. Advanced OA is typically characterized by progressive erosion of the articular cartilage in combination with degradation of the subchondral bone(Loeser 2004). There is some evidence suggesting that cartilage and bone changes are inter-related in OA. Subchondral bone sclerosis and formation of osteophytes are typical features of OA. These factors affect cellular changes such as chondrocyte clustering in the earlier stages and increased chondrocyte apoptosis due to caspases in advanced OA(Loeser 2004). OA is therefore a multi-faceted disease affecting cartilage, synovium, and bone and involving interplay of multiple factors that create a negative cycle of progressive joint degeneration.

Secondary OA also exists in humans where cartilage changes occur as a consequence of a trauma or trigger which hampers the mechanical integrity of the tissue, usually by causing damage to the collagen network(Buckwalter and Brown 2004). Different causes of secondary OA have been identified such as high intensity impact joint loading, intra-articular fractures, ligament injuries and several metabolic disorders (Buckwalter and Martin 2006).

Etiology of OA remains unclear to this day. Primary OA is correlated with increasing age but it is not necessarily considered as a normal ageing process(Crepaldi and Punzi 2003). Large scale follow-up studies in human populations have helped identify risk factors for primary OA(Buckwalter, Saltzman et al. 2004, Felson 2004, Cimmino and Parodi 2005). One, is the effect of gender with OA being more prevalent in women than men(Buckwalter and Lappin 2000). Another risk factor is high BMI or body weight(Schouten 1992). This factor combined with malalignment of joint puts the patient at high risk for OA(Sharma, Lou et al. 2000). Trauma to the knee not limited to accidents or sports injury(Gelber, Hochberg et al. 2000) particularly in the form of a meniscectomy(Roos, Lauren et al. 1998) also creates a high risk.

OA is often observed to be clustered in families leading to a hypothesis that genetics may play a role as a risk factor as well(Cicuttini and Spector 1996). In a twin study, heritability of OA was estimated to range from 39-65%(Spector, Cicuttini et al. 1996). However, OA is not caused by a single gene mutation. Multiple genetic loci for susceptible OA genes have been identified but these factors are not comprehensive (Aigner and Dudhia 2003, Peach, Carr et al. 2005). OA is a multifactorial complex disease that researchers continue to try and understand better.

Prevalence

OA prevalence increases as people age. In the US, 27 million people suffer from clinical OA. OA is the most common form of arthritis. For population > 60 yrs., the prevalence rate of symptomatic knee OA is 10% in men and 13% in women. This number is expected to increase as the ageing population rises as well as the obesity epidemic (Zhang and Jordan 2010).

Various studies have been performed to estimate the prevalence of OA. The age standardized prevalence of radiographic knee OA in adults age ≥ 45 was 19.2% among the participants in the Framingham Study and 27.8% in the Johnston County OA Project (Lawrence, Felson et al. 2008). In the third National Health and Nutrition Examination Survey (NHANES III), approximately 37% of participants age >60 years or older had radiographic knee OA (Lawrence, Felson et al. 2008).

The table below shows the prevalence of OA for various joints as described by different studies.

Table 1. Prevalence of OA

Anatomic site	Age	Source	Male patients (%)	Female patients (%)	Total
Hip	≥45	Johnston County OA project (Jordan, Helmick et al. 2009)	25.7	26.9	27.0
Hand	≥26	Framingham OA study (Zhang, Niu et al. 2002)	25.9	28.2	27.2
Knee	≥26	Framingham OA study (Felson, Naimark et al. 1987)	14.1	13.7	13.8
All joints	≥45	Framingham OA study (Felson, Naimark et al. 1987)	18.6	19.3	19.2
All joints	≥60	NHANES III (Dillon, Rasch et al. 2006)	31.2	42.1	37.4

In addition to significantly affecting patients' quality of life, OA also presents a large economic burden (Bitton 2009). In a study done in 1997, total medical expenditures for arthritis and other rheumatic conditions was $233.5 billion. By 2003, these costs

increased to #321.8billion (factoring in inflation) (Yelin, Murphy et al. 2007). A significant portion of these costs is attributed to OA and an estimate by Leigh et al, calculated the total annual costs of OA at 89.1 billion (Leigh, Seavey et al. 2001). While these are the direct costs of OA, there is also an indirect cost which includes lost wages, lost productivity and expenses from home care. A study based on claims database analysis calculated the indirect costs of OA at $4603 per person per year(White, Birnbaum et al. 2008).

Treatment Strategies

Currently, there are no clinically approved disease modifying OA drugs (DMOADs) that have shown efficacy for OA. Current treatment methods are targeted towards reducing pain (symptomatic treatment) rather than trying to treat the underlying cause of the disease. Another issue with current symptomatic OA drugs are the side-effect profiles which cause concerns particularly in chronic applications (Wieland, Michaelis et al. 2005). Researchers have suggested that treatment of OA should be tailored individually as there is a substantial discordance between radiographically diagnosed OA and knee pain. Depending on the patient, non-pharmacological treatments including exercises and weight reduction should also be discussed by the physician (Dieppe and Lohmander 2005)

Pharmacological

The first line oral analgesic for knee OA is acetaminophen. It is widely recommended due to its favorable safety profile. In cases where patients do not respond to acetaminophen, the next line of treatment is non-steroidal anti-inflammatory drugs (NSAIDs). The principal targets for NSAIDs are the isoforms of cyclooxygenase, COX1

and COX2. COX1 is constitutively expressed in many cell types, whereas COX2 is induced at the site of inflammation (Vane, Bakhle et al. 1998) . However, NSAIDs exhibit a risk of gastrointestinal side effects as the principle targets are also expressed in the kidney and other organs. Selective COX2 inhibitors were introduced in 1999, which provide equivalent efficacy while reducing the risk of GI complications(Warner, Giuliano et al. 1999). Recently, the cardiovascular safety of COX-2 selective and other NSAIDs is under scrutiny (Petit-Zeman 2004, Topol 2004). Currently, COX-2 selective medications are contraindicated for people with ischemic heart disease and hypertension (Wieland, Michaelis et al. 2005).

Opioid analgesics are also useful alternatives in patients who cannot tolerate NSAIDs. Glucosamine and chondroitin products are also widely used for pain management in OA though their efficacy remains controversial (Wieland, Michaelis et al. 2005).

Intra-articular injection of corticosteroids are also used to treat pain in OA. However, injections can only be given up to 4x/year as they are invasive and it is difficult to retain the drug in the joint space for a long time to achieve sustained efficacy (Gerwin, Hops et al. 2006). These therapies seem to provide temporary relief of pain in certain patients, but no convincing evidence for disease-modifying effects has been demonstrated (Ayral 2001).

Disease Modifying OA Drugs

While no DMOADs have been currently approved, there are a few DMOADs in various phases of development. There a variety of compounds each with its own mechanism of action. Researchers suggest that initial degenerative changes are easier to

reverse and hence, early detection of OA is crucial. Using the knowledge about signaling pathways in chondrocytes and identifying various molecules that play a role in catabolic and anabolic processes, researchers are trying to develop DMOADs.

MMP-inhibitors have been tested which inhibit MMP gene expression for genes that have been implicated in OA (Burrage et al. 2007, Cawston et al. 2006, Murphy et al. 2005). However, these MMPi's have had musculoskeletal side effects leading to failure in early clinical phase trials. Researchers are now trying to focus on selective MMPi's vs. broad spectrum inhibitors (Fingleton 2007). MMP-13 is one of the important MMPs expressed in OA cartilage and a MMP-13 inhibitor might be a viable target to pursue. In addition to MMPs, researchers have also tested IL-1b inhibitors. IL-1b is a pro-inflammatory cytokine expressed in OA and an IL-1 inhibitor showed promise in small animal studies (Hunter 2011). However, this did not translate to humans as IL-1 receptor antagonist in various forms failed to meet its pain and structure endpoints (NIH 2008).

In addition to articular cartilage, subchondral bone turnover has also been implicated in OA. Hence, drugs originally targeted for osteoporosis are being proposed as candidates for OA treatment. Calcitonin, promotes inhibition of bone resorption. A human clinical trial of salmon calcitonin (sCT) led to reduced levels of type II collagen and a pilot study exhibited decrease in pain scores (Karsdal, Byrjalsen et al. 2010). sCT is currently being tested in ongoing clinical trials to examine its effect on OA (NIH 2012)

Bone morphogenetic protein (BMP) has been used clinically in patients. BMP-7 is a member of the TGFβ superfamily and is known to have reparative effects on cartilage. Individuals with OA have decreased levels of BMP-7 and increased levels of

extracellular BMP antagonists (Hunter 2011). There is an ongoing clinical trial testing the efficacy of BMP-7 in knee OA (NIH 2010).

Growth factor changes have been implicated in OA as well. FGF-18 has been reported to have anabolic effects on the cartilage. It activates FGF receptor 2 and increases matrix formation while it inhibits cell proliferation. Preclinical studies showed potential of FGF-18 in a rat OA model (Moore, Bendele et al. 2005). Based on these studies, FGF-18 is currently the focus of an ongoing clinical trial (NIH 2010).

Apart from these, there are other agents in early stages of development (not in phase II trials). These include cathepsin K, proteoglycan 4 (lubricin), receptor activator of nuclear factor κB ligand (RANKL) and aggrecanase inhibitors (Hunter 2011).

One major obstacle is the difficulty in developing diagnostic methods for early cartilage degeneration, and subsequently for monitoring the effect of these novel pharmaceuticals (Goldring 2006, Qvist et al. 2008). In order to determine the efficacy of these novel medications, it is important to develop efficient methods that are capable of detecting the effects of each treatment in both pre-clinical and clinical stages.

Surgical Treatments

Advanced OA might require surgical intervention if medical treatment does not sufficiently alleviate pain (Jordan et al. 2003). While knee replacement is the most common technique, other options are also available.

Arthroscopic procedures such as arthroscopic lavage and debridement have been used in patients who do not respond to pharmaceuticals (Frizziero et al. 2005, Segal et al. 2006). High tibial osteotomy which involves surgical realignment of the loading axis of the limb has been used to treat medical compartment OA of the knee (Brouwer et al.

2005). In these procedures it is difficult to determine which patients will benefit the most and hence the results are still somewhat contradictory.

Joint replacement, while expensive, has been evaluated as being cost effective. It can alleviate pain and improve joint functionality as well. Timing of surgery is important to consider during joint replacement so that the patient gets the most benefit out of this procedure (Fortin, Penrod et al. 2002). The annual rate of total joint replacement is increasing with OA being the most common indication for total knee replacement (Katz 2006).

Cartilage repair techniques

Currently several cartilage repair techniques are in clinical use. These include osteochondral transplants, microfracture technique and autologous chondrocyte implantation (Chiang and Jiang 2009). These are targeted towards repairing articular cartilage lesions. These are limited in use for localized cartilage lesions, often of traumatic origin rather than treating primary OA (Chiang and Jiang 2009).

Development of efficient techniques and materials for cartilage repair is an important area of research. Biologic solutions based on tissue engineering techniques are also being explored as options (Nesic et al. 2006, Schurman et al. 2004).

Small Animal models for OA

OA is a multi-factorial disease influenced by a variety of genetic and environmental factors. The need to understand the molecular events that occur in the joint in addition to having a platform for preclinical testing, has required researchers to develop suitable small animal OA models.

Most models involve surgical insults in order to cause mechanical stress in the joint considering that injury is a common predisposing factor towards OA. Models have been developed in sheep (Cake et al., 2004), dogs (Mastberger et al., 2006), rabbits (Inouye et al., 1973), guinea pigs (Bendele et al., 1991), rats (Hayami et al., 2006; Laurent et al., 2006; Moore et al., 2005), and mice (Bendele, 2001). Small animals in the form of rats and mice allow for relatively quick onset of the disease and are less expensive.

Rat Models

Surgically induced destabilization of joints is the most widely used OA induction method. Most induction methods duplicate known injuries in humans such as anterior cruciate ligament transection (ACLT) and meniscal injury. ACLT or ACLT in combination with a partial medial meniscectomy has been used to induce OA in rats. It leads to PG loss, cartilage surface damage as well as subchondral bone sclerosis and osteophyte progression (Bendele 2002). The medial meniscal tear (MMT) model, is the most widely used model for inducing OA in rats(Gerwin, Bendele et al. 2010). It involves transection of the medial meniscus which leads to rapidly progressive cartilage degeneration indicated by chondrocyte & PG loss, fibrillation and osteophyte formation. Progressive changes occur and are detectable at 3 weeks and by 6 weeks tibial cartilage degeneration is focally severe with degeneration of surrounding matrix and prominent osteophytes (Moore, Bendele et al. 2005).

Apart from surgical destabilization, chemically induced joint degeneration has also been used to study effects of pain in rats. A common model for this is injection of monosodium iodoacetate. MIA is an inhibitor of glycolysis and induces chondrocyte

apoptosis and joint inflammation. Its utility as an OA injury model is debatable though it is validated as a suitable model for pain (Bendele 2002). Other agents that are used to induce cartilage degeneration include papain, collagenase and chondroitinase which degrade ECM components but may not be relevant to modeling human OA as the processes that precede and induce proteolysis in human OA do not occur (Little and Smith 2008). Additionally, the reagents may be quite different from the compounds that exist in human disease as well as in causing much higher degree of inflammation as compared to human OA.

Murine Models

Murine models have been gaining popularity due to the homogeneity of genetics, ability to inbreed and option to create genetically modified strains. However, surgical induction in mice is difficult due to the small size of joints.

Microsurgical tools have been used to create mouse meniscectomy model that involved medial collateral ligament (MCL) transection coupled with medial meniscectomy. This leads to mild cartilage lesions on the medial plateau by 3-4 weeks (Clements et al., 2003).

Spontaneous OA Models

Age-onset development of OA occurs in STR, DBA/1, and C57 Black mouse strains. These spontaneous models may help us understand the mechanisms beneath some human forms of OA (Yamamoto et al., 2005). The highest incidence of this type of OA occurs in the STR/1N strain (Jay, 1951) and the related STR/ort strain (Sokoloff and Jay, 1956). In this model, cartilage lesions are detected histologically as early as 8 weeks of age and appear at the insertion of the medial collateral ligament and the medial tibial

plateau (Mason et al., 2001). Males have a higher incidence than females, and cartilage loss is most prevalent in the medial compartments of the knee joint. Interestingly, spontaneous obesity develops at three months of age in these mice, even when kept on a standard diet. Histological evaluation of knee joints from STR/ort strain using TUNEL assays showed an increasing number of apoptotic cells in cartilage covering medial tibialand femoral bone with advanced histological lesions (Mistry et al., 2004). This finding may be consistent with preceding biomechanical or metabolic stress on the cartilage (Mason et al., 2001). C57 Black mice are also susceptible to developing OA lesions in knee joints as a result of a genetic mutation with recessive Mendelian inheritance (Silberberg and Silberberg, 1960). Incidence and severity of OA based on histopathological cartilage damage increases with age in both males and females from 20% at 2 months to 80% at 16 months (Yamamoto et al., 2005).One limitation with these models is the cost of experimentation as the animals need to be housed and maintained for up to a year for testing.

Limitations

The pharmaceutical industry uses surgical models for pre-clinical studies extensively due to rapid, reproducible results. However, there are a few limitations to be considered. One, OA is not always caused by joint trauma and a lot of patients do not have a history of injury limiting our ability to translate data. Two, surgically induced OA models cause rapid damage whereas in humans OA takes several years to develop. Third, the surgery itself may be a confounding factor as it can damage other structures and start a wound healing cascade different from OA. Another important factor is that surgical

models lead to continued joint damage post-surgery which can limit the evaluation for therapies since the damage may be too aggressive (Little and Smith 2008).

With genetic models, the mice can be difficult to breed and maintain. It still isn't clear what predisposes an individual animal to OA – is it the direct involvement of the gene or the developmental changes that occur downstream due to gene deletion. Another limitation with genetic models is that treatment interventions are difficult to test unless the gene abnormality occurs during adulthood/or upon induction of the disease.

Imaging Techniques for Cartilage

Non-destructive imaging of cartilage to assess the composition and structure of articular cartilage remains an important need and there are a variety of techniques for this task. The spatial resolution necessary for assessing cartilage is usually the deciding factor in choosing what technique to use.

Traditional radiography and computed tomography (CT) techniques allow for evaluating changes in the bony matrix such as presence of osteophytes and joint space narrowing. Magnetic resonance imaging (MRI) allows for visualization of the cartilage. Within MRI, there are a variety of techniques to assess the cartilage such as 2D FSE, 3D FSE, 3D driven equilibrium Fourier transform etc. Each have their own strengths and limitations(Roemer, Crema et al. 2011). 3D MRI data can also be used for quantitative measurement of the cartilage. Trained users segment the bone and cartilage interface to isolate the cartilage area for evaluation. Contrast agents based MRI such as delayed gadolinium-enhanced MRI of cartilage (dGEMRIC) allows for accurate measurement of sGAG concentration in healthy and degrading joints (Winalski and Rajiah 2011).

Recent research has also been exploring ultrasound as a method to analyze collagen structure in the cartilage. Sonography has demonstrated changes in the hyaline cartilage from early to late disease stages and in OA patients with synovitis, joint effusion with synovial thickening and proliferation can be observed by gray-scale ultrasound (Iagnocco 2010). Fourier transform infrared imaging spectroscopy (FT-IRIS) has also been shown to detect changes in sGAG content based on frequency absorbance spectrums (Rieppo, Hyttinen et al. 2009).

Contrast based CT imaging

CT imaging was introduced in the early 1970's and has since proven to be a valuable diagnostic tool (Holdsworth, 2002). Clinical CT imaging was targeted towards humans to generate two-dimensional images of internal structures; however, the resolution did not enable visualization for small animal models. With advances in technology, higher resolution images can be obtained, and today μCT systems are defined as systems which can perform volumetric CT analysis with an isotropic voxel spacing of < 100 μm. Clinical CT imaging does not have the resolution to verify OA progression. However, μCT is used to examine OA progression in small animal models by assessing cartilage using contrast agents and subchondral bone based on X-ray attenuation (Holdsworth, 2002).

The working principle for μCT imaging is based on generating contrast by X-ray attenuation. As the X-ray beam penetrates a sample, it is attenuated based on the material properties of the object such as acquiring X-rays of fractured bone. An X-ray projection of the sample represents an image of the sum of local attenuations along the X-ray beam. To generate a 3D image, cameras capture X-ray attenuation data from many different

viewing angles. The collected data is run through image reconstruction algorithms, which produce 2D grayscale pixel matrices as slices of the object. After this step, the slices are processed and stacked to produce 3D images (Bartling S. H. , 2007).

EPIC-µCT

Articular cartilage degradation is a primary characteristic of OA. Even though µCT provides an excellent option to visualize bone morphology, cartilage imaging and quantification is a challenge due to its low radiodensity. Traditionally, changes in cartilage have been evaluated by histology, which is time-consuming and destructive. Recent research has shown that specific contrast agents have the ability to increase contrast of cartilage to allow for measurements of morphology and composition of the tissue (Xie et al., 2009, Palmer et al., 2006, Silvast et al., 2009a). Within the cartilage extracellular matrix, negatively charged sulfated glycosaminoglycans (sGAGs) are attached to the PG backbone, and these allow for electrostatic interactions with contrast agents. sGAGs are of importance to researchers as a loss of sGAGs is an indicator of early OA cartilage destruction (Wakitani et al., 2007).

Hexabrix^{TM} 320 (Covidien, Mansfield MA), a clinically available CT contrast agent containing ioxaglate (a negatively charged hexaiodinated dimer), was the first ionic agent used to increase cartilage radiopacity through EPIC-µCT. Specimens to be imaged using EPIC-µCT are first equilibrated in a solution containing an ionic contrast agent like Hexabrix^{TM} and then scanned with a µCT machine (Palmer et al., 2006). Because of the Hexabrix^{TM} molecule's negative charge, incubation of cartilage samples with Hexabrix^{TM} yielded an equilibrium distribution of the agent that was inversely related to the density of the negatively charged sGAGs. The EPIC-µCT technique was shown to be effective in

visualizing cartilage in an *in vitro* degradation model whereas, for *ex vivo* proof of concept on an intact joint, a rabbit femur was imaged (Palmer et al., 2006).

EPIC-µCT has been validated with histological measurements of thickness and needle probe testing. A strong correlation between measurement of articular cartilage thickness with results from EPIC-µCT compared to both histology and needle probe testing was observed. The EPIC-µCT technique was also shown to be precise with a low coefficient of variation in measurement of cartilage volume, surface, and thickness. A follow up study in an *ex vivo* rat model determined 30 minutes as a suitable incubation time and 40% Hexabrix^{TM} as a suitable concentration to achieve desired contrast (Xie et al., 2009). In this study, sGAG optical density was compared to cartilage attenuation values and both were directly correlated. sGAG optical density decreased as cartilage attenuation increased with age. These studies establish EPIC-µCT as a viable technique to measure morphologic changes in cartilage over time (Xie et al., 2010, Xie et al., 2009).

Cartilage has recently been visualized *in vivo* using EPIC-µCT as well. The *in vivo* environment presents various challenges for examining cartilage. Some of the challenges include diffusion of contrast agent *in vivo*, injection of agent, retention of agent in the joint cavity as well as the ability to differentiate between cartilage and surrounding soft tissue and synovial fluid (Palmer et al., 2006). Piscaer et al. recently conducted a study that assessed cartilage degradation in an *in vivo* rat model (Piscaer et al., 2008). MIA, a chemical that causes chondrocyte death leading to cartilage degradation, was injected into rat knees. An equilibrium partition, though, was not reached *in vivo* due to diffusion from the joint cavity. However, a decrease in osmolarity and a higher concentration of Hexabrix^{TM}used*in vivo* enabled visualization of degraded

cartilage as early as 4 days in the MIA model (Piscaer et al., 2008). At the end of 44 days, there was a significant decrease in cartilage volume and increase in cartilage attenuation compared to the controls, indicating a loss of sGAGs and degradation of cartilage in the MIA models. Measuring contrast dye kinetics, Hexabrix™ was shown to absorb more readily in the degraded MIA animal cartilage than normal cartilage.

Current imaging standards for EPIC-μCT of cartilage employ anionic contrast agents such as Hexabrix™ and Cysto-Conray™ II (Covidien Mansfield MA), a clinically available CT contrast agent containing iothalamate (a tri-iodinated monomer). While using these contrast agents is the current standard of practice, one limitation is their low sensitivity to changes in sGAGs, a major component of cartilaginous tissue. Negatively charged sGAGs repel anionic molecules, which results in limited diffusion of the imaging agents into cartilage. To address this issue, high concentrations of anionic contrast agents must be used to achieve linear correlations between X-ray attenuation and sGAGs (Bansal et al., 2010).

Recent research has also explored the use of cationic contrast agents for CT imaging. Cationic agents distribute into articular cartilage and generate a positive relationship with GAG content. Instead of an inverse distribution, cationic agents rely on electrostatic attraction to achieve a high concentration within the tissue. These agents have been tested using osteochondral plugs and future applications involve testing these agents in small animal OA models ex-vivo (Bansal, Joshi et al. 2011).

CHAPTER 3

EPIC-μCT AS A TOOL FOR LOCALIZED 3D ANALYSIS OF CARTILAGE COMPOSITION & MORPHOLOGY IN RAT JOINT DEGENERATION MODELS[b]

Abstract

Current histological scoring methods to evaluate efficacy of potential therapeutics for slowing or preventing joint degeneration are time-consuming and semi-quantitative in nature. Hence, there is a need to develop and standardize quantitative outcome measures to define sensitive metrics for studying potential therapeutics. EPIC-μCT allows for quantitative analysis of articular cartilage in small animal models. We evaluated the hypothesis that EPIC-μCT can be used to quantitatively characterize morphological and compositional changes in the tibial articular cartilage in two distinct models of joint degeneration and define localized regions of interest to detect degenerative cartilage changes. First, we induced joint degeneration by injecting monosodium iodoacetate (MIA) or by performing medial meniscal transection (MMT) in rat. Three weeks post-surgery, tibiae were analyzed using EPIC-μCT and histology. EPIC-μCT allowed for measurement of 3D morphological changes in cartilage thickness, volume and composition. Extensive cartilage degeneration was observed throughout the joint in the MIA model after 3 weeks. In contrast, the MMT model showed more localized

---

[b] Portions of this chapter were adapted from Thote T, Lin AS, Moran SM, Guldberg RE, Willett NJ. Localized 3D analysis of cartilage composition and morphology in small animal models of joint degeneration. Osteoarthritis Cartilage 21(8): 1132-1141. License Number: 3370890841966

degeneration with regional thickening of the medial tibial plateau and a decrease in attenuation consistent with PG depletion. Focal lesions were also observed and 3D volume calculated as an additional outcome metric. The MMT model showed similar features to human OA, including localized lesion formation and PG loss, while the MIA model displayed extensive cartilage degeneration throughout the joint. EPIC-μCT imaging provides a rapid and quantitative screening tool for preclinical evaluation of OA therapeutics.

Introduction

OA affects 27 million people in the US (Lawrence, Felson et al. 2008). Current treatment methods are targeted towards pain relief for OA often in the form of non-steroidal anti-inflammatory drugs (NSAIDs) (Felson, Lawrence et al. 2000). However, there are currently no clinically approved therapeutics that can halt the progression of OA by controlling cartilage erosion and chondrocyte loss (Abadie, Ethgen et al. 2004).

Developing disease modifying OA drugs (DMOADs) remains an unmet need for OA patients. Development of new imaging technologies is one of the requirements to better test potential therapeutics. Microcomputed tomography (μCT) has traditionally provided 3D, quantitative analysis of hard tissues. This imaging methodology has recently been modified to facilitate application to soft tissues, such as cartilage, using contrast agents. EPIC-μCT, allows for non-destructive evaluation of cartilage morphology and composition (Palmer, Guldberg et al. 2006). Previous studies have used different variations of μCT, such as EPIC-μCT and in vivo μCT arthrography to image cartilage in multiple joint degeneration models (Piscaer, van Osch et al. 2008; Piscaer,

Waarsing et al. 2008; Xie, Lin et al. 2009; Xie, Lin et al. 2010; Siebelt, Waarsing et al. 2011; Kotwal, Li et al. 2012; Xie, Lin et al. 2012).

Several surgically and chemically induced models of OA have been developed in different species as platforms to evaluate disease pathology as well as to screen therapeutics (Oegema 1999; Bendele 2001). In this aim, two joint degeneration rat models commonly used to screen OA therapies were characterized—chemical induction of joint degeneration using monosodium iodoacetate (MIA) and surgical induction of joint degeneration via medial meniscus transection (MMT) (Bendele 2001; Bove, Flatters et al. 2009). Each method presents advantages for use in small animal models of joint degeneration. The MIA model is quick, easy, reproducible, and animals exhibit signs of OA related pain (Smith, Little et al. 1997). The MMT model is characterized by progressive cartilage degeneration involving chondrocyte and PG loss, osteophyte and lesion formation, collagen degradation and cartilage fibrillation (An and Friedman 1999; Janusz, Bendele et al. 2002; Little and Smith 2008; Gerwin, Bendele et al. 2010). A major difference in the two models is that the MIA model leads to global degenerative changes whereas the MMT model leads to more localized damage. The MIA model is also typically more aggressive and associated with increased joint pain. While a high dose MIA model—where PGs are nearly completely depleted—has previously been characterized using EPIC-μCT (Xie, Lin et al. 2012), EPIC-μCT has not been used to characterize a less aggressive low dose MIA model or the MMT model.

EPIC-μCT allows for high resolution 3D quantification of cartilage morphology and composition. It is a relatively high throughput technique, provides 3D volumetric data, and enables increased sensitivity and 3D visualization. The objectives of this study

were to use EPIC-μCT to quantitatively characterize morphological and compositional changes in the tibial articular cartilage in two distinct models of joint degeneration and define localized regions of interest to detect degenerative cartilage changes. We hypothesized that EPIC-μCT would be successful in detecting localized changes in articular cartilage and that the MIA model would show extensive cartilage degradation whereas the MMT model would have focal areas of damage.

Materials and Methods

Induction of Joint Degeneration

Georgia Institute of Technology Institutional Animal Care and Use Committee approved all experimental animal procedures (IACUC protocol #A09007). Two groups of rats were used in this study – 8-week old Wistar rats injected with MIA and weight matched Lewis rats (300-325g) that underwent MMT surgery (Janusz, Bendele et al. 2002, Moore, Bendele et al. 2005, Xie, Lin et al. 2012).

Eight 8-week old male Wistar rats (Charles River, Wilmington, MA) were acclimated for one week. After anesthetizing with isoflurane, 0.3mg MIA (Sigma-Aldrich, St. Louis, MO) in 50μl saline was injected into the joint space through the infrapatellar ligament of the left knee. Right knees were injected with 50μl saline as a contralateral control.

Seven weight matched adult male Lewis rats (Charles River, Wilmington, MA; 300-325g) were acclimated for one week. The animals were anesthetized with isoflurane, and a small incision through the skin was made on the medial aspect of the left femoro-tibial joint. The medial collateral ligament (MCL) was exposed by blunt dissection and

transected to visualize the joint space and medial meniscus. The meniscus was transected completely at its narrowest point. The skin was closed with 4.0 silk sutures and then stapled using wound clips. All surgical sites were observed daily for signs of abnormal healing.

Assessment of Cartilage

Rats were euthanized via CO_2 inhalation at 3 weeks after MIA injection or MMT surgery. Tibiae were harvested, dissected free of surrounding tissues, and fixed in 10% neutral buffered formalin (NBF, EMD Chemicals, Gibbstown, NJ) for 3-4 days and then transferred to 70% ethanol (Palmer, Guldberg et al. 2006).

For EPIC-µCT, the proximal end of each tibia was immersed in 2ml of 30% Hexabrix 320 contrast agent (Covidien, Hazelwood, MO) and 70% ion-free PBS at 37ºC for 30 minutes, an incubation period known to result in equilibration of the agent (Palmer, Guldberg et al. 2006, Xie, Lin et al. 2009). Proximal tibiae were scanned using a µCT 40 (Scanco Medical, Brüttisellen, Switzerland) at 45kVp, 177µA, 200ms integration time, and a voxel size of 16µm(Xie, Lin et al. 2009).

Following scanning, tibiae were decalcified in Cal-Ex II (Fisher Scientific, Waltham, MA) for 14 days. Samples were routinely paraffin embedded. For comparison with EPIC-µCT images, sagittal sections were cut at 5µm thickness. Sections were stained for sGAGs with 0.5% Safranin-O and 0.2% Fast Green counterstain or hematoxylin& eosin. For each sample, three sagittal sections were used for thickness histomorphometry analysis and digital images of each section were captured. The cartilage thickness of each section was defined as the average value of 5 manual

thickness measurements at regular intervals perpendicular to the cartilage surface and the values for the three sections were then averaged.

µCT regional analysis

Scanco evaluation software was used to assess 3D morphology and composition. Raw scan data were automatically reconstructed to 2D grayscale tomograms. These were rotated to sagittal sections, and the cartilage was contoured to separate it from trabecular bone and surrounding air (Palmer, Guldberg et al. 2006, Xie, Lin et al. 2012). The cartilage was segmented using a bandpass filter with a minimum threshold value of 175 to eliminate air and 225 to eliminate bone from the raw image following which 3D images were generated. The threshold values were globally applied for both the left and right tibiae of all animals.

The MMT surgery produces localized cartilage degeneration on the medial plateau of the tibia. To observe localized effects of joint degeneration, we evaluated the medial tibial plateau in the MMT group. The regional analyses were replicated for the MIA tibiae for comparison. Four regional analyses were performed using different volumes of interest (VOI). For the MMT model, images were evaluated for: (1) Full articular cartilage in the proximal tibia including medial and lateral aspects (2) Medial plateau only (3) Medial 1/3 of the medial tibial plateau (4) Focal lesions on the medial plateau only (Fig 2). For the MIA model, only analyses (1) and (2) were performed for overall tibial articular cartilage and tibial medial articular cartilage respectively. Two outcome measures were defined for evaluation of focal defects: erosion (defect extended to less than 50% of cartilage thickness) and lesion (defect extended to more than 50% of cartilage thickness) (Pritzker and Aigner 2010). To define VOIs of focal lesions, manual

contouring was performed in the isolated lesion area (typically ~8 slices). Within this VOI, segmented cartilage volume was subtracted from the total volume evaluated to compute lesion volume.

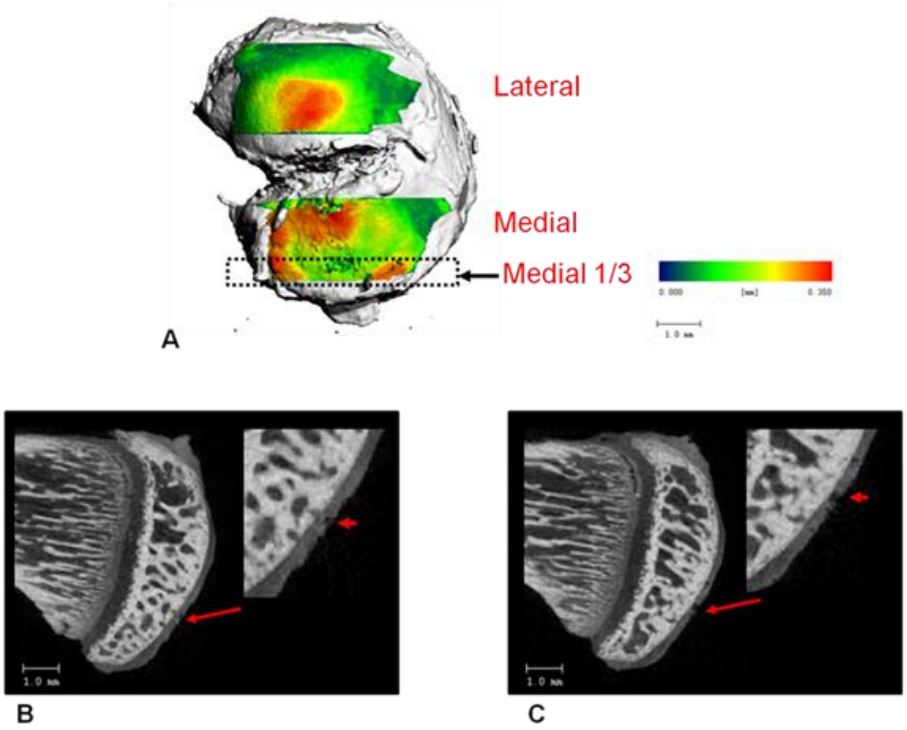

Figure 2.Representative image illustrating EPIC-µCT image analysis (tibial cartilage overlaid on bone) and volume of interest (VOI) designations. Pseudocolor coding (indicated at bottom) displays larger thicknesses in red and smaller thicknesses in blue B: Representative grayscale EPIC-µCT images of cartilage showing erosions (B) and lesion (C) (Inset shows zoomed in view). Lesion locations were identified by manually examining sagittal grayscale images slice by slice.

Statistical analysis

All data are presented as mean ± standard error of the mean (SEM). All data were expressed as mean ± standard deviation of the mean. The means of cartilage morphology variables—cartilage thickness, volume, and attenuation—fit a Gaussian distribution (Kolmogorov-Smirnov test) and were evaluated using paired t-tests to compare

experimental and control tibiae for MMT and MIA groups separately. Each individual region (Overall cartilage, medial tibial plateau and medial 1/3 of medial tibial plateau) was evaluated independently with separate paired t-tests for each of the cartilage morphology variables listed above. All analysis was done using GraphPad Prism (GraphPad Software Inc. 5.01, La Jolla, CA). Statistical significance was set at a 95% confidence interval ($p < 0.05$).

Results

MIA Model Characterization

MIA articular cartilage analysis

Representative images of tibial articular cartilage sections stained with Safranin-O in comparison with EPIC-μCT images are shown (Fig3). At three weeks post injection, the MIA cartilage displayed extensive PG loss which was not observed in the saline injected contralateral control (Fig 3). Images of sagittal sections from the medial tibial plateau of the tibia generated by EPIC-μCT for MIA samples are also shown (Fig 3).

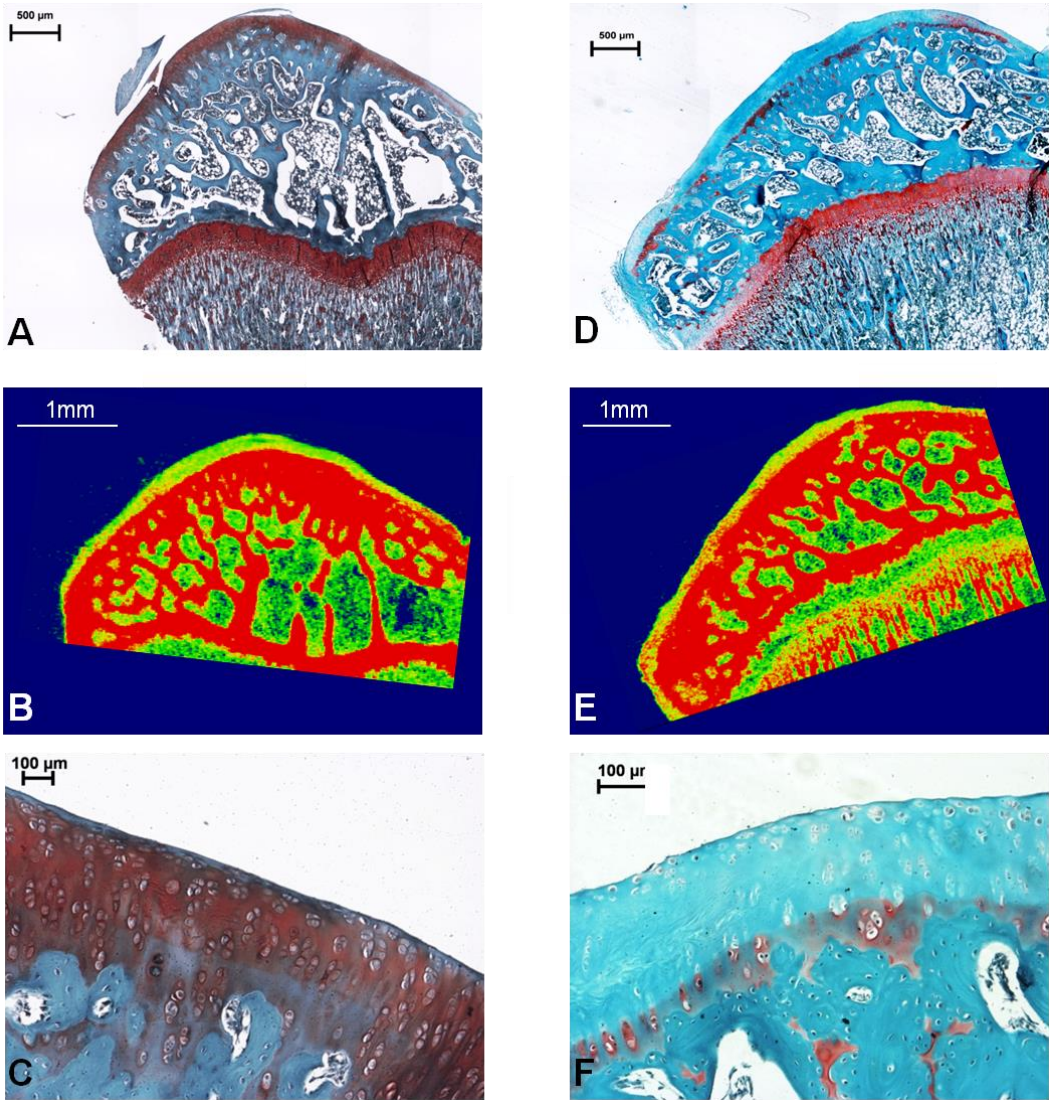

Figure 3.Histology and EPIC-µCT images of tibial articular cartilage in the MIA model. A-C: Representative saline contralateral control section, safranin-O stained, 4X (A), corresponding EPIC-µCT thickness map from the same sample (B) and 10X safranin-O section (C). D-F: Representative MIA injected sections, safranin-O stained, 4X (D), corresponding EPIC-µCT thickness map from the same sample (E) and 10X safranin-O section (F).

Using the EPIC-µCT technique, the overall tibial cartilage was quantitatively evaluated for thickness, volume, and attenuation. At three weeks post injection, cartilage thickness in MIA tibiae decreased by 30% compared to saline contralateral controls (Fig

4). Cartilage attenuation in MIA tibiae increased by 18% compared to saline contralateral controls (Fig4).

Following overall cartilage analysis, the medial tibial articular cartilage was evaluated separately. Average cartilage thickness and volume were 31% and 18% lower, respectively, compared to saline contralateral controls (Fig 4). Average attenuation was 22% higher than saline contralateral controls (Fig 4). The decrease in cartilage volume was not observed when assessing the overall tibial plateau.

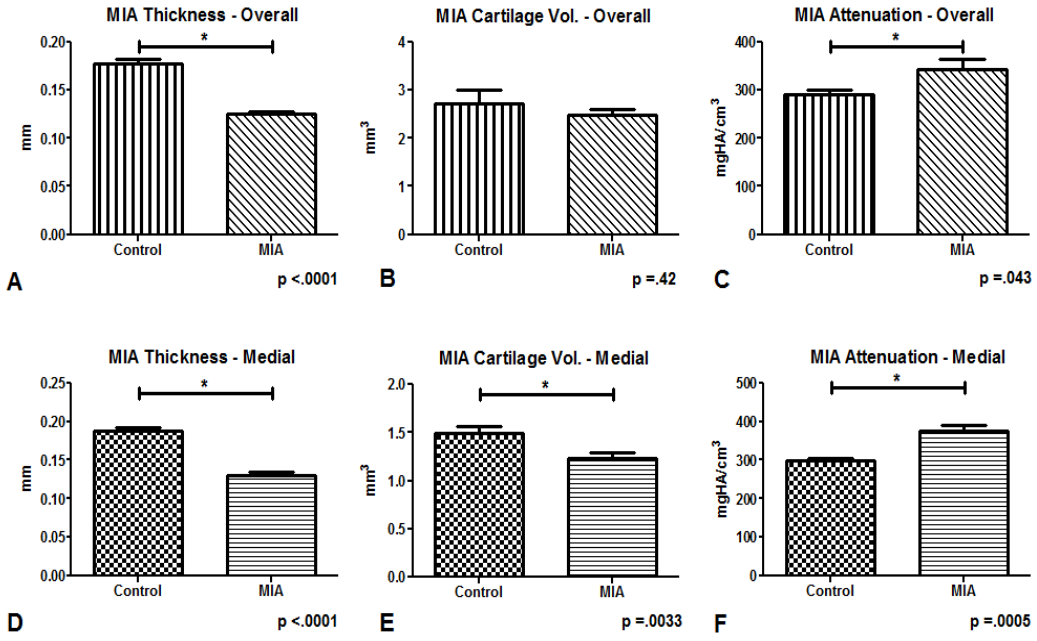

Figure 4. Tibial articular cartilage variables quantified for MIA and saline contralateral control knees (paired comparisons). A-C: Overall tibial articular cartilage variables - Cartilage thickness (A); cartilage volume (B); cartilage attenuation (C). D-F: Medial tibial articular cartilage variables - Cartilage attenuation (D); cartilage thickness (E); cartilage volume (F). At 3 weeks post injection, overall and medial tibial cartilage thickness from MIA-injected joints was significantly lower than saline contralateral control cartilage. Overall and medial tibial cartilage attenuation from MIA-injected joints were significantly higher than saline contralateral controls. Medial tibial cartilage volume from MIA-injected joints was significantly lower than saline contralateral controls. * = $p < .05$, n=8

MMT MODEL CHARACTERIZATION

MMT tibial articular cartilage analysis

Representative images of tibial articular cartilage sections stained with Safranin-O in comparison with EPIC-µCT images are shown (Fig 5). The MMT cartilage displayed erosion on the histology image which was not observed on the contralateral control. The EPIC-µCT image of the MMT tibia also displayed both an erosion and a lesion on the sagittal section of the medial tibial plateau (Fig 5).

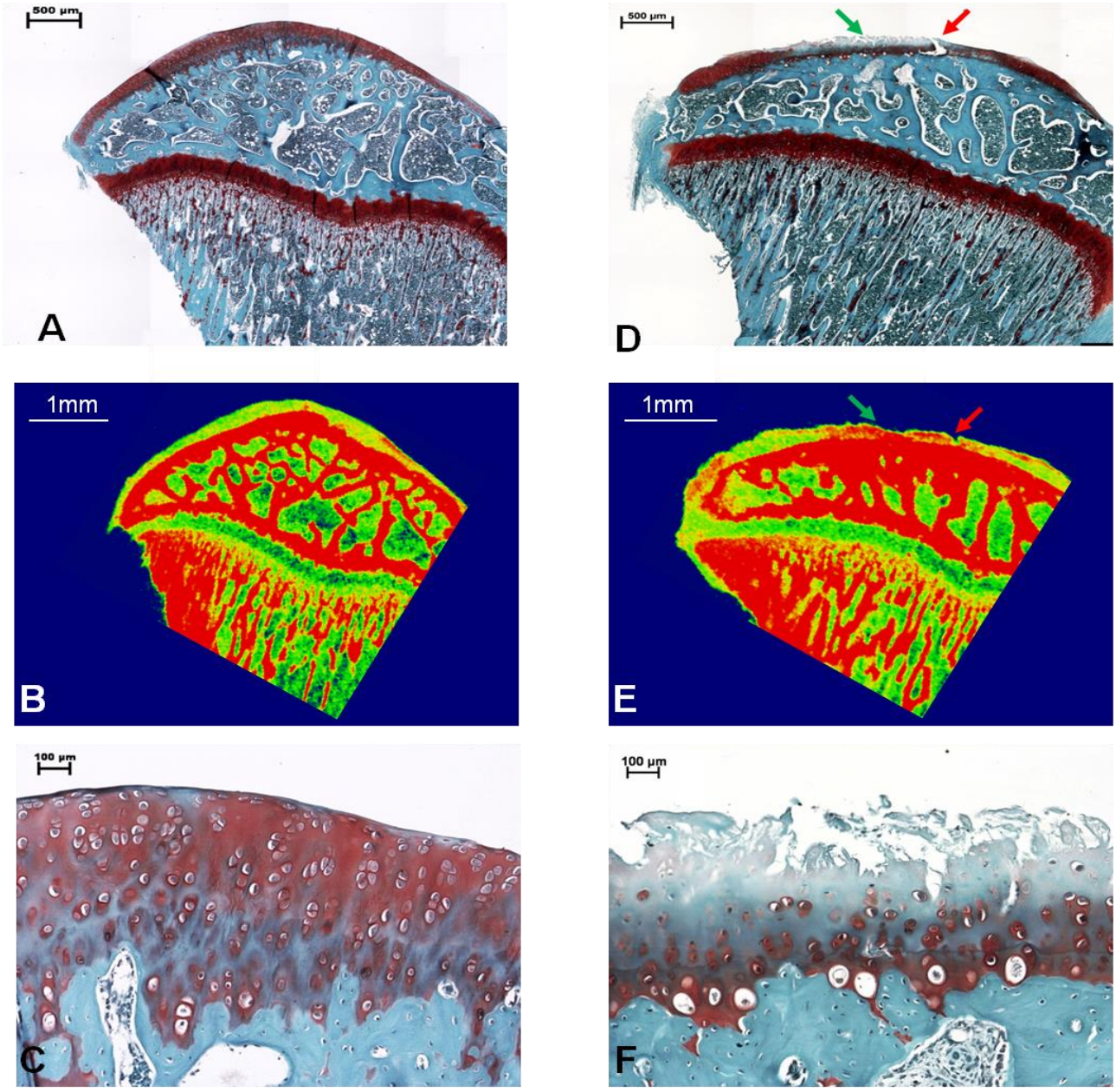

Figure 5. Histology and EPIC-µCT images of tibial articular cartilage in the MMT model 3 weeks post injection. A-C: Representative safranin-O stained control section, 4X (A), corresponding grayscale EPIC-µCT section (B) and 10X safranin-O section (C). D-F: Representative safranin-O stained MMT section, 4X (D), corresponding grayscale EPIC-µCT section (E) and 10X safranin-O section (F). Green arrow in D & E indicate fibrillation site and red arrow in D & E indicate lesion site.

Cartilage histomorphometry measurements similarly showed a significant increase in the thickness of the medial tibial plateau in the MMT tibiae compared to the contralateral controls (Fig 6).

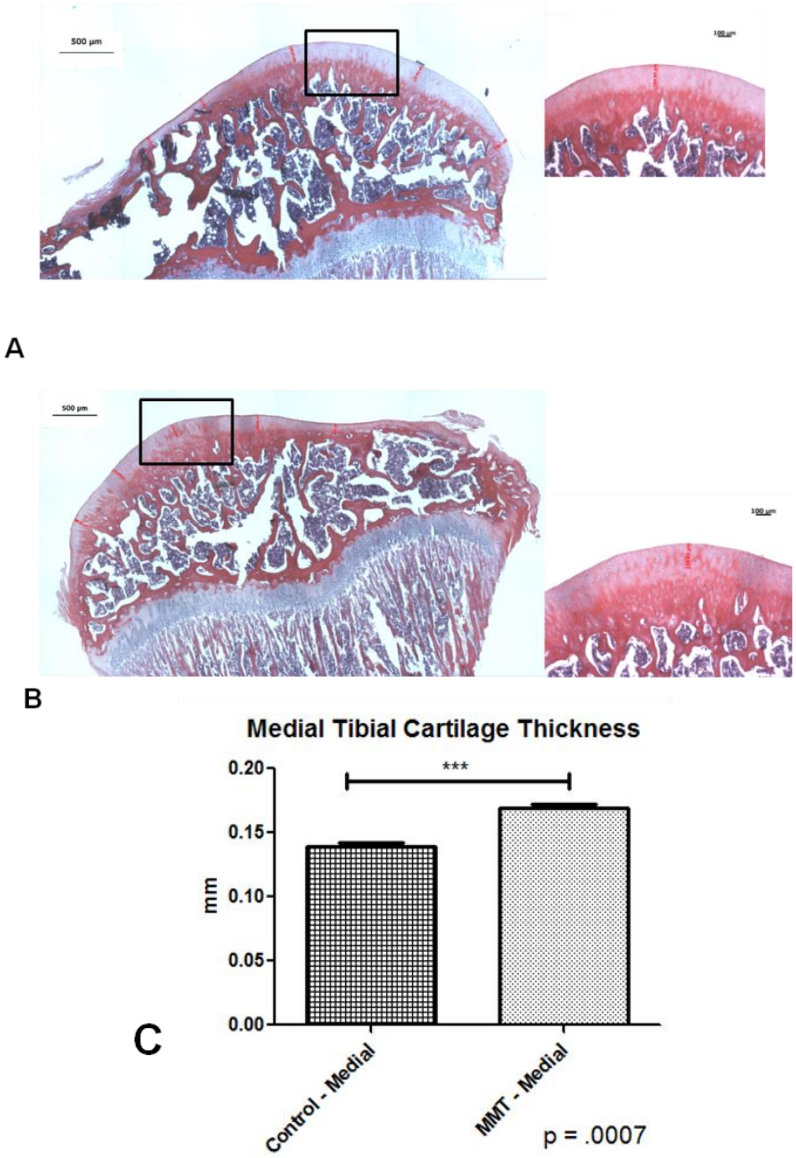

Figure 6. Histology thickness measurements for medial tibial plateau. A-B: H&E stained sagittal sections of medial tibial plateau from contralateral control knee (A) and MMT knee (B). Insets show zoomed in region at 4x indicated by black box C: Histomorphometry measurements showing a significant increase in medial tibial cartilage thickness in MMT knees compared to contralateral control. Red lines on Fig A& B indicate thickness measurements. 5 measurements were taken per slice and each sample had 3 sagittal slices. Individual measurements from each slice were averaged and then measurements for all 3 slices were averaged together to calculate medial tibial cartilage thickness (n = 4, *** = $p < .001$)

Using the EPIC-μCT technique, the overall tibial cartilage was quantitatively evaluated for thickness, volume, and attenuation for the medial and lateral plateaus combined. The MMT joints did not show any difference in thickness (Fig 7).Average volume was significantly higher in the MMT tibiae (26.6%) compared to the contralateral controls (Fig 7). No significant difference in cartilage attenuation was observed when analyzing the overall tibial cartilage (Fig 7).

The MMT medial tibial cartilage had significantly higher thickness and volume by 31% and 70% compared to contralateral controls (Fig 7). In the analyses of cartilage in the full tibial plateau, cartilage attenuation was 25% higher in the MMT medial tibiae than contralateral controls (Fig 7). Though no change in average attenuation was observed for cartilage in the full tibial plateau, isolating the medial plateau resulted in detection of a significant difference in articular cartilage attenuation for MMT tibiae compared to controls.

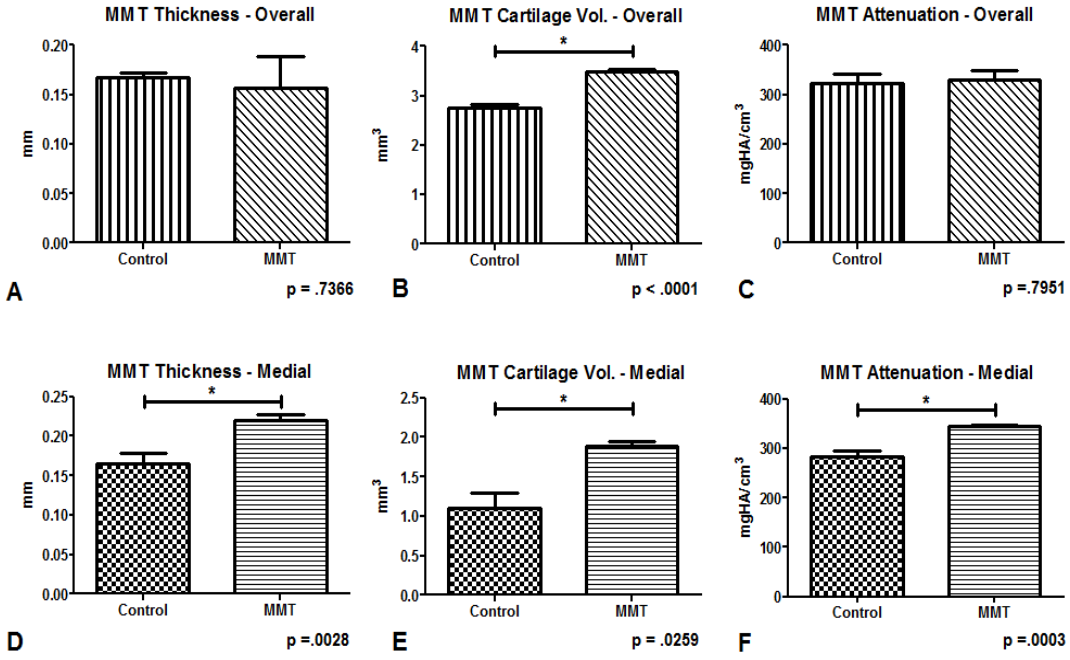

Figure 7. Tibial articular cartilage variables quantified for MMT and contralateral control knees (paired comparisons). A-C: Overall tibial articular cartilage variables - Cartilage thickness (A); cartilage volume (B); cartilage attenuation (C). D-F: Medial tibial articular cartilage variables - Cartilage attenuation (D); cartilage thickness (E); cartilage volume (F). At 3 weeks post-surgery, overall and medial cartilage volume from MMT joints was significantly higher than contralateral control cartilage. Medial tibial cartilage thickness and attenuation from MMT joints were significantly higher than contralateral controls. * = $p < .05$, n=7

<u>MMT Medial 1/3 of medial tibial articular cartilage analysis</u>

Following analysis of the medial tibial plateau, further localized analysis was performed for the medial 1/3 of the medial tibial plateau. Evaluating this region, similar results were observed as with the whole medial plateau. Average cartilage thickness and volume in the MMT tibiae were 50% and 90% higher, respectively, compared to contralateral controls; average cartilage attenuation was 35% higher compared to controls (Fig 8).

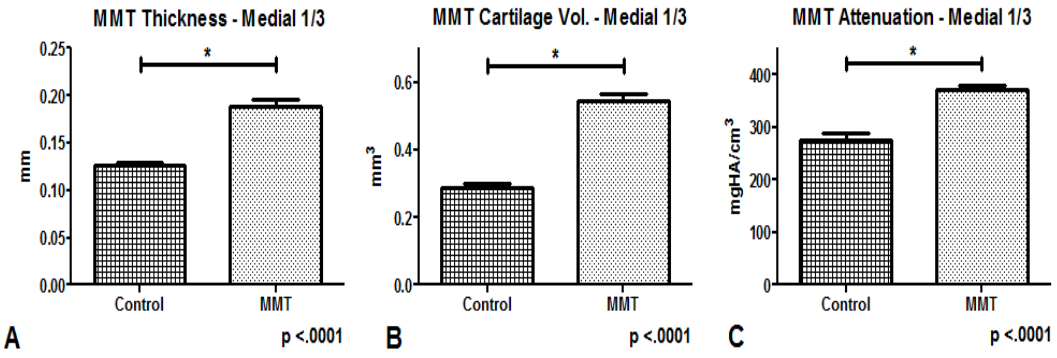

Figure 8. Medial 1/3 tibial articular cartilage variables quantified for MMT and contralateral control knees (paired comparisons). A: Cartilage thickness; B: cartilage volume; C: cartilage attenuation. Cartilage thickness and volume from MMT surgery tibiae were significantly higher than contralateral control cartilage. Average cartilage attenuation in MMT surgery tibiae was significantly higher than the respective contralateral control tibiae. * = p <.05, n=7

The grayscale 2D images from the medial plateau of the MMT animals were viewed slice by slice to locate, visualize, and quantify focal defects. Pseudo-color attenuation maps were generated based on these images. Sagittal sections from the attenuation maps showed higher attenuation on the MMT tibiae near the lesion sites (Fig 9). In addition to differences in attenuation, surface defects on the cartilage were also observed. Two MMT samples had three lesions and six MMT samples had one lesion each on the medial tibial articular cartilage. Six MMT samples had one erosion and one MMT sample had two erosions on the medial tibial articular cartilage. The average number of lesions was 1.57 ± .37 and average number of erosions was 1.14 ± .14 for the MMT tibiae, and no defects were observed on the controls. The average lesion volume was 0.00393 ± .003 mm3 for MMT tibiae, and no lesions were found on any of the contralateral controls (Fig 9).

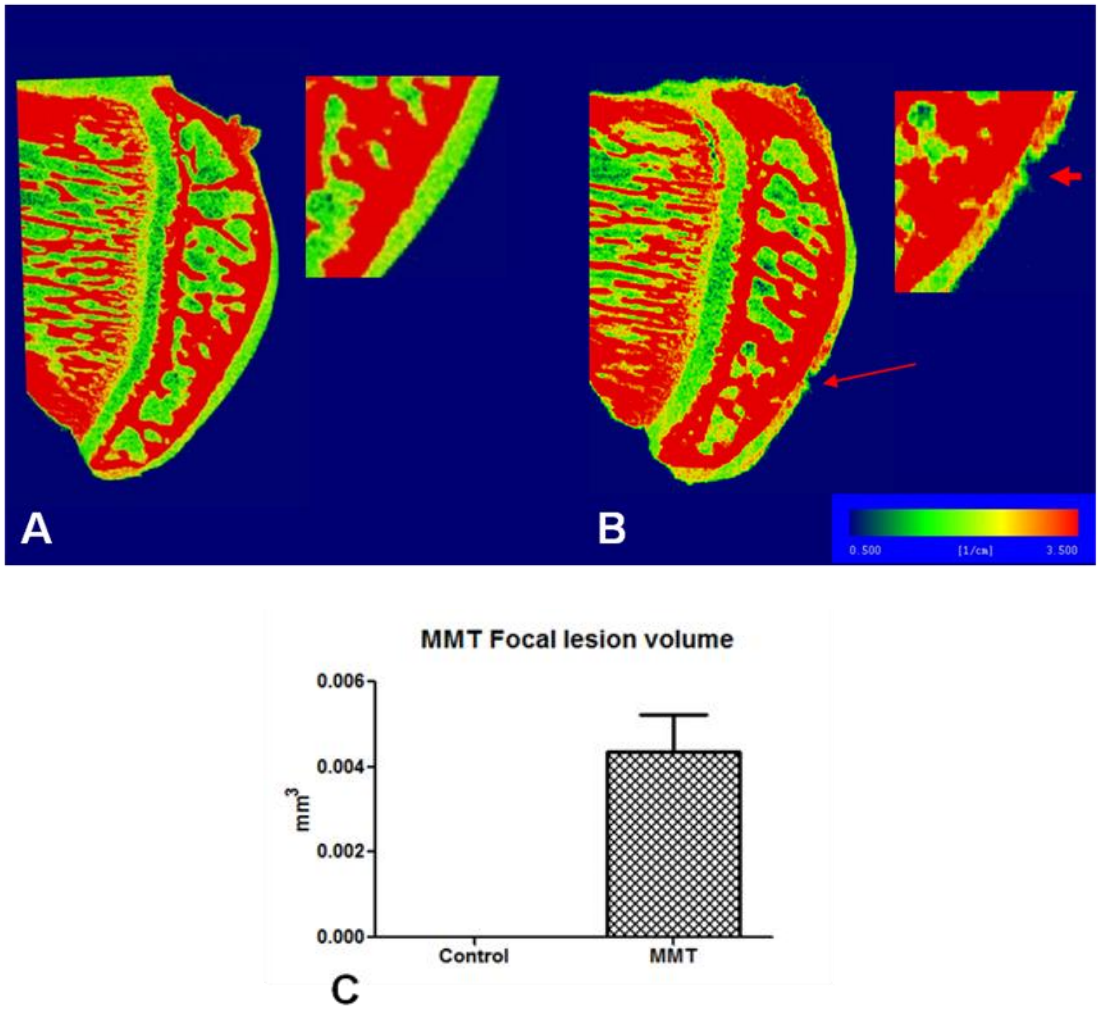

Figure 9. Representative sagittal attenuation maps of medial tibial plateau for control (A) and MMT (B) (Inset shows zoomed in view). Red displays higher attenuation levels and green indicates lower attenuation. Red arrow indicates lesion site in MMT. Higher levels of attenuation were seen surrounding the lesion site for MMT tibiae. C: Focal lesion volume quantification for MMT tibiae.

The average focal lesion volume was only 7.2% of the average medial 1/3 medial cartilage volume and 2.1% of the average medial plateau cartilage volume. The average focal lesion volume accounted for only .13% of the full cartilage volume when medial and lateral plateaus were combined. Because lesion volumes represented such a small region in proportion to the full cartilage volume, localized assessment clearly enhanced detection of morphometric differences between MMT and controls.

Discussion

The study of animal models of joint degeneration is essential for evaluating potential therapeutics and understanding the pathogenesis of cartilage loss. Studying the progression of OA in humans is challenging because of poor evaluative tools and limited access to diseased tissue during early development and through disease progression. Suitable animal models for research are consistent, reproducible, have an appropriate time frame of progression for high-throughput screening and recapitulate human pathology (Little and Smith 2008). Cartilage degeneration has been previously demonstrated in the two most widely used methods of joint degeneration in small animals—the MMT model (Bendele 2001, Janusz, Bendele et al. 2002, Moore, Bendele et al. 2005, Wancket, Baragi et al. 2005, Bove, Laemont et al. 2006) and the MIA model (Kalbhen 1987, Guingamp, Gegout-Pottie et al. 1997, Fernihough, Gentry et al. 2004, Wancket, Baragi et al. 2005). Histopathology was the primary analytical method for these previous studies. EPIC-μCT allows for efficient, non-destructive 3D imaging and localized analysis, providing quantitative methods to assess cartilage thickness, attenuation and volume among other variables. For this study, the MIA and MMT models were quantitatively characterized via EPIC-μCT to measure localized variables of attenuation, thickness and volume.

The results from the current low dose MIA study indicated an overall thinning of the cartilage layer. These are consistent with a previous dose response study for MIA which showed that 0.3mg was the lowest dose that caused articular cartilage damage covering the entire articular surface (Guingamp, Gegout-Pottie et al. 1997). In another study, Safranin-O staining indicated hypertrophied and disorganized chondrocytes as well

as degeneration of the cartilage surface at 3 weeks at the 0.3mg dose and more extensive damage at a 3mg dose (Kobayashi, Imaizumi et al. 2003). It is to be noted that these previous studies did not assess global and regional degeneration of the cartilage nor did they use quantitative techniques. In the current study, attenuation was significantly increased in the MIA joints, which was indicative of decreased PG content. Similarly, the Safranin-O staining showed severely depleted sGAGs. In regional analyses and the overall tibial plateau, the low-dose MIA model showed reduced cartilage thickness, volume as well as increased attenuation.

The MIA model remains the current standard to assess pain therapeutics asit is easy to use and is reproducible. Hence, some studies have tested DMOADs and NSAIDs in this model due to its widespread prevalence (Smith, Little et al. 1997, Bove, Calcaterra et al. 2003, Combe, Bramwell et al. 2004, Bar-Yehuda, Rath-Wolfson et al. 2009, Fitzpatrick, Green et al. 2011). Our results showed uniform thinning and PG loss even in this low dose MIA model. This is not a typical presentation of human OA and does not correspond with many of the OARSI recommended OA histopathology grading features(Gerwin, Bendele et al. 2010). The MIA model represents biochemically induced OA and disease progression is expedited in the low dose model. This can be an issue regarding the suitability of this model to test disease modifying therapeutics for knee OA. Additionally, transcriptional profiling of gene expression has shown little overlap with this model and human OA and the disease process induced by MIA causes rapid cartilage and subchondral bone damage (at < 3 weeks). This extensive damage suggests that the time-frame of disease progression is much faster in the MIA model than OA progression in humans (Guingamp, Gegout-Pottie et al. 1997, Combe, Bramwell et al. 2004, Barve,

Minnerly et al. 2007). Thus, the MIA model shows different genetic, compositional and morphological changes than normally observed in human OA. Despite this, the MIA model does have an advantage in detecting joint pain-related behaviors due to the rapid damage caused to the articular cartilage (Little and Smith 2008). It remains the more popular model for testing therapeutics targeted towards OA symptoms but has limited utility for testing DMOADs.

In the MMT model, overall and regional changes in cartilage parameters were detected. While changes were detectable at the overall level, most were in the medial 1/3 region. This observation that cartilage damage was most extensive in the outer 1/3 was similar to previous reports in the rat MMT model and attributed to the fact that this is the load bearing region that is destabilized (Bendele, McComb et al. 1999, Janusz, Bendele et al. 2002, Moore, Bendele et al. 2005). Though the medial 1/3 of the medial tibial plateau displayed cartilage thickening in the MMT model, focal lesions were also observed. A previous study supported the identification of localized lesions in the MMT model through immunostaining for type II collagen neoepitope antigen (TIINE) antibody (Wancket, Baragi et al. 2005). These lesions had not been previously quantified. Results from the present study showed that the lesion volume accounted for a small percentage (2.1%) of the medial plateau cartilage volume. The lesions compared to the full tibial articular cartilage layer occupied an even smaller fraction of the total volume, making cartilage changes challenging to detect when performing an overall cartilage analysis.

The increase in thickness for the medial plateau contradicts studies that have shown cartilage thickness to be reduced in MMT rats at 3 weeks (Janusz, Bendele et al. 2002, Moore, Bendele et al. 2005). To confirm this thickness increase that was measured

via EPIC-μCT, histomorphometric measurements were made and similarly showed a significant increase in cartilage thickness in the medial tibial plateau of the MMT animals compared to contralateral controls. Other studies have also reported thickening of OA cartilage in humans, beagles and rabbits (Muir H 1987, Arokoski, Jurvelin et al. 2000, Calvo, Palacios et al. 2001, Oeppen, Connolly et al. 2004, Cotofana, Buck et al. 2012). Another study in dogs, reported a transient episode of chondrocyte proliferation and increased matrix production within the lesion site and superficial zone of the adjacent articular cartilage in response to destabilization of joints (Pinals 1996).

In addition to thickening of cartilage, another factor contributing to the increase in thickness/volume could be cartilage-like structures called chondrophytes. Thickening of marginal zone cartilage and generation of chondrophytes and osteophytes has also been reported as a result of destabilization of the joint or injury in many animal models including the MMT model at 3 weeks (Pinals 1996, Bendele 2001, Bove, Laemont et al. 2006, Blaney Davidson, Vitters et al. 2007, Wei, Kulkarni et al. 2010). A previous study hypothesized that the observed peripheral thickening could be an adaptive or compensatory mechanism to increase articular cartilage surface though no data was presented on PG content (Arokoski, Jurvelin et al. 2000). The cartilage volume from the MMT tibiae in the medial 1/3 region increased by 90% compared to the control tibiae. Formation of these chondrophyte/osteophyte structures could augment measured cartilage volume and thickness because diffusion of contrast agent into the chondrophyte would be expected to be similar to that of articular cartilage. Even though we observed higher volume and thickness, the average attenuation remained higher for the MMT tibiae indicating lower cartilage quality and depleted PG content.

OA is a multifactorial disease and there are several contributing factors to disease progression. Focal lesions on the articular cartilage have been observed in humans with early stage OA, and are considered to be among factors involved in OA progression (Clouet, Vinatier et al. 2009). The MMT model displayed focal lesions when regional analysis was performed using EPIC-μCT. While histology can identify lesions, the 2D nature of the technique means that lesion incidence and overall volumes cannot be quantified. EPIC-μCT allowed for both slice-by-slice visualization and volumetric quantification of these lesions. Our ability to further discern the sensitivity of the EPIC-μCT technique to measure more subtle PG changes was limited by the fact that sham surgery was not performed. Contralateral control limbs were used as negative controls as sham surgeries do not develop lesions (Allen, Mata et al. 2012), and this additionally allowed us to minimize animal numbers. The MMT model displayed several characteristics similar to OA characteristics in humans such as peripheral thickening, loss of PGs, erosion of cartilage and localized lesions.

Though the objectives of this study were not to directly compare MIA and MMT models, some interesting overall observations exist. The data show widespread cartilage degeneration in the low dose MIA model and localized degradation in the MMT model. The MIA model appears to cause greater damage in full tibial plateau cartilage compared to controls; whereas, this difference at the full tibial plateau level was not detected in the MMT model at 3 weeks. It should be noted that two different strains of rats were used in this study. Based on previous studies, the standard rat strain for the MIA model is Wistar and for the MMT model is Lewis (Gerwin, Bendele et al. 2010). Direct comparison of absolute quantitative values are not appropriate and thus, not performed. Although there

may be variations in the response of different strains to the two methods used to induce joint degeneration, this limitation does not alter the conclusions of the study. Another limitation of our analysis was that all measurements were performed in the sagittal plane as established previously in the EPIC-μCT protocol, and this limited our ability to perform comparisons to the OARSI histomorphometric standards(Grogan, Miyaki et al. 2009).

CHAPTER 4

SENSITIVITY OF EPIC-μCT ANALYSIS TO QUANTIFY EFFECTS OF BROAD SPECTRUM MMP INHIBITOR IN RAT MEDIAL MENISCAL TEAR MODEL

Abstract

Cartilage degeneration is the signature pathology feature of degenerative joint diseases, which are the most common cause of pain and disability in the United States. The development of effective therapies for cartilage protection has been limited by a lack of efficient quantitative cartilage imaging modalities in preclinical in vivo models. EPIC-μCT can quantitatively analyze articular cartilage and has been used to characterize the rat MMT model. The application of this technique to test therapeutic efficacy of a disease modifying OA drug (DMOAD) has not yet been tested. Also, the technique while used to characterize the MMT model has not been validated via a direct comparison to histology. The objective of this study was two-fold: first, to validate EPIC-μCT in the rat MMT model; and second, to quantitatively assess the sensitivity of EPIC-μCT to detect the effects of matrix metalloproteinase inhibitor (MMPi) therapy on cartilage degeneration. EPIC-μCT was shown to provide simultaneous 3D quantification of multiple parameters of joint health, including cartilage degeneration and osteophyte formation. In MMT animals treated with MMPi, OA progression was diminished, as measured by 3D parameters such as lesion volume and osteophyte size. A post-hoc power analysis showed that EPIC-μCT was significantly more sensitive than histopathology requiring approximately 50% fewer animals to detect a therapeutic effect of MMPi. This is the first

study to demonstrate that EPIC-μCT has higher sensitivity than composite histopathology scoring and that 3D imaging provides more information to distinguish the specific effects of a therapy on cartilage. EPIC-μCT is a powerful tool that will provide robust, reproducible and quick methodology to identify new cartilage protective drugs in the pre-clinical development stage.

Introduction

OA is characterized by the progressive loss of normal structure and function of articular cartilage(Loeser, Goldring et al. 2012). OA affects the entire joint including the subchondral bone, the synovium andperiarticular tissues (Loeser, Goldring et al. 2012). People with OA and cartilage injury can experience severe pain and limited motion. Currently there are no FDA approved drugs that can modify cartilage degeneration, resulting in the need for improved therapeutics.

Development of new therapeutics requires multiple steps starting with *in vitro* screening, small animal testing, large animal testing and eventually clinical trials. Substantial progress has been made in recent years to improve throughput, decrease costs, and provide better data with predictive indicators of the potential efficacy of a drug in humans. Much of this progress has been at the *in vitro* screening stage with techniques that include microarrays, microfluidics, and multiplex systems; however, the *in vivo* stages for screening of joint therapeutics remain slow, expensive, and with few quantitative outcomes.

In order to screen prospective therapeutics, the MMT model in the rat is becoming the accepted standard as the primary *in vivo* screening model. The model displays similarities with pathologies observed in human OA such as PG loss, erosion/lesion

formation, osteophytes and subchondral bone sclerosis (Gerwin, Bendele et al. 2010). A number of pharmaceutical companies have recently used this model to screen potential therapeutics including Pfizer, Lilly Research Corp, Wyeth and Abbott Laboratories (Bove, Laemont et al. 2006, Baragi, Becher et al. 2009, Flannery, Zollner et al. 2009, Mapp, Walsh et al. 2010, Wei, Kulkarni et al. 2010). Most of these studies use histological analysis with semi-quantitative pathological scoring for assessing therapeutic efficacy as it is the current gold standard. A major limitation of this technique couple with the rat MMT model is that it requires at least three weeks of treatment to demonstrate efficacy of potential therapeutics with a minimum of 20 animals per group (Gerwin, Bendele et al. 2010). The testing of drugs in an efficient and less expensive manner is limited by the high animal number requirement and long dosing period.

The development of 3D high resolution imaging techniques that provide quantitative structural and compositional analyses in addition to traditional histological assessment has become a milestone that has expedited the development of novel therapeutics in some fields. In the musculoskeletal field, this approach is true for μCT analysis of hard tissues, such as analyzing the efficacy of osteoporosis therapies for bone (Borah, Dufresne et al. 2004, Kleerekoper 2006, O'Neal, Diab et al. 2010, Kawai, Modder et al. 2011). The ability to quantify 3D changes in bone microarchitecture provided substantial new insight into the mechanism of disease progression and accelerated the development of effective therapies for osteoporosis which are now clinically available (Borah, Dufresne et al. 2004, Kleerekoper 2006, O'Neal, Diab et al. 2010, Kawai, Modder et al. 2011). Similar 3D analysis of soft tissues has been limited; however, in recent years, there has been progress using contrast enhanced imaging

techniques for soft tissues. These are often based on equilibration of an ionic contrast agent into the soft tissue and then correlating the attenuation of the contrast agent to structural and biological parameters. As described earlier, EPIC-μCT allows for quantitative imaging of cartilage (Palmer, Guldberg et al. 2006). Using this technique we have shown that we can measure structural and compositional parameters of cartilage including PG loss, incidence of lesions and erosions, and volume of lesions; our next objective was to use this technique to evaluate the efficacy of a disease modifying therapy in a preclinical model of OA (Thote, Lin et al. 2013).

The aim of this study were two-fold: first, to perform a direct comparison of EPIC-μCT analysis to histopathological scoring looking at the development of OA in the rat MMT model; and then, to use EPIC-μCT to quantitatively assess the efficacy of a therapy for OA, in this case an MMPi, and similarly perform a direct comparison to the gold standard of histopathology. Our hypothesis was that EPIC-μCT would provide a more sensitive analytical method than histopathology requiring fewer samples and allowing for the quantitative analysis of more parameters.

Materials and Methods

Induction of Joint Degeneration

All animal studies were conducted at Abbvie Laboratories in accordance with Institutional Animal Care and Use Committee (IACUC) guidelines and the National Institutes of Health Guide for Care and Use of Laboratory Animals. Abbvie Laboratories facilities are accredited by the Association for the Assessment and Accreditation of Laboratory Animal Care (AAALAC).

Weight matched Lewis rats (300-325g) were subjected to MMT surgery based on previously established studies (Janusz, Bendele et al. 2002, Moore, Bendele et al. 2005, Xie, Lin et al. 2012). Two separate studies were performed. In the first study animals were separated into two groups: sham surgery or MMT surgery. The sham surgery was performed by exposing the joint and transecting the medial collateral ligament. In MMT animals the exposed meniscus was then transected at its narrowest point. The joint and skin were then closed with sutures. Animals were euthanized at 7, 14, or 21 days (at each of the time points, n=5-6 for MMT and n=3 for sham animals). In the second study animals were separated into three groups: Sham surgery (n=15), MMT +MMPi (n = 19) and MMT+vehicle (n=21). The MMPi used in this study (biaryl ether retro-hydroxamate) is a broad-spectrum, matrix metalloproteinase (MMP) inhibitor (Upadhyay, Baker et al. 2013). Rats were administered the MMPi drug (30mg/kg) orally 2x/day for 21 days post-surgery.

Histopathology Scoring

The scoring of the joints was done using parameters from the scoring scheme described by Gerwin et al. (Gerwin, Bendele et al. 2010). Sections were analyzed microscopically and scored by a trained pathologist. For each knee, three sections were scored and then the average of the scores was used. Parameters that were scored include: cartilage degeneration for each zone (3 zones), a 3 zone sum of cartilage degeneration, subchondral bone, and osteophytes. Osteophyte width, width of the marginal zone, and cartilage degeneration width (performed in the MMPi study only) were measured separately by ocular micrometers. Detailed descriptions of the different scoring parameters were previously published (Gerwin, Bendele et al. 2010).

μCT regional analysis

The MMT surgery involved an injury to the medial side of the knee joint through transection of the medial meniscus. As a result, the medial plateau of the tibia was more susceptible to injury. To observe localized effects of joint degeneration, we evaluated the medial tibial plateau in all groups. (Gerwin, Bendele et al. 2010).

Scanco evaluation software was used to assess 3D morphology and composition. Raw data were automatically reconstructed to 2D grayscale tomograms. These were rotated to sagittal sections, and the cartilage was contoured to separate it from trabecular bone and surrounding air (Palmer, Guldberg et al. 2006, Xie, Lin et al. 2012). The cartilage was segmented using a threshold value of 175-225 and then 3D images were generated. Four regional analyses were performed using different volumes of interest (VOI). For the MMT model, images were evaluated for: (1) Medial plateau only (2) Medial 1/3 of the medial tibial plateau (3) Focal lesions on the medial plateau only (Fig 10). Two outcome measures were defined for evaluation of focal defects: erosion (defect extended to less than 50% of cartilage thickness) and lesion (defect extended to more than 50% of cartilage thickness) (Pritzker and Aigner 2010). To define VOIs of focal lesions, manual contouring was performed in the isolated lesion area (typically ≈ 8 slices) to simulate the curvature of the surrounding cartilage surface excluding the subchondral bone and surrounding air. Within this VOI, segmented cartilage volume was subtracted from the total volume evaluated to compute lesion volume.

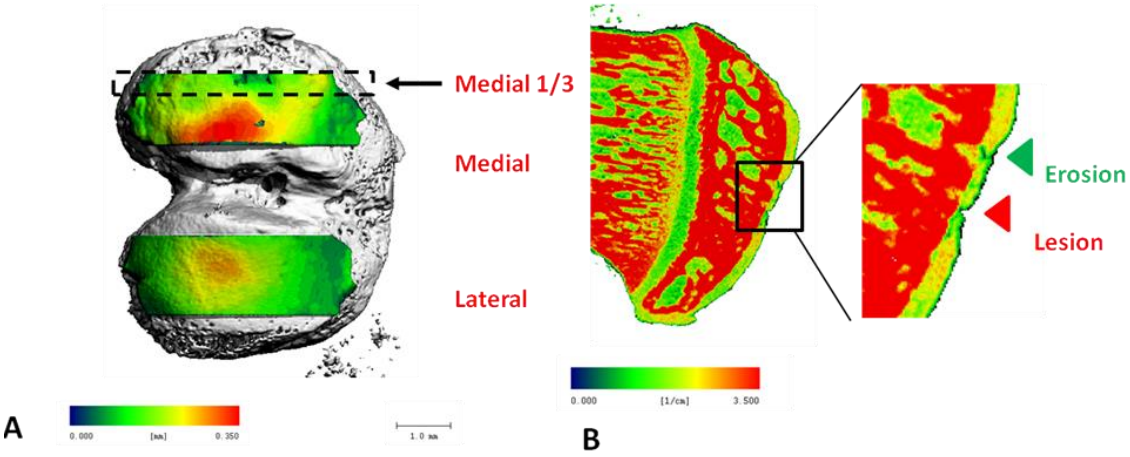

Figure 10. Representative CT images indicating articular cartilage volume of interest and cartilage degeneration. A: Rat tibial articular cartilage overlay on bone indicating volumes of interest. B: Representative image illustrating erosions (cartilage defect < 50% of thickness) and lesion (cartilage defect > 50% of thickness)

Analysis of the osteophytes was performed after the 2D grayscale tomograms were rotated to coronal sections (Fig 11). The medial marginal area was contoured for osteophyte growth. The marginal osteophyte was segmented using two different threshold values: 1) 130-1000 to include both mineralized matrix and cartilage, 2) 265-1000 to include only the mineralized matrix. Outcome measures defined for marginal osteophytes included total osteophyte volume, total osteophyte thickness, mineralized osteophyte volume and cartilaginous osteophyte volume.

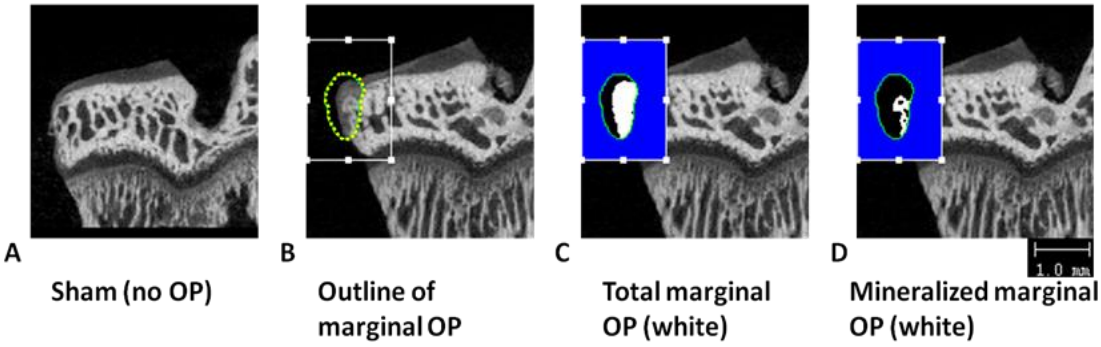

Figure 11. Representative images illustrating osteophytes in coronal tibial section No osteophyte (OP) in sham joint (A), outline of osteophyte in MMT joint (B), total osteophyte (indicated in white) in MMT joint (C) and mineralized matrix (indicated in white) in MMT joint (D)

Statistical analysis

All data were expressed as mean ± standard error. Cartilage morphology parameters were evaluated using ANOVA with a Tukey test to compare between selected groups using GraphPad Prism Software (GraphPad Prism Software Inc. 5.01, La Jolla, CA). Statistical significance was set at a 95% confidence interval ($p < 0.05$).

Power analysis was performed by selecting a desired power of 0.8. Effect size was calculated for unequal sample sizes based on t-test data between the MMPi treated and vehicle treated group. These data were used to calculate the total sample size using G*Power (G*Power Version 3.1.3, Universitat Kiel, Germany).

Results

MMT Time-point Study

The rat MMT model was analyzed using both EPIC-μCT and histopathology. These results were directly compared for the same set of samples. Representative coronal sections from histology and EPIC-μCT display qualitatively similar results in disease progression over three weeks (Fig 12). Osteophytes, erosions and PG loss can be observed in the comparable EPIC-μCT and histology sections.

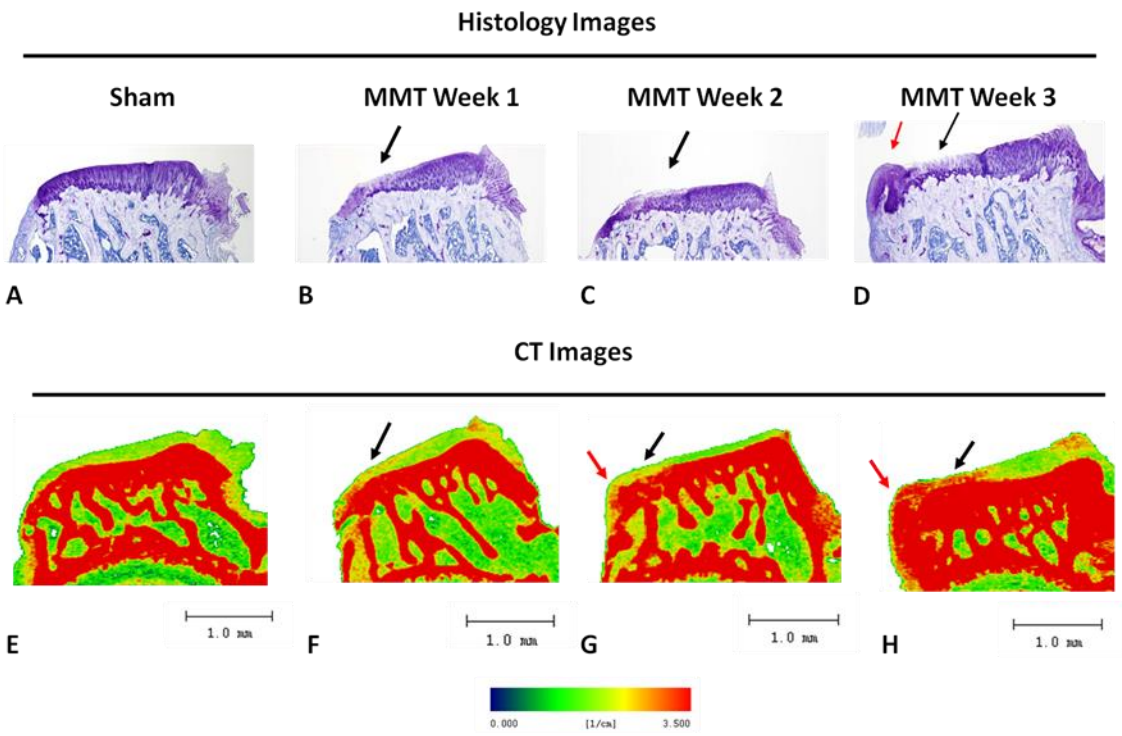

Figure 12.Representative histology and EPIC-µCT images depicting OA progression over 3 weeks. A – D: Toluidine blue stained MMT joints showing no damage in sham (A), cartilage surface erosion at week 1 in MMT joint (B), increased cartilage surface erosion at week 2 in MMT joint (C) and development of osteophyte (red arrow) and severe cartilage erosion at week 3 in MMT joint (D). E-H: Corresponding EPIC-µCT images for the samples as sectioned via histology indicating progression of cartilage degradation. No damage observed in sham (E) or week 1 MMT joint (B). Increased areas of attenuation observed in MMT joints at week 2 (G) and 3 (H) as indicated by black arrow. Red arrow indicates area of mineralization within marginal osteophyte at week 2 and week 3 in MMT joints. Red indicates higher attenuation corresponding to lower proteoglycan content.

Histology sections were scored by a histopathologist based on the scheme described by Gerwin et al (Table 2). The results include tibial 3-zone sum score, total cartilage degeneration score, the osteophyte width, and the total joint score (Gerwin, Bendele et al. 2010).

Table 2. Histology data for joint parameters for sham and MMT animals at weeks 1, 2 & 3. Data presented are with SD.

	Sham - All time points (n = 3 at each time point)	MMT @ Week 1 (n = 6)	MMT @ Week 2 (n = 6)	MMT @ Week 3 (n = 6)
Cart Deg MFC (0-15)	0	0	0	0.67 ± 1
Cart Deg MTP z1 (0-5)	0	3.5 ± 1	4.67 ± 0.52	4.5 ± 1
Cart Deg MTP z2 (0-5)	0	3.17 ± 1	4 ± 0.63	4.17 ± 1
Cart Deg MTP z3 (0-5)	0	0	0	0
3 Zone Sum	0	6.67 ± 2	8.67 ± 0.52	8.67 ± 1
Total Cart Deg Score	0	6.67 ± 2	8.67 ± 0.52	9.33 ± 1
Osteophyte Score (0-4)	0	1 ± 1	2.67 ± 1.51	4 ± 0
Osteophyte Width (μm)	0	175 ± 192	370.83 ± 190.67	741.67 ± 130
Subchondral Bone Score MTP (0-5)	0	.17 ± 0	1.33 ± 0.82	1.67 ± 1
Total Joint Score	0	7.67 ± 3	11.33± 1.75	13.33 ± 1

Progression of the MMT model from week 1 to week 3 was analyzed. At week 1, the 3 zone sum score was significantly higher in the MMT animals compared to sham. This increase was consistent up to week 3 though no significant difference between these values at week 1 and week 3 were observed (Fig 13). EPIC-μCT data showed a significant increase in cartilage attenuation at week 2 in MMT animals, but no difference was observed at week 1. Lesion volume significantly increased between 2 and 3 weeks post-surgery in MMT treated animals (Fig 13).

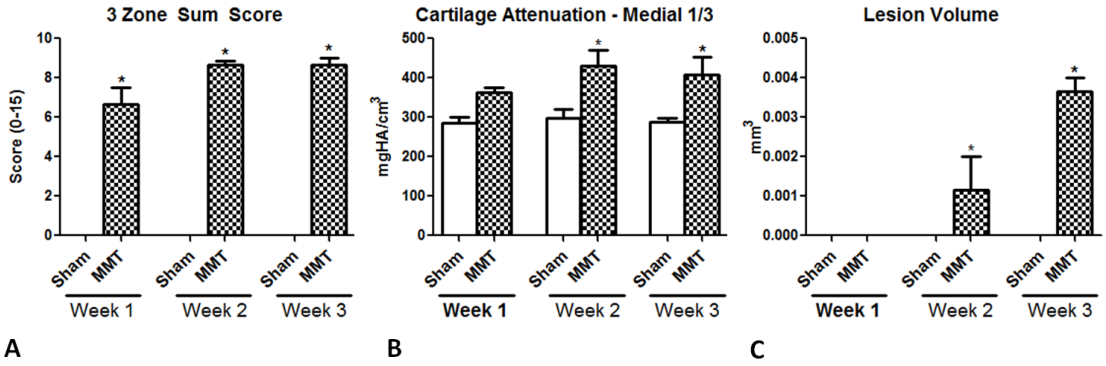

Figure 13. Quantification of cartilage degeneration in MMT joints over 3 weeks. A. Histo-pathological 3 zone sum score is significantly increased in MMT joints at weeks 1, 2 and 3 compared to shams B. Cartilage attenuation is significantly increased in MMT joints at weeks 2 & 3 compared to shams. C. Cartilage lesion volume is significantly increased in MMT joints at week 3 compared to shams, and MMT joints at week 1 & 2. n = 5-6/group for CT data; n= 3 for sham and n = 5-6 for MMT for histology data.

Additional parameters, including cartilage thickness, volume and lesion and erosion incidence, were measured by EPIC-μCT. Lesion incidence was significant at week 3 and erosions were significant as early as week 2 (Table 3).

Table 3. Average incidence of lesions and erosions in sham and MMT groups

		Lesion	Erosion
Week 1	Sham	0	0
	MMT	0	0.167 ± 0.408
Week 2	Sham	0	0
	MMT	0.4 ± 0.548	0.6 ± 0.548*
Week 3	Sham	0	0
	MMT	2 ± 0.894$^{\$,\%}$	2 ± 0.894$^{\#}$

*= $p < 0.05$, erosions at MMT week 2 significantly different from MMT week 3
= $p < 0.05$, erosions at MMT week 3 significantly different from sham week 3
$ = $p < 0.05$, lesions at MMT week 1 significantly different from MMT week 3
% = $p < 0.05$, lesions at MMT week 3 significantly different from sham week 3

Osteophytes were observed in the MMT animals on the medial tibial plateau via both EPIC-µCT and histopathology. The marginal tissue thickness was significantly higher in the MMT animals compared to sham animals at week 2 (above the 200 µm cut off for classification of an osteophyte, Fig. 14). Similarly, EPIC-µCT measurements showed a significantly higher 3D average marginal thickness in MMT animals compared to shams at week 2. EPIC-µCT also allowed for measurements of additional osteophyte parameters - total volume and mineral volume. Marginal total volume and mineral volume were all increased in MMT animals by 2 weeks post-surgery (Fig 14).

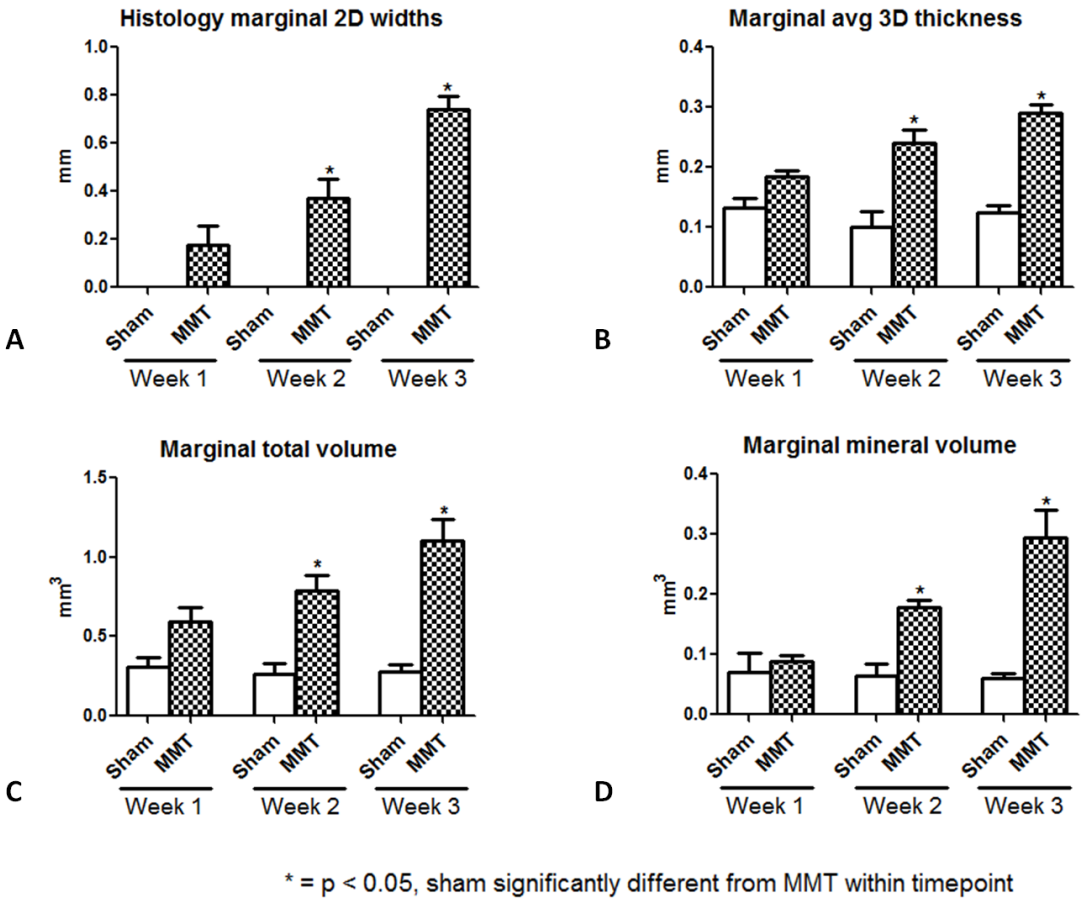

Figure 14. Osteophyte progression in MMT animals over 3 weeks. A. Osteophyte widths as calculated via histo-pathology scoring show an increase in MMT joints compared to shams at week 2 and week 3. B-D: Marginal average 3D thickness (B), marginal total volume (C) and marginal mineral volume (D) as calculated via EPIC-μCT show an increase in MMT joints compared to shams at week 2 and 3. n = 5-6/group for CT data; n= 3 for sham and n = 5-6 for MMT for histology data.

* = $p < 0.05$, sham significantly different from MMT at week 2; $ = $p < 0.05$, sham significantly different from MMT at week 3

A correlation analysis (Fig 15) was performed comparing EPIC-µCT 3D thickness and 2D histopathology tissue widths and a significant correlation was observed between measurements from the two techniques (r^2=0.8268, $p<0.05$).

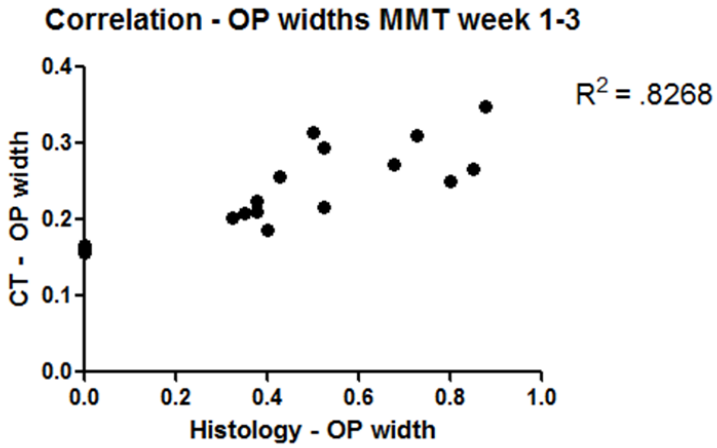

Figure 15. Correlation analysis between CT OP width and histology OP width

MMPi Study

EPIC-µCT and histopathology analyses were performed on the sham, vehicle treated, and MMPi treated samples at 3 weeks post-surgery. Representative coronal sections from histology and EPIC-µCT coronal sections are presented from each group (Fig. 16). Similar degeneration, lesion formation and osteophyte appearance are observed between the EPIC-µCT and histology images.

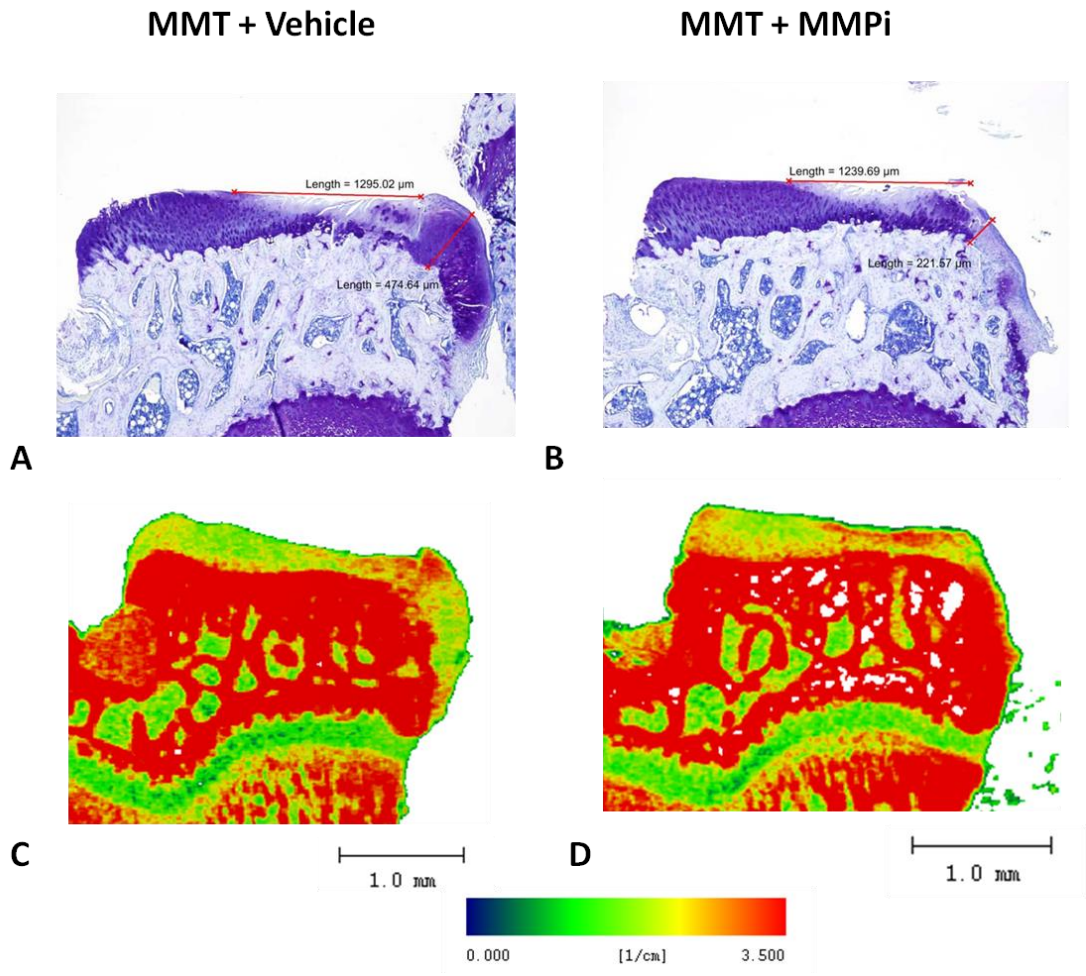

Figure 16. Representative histology and EPIC-µCT images depicting effect of MMPi on MMT joints. A – B: Toluidine blue stained MMT joints showing reduced osteophyte formation in MMPi treated joint (B) compared to vehicle treated joint (A). C-D: Corresponding EPIC-µCT images for the samples as sectioned via histology indicating reduced osteophyte formation in MMPi treated joint (D) compared to vehicle treated joint (C). Red indicates higher attenuation corresponding to lower proteoglycan content

A significant decrease in the tibial 3 zone sum score, the osteophyte width, and the subchondral bone score was observed via histopathology scoring. Other parameters—total cartilage degeneration, cartilage matrix loss at 0% depth, and total joint score—did not show a significant effect of MMPi treatment (Table 4)

Table 4. Histopathology data from MMPi study

	Sham (n=6)	Vehicle (n=19)	MMPi (n=21)
Cart Deg MFC (0-15)	1.6 ± 0.8	2.8 ± 1.7	4.6 ± 2.0
Cart Deg MTP z1 (0-5)	0.2 ± 0.4	4.2 ± 0.9	4.1 ± 0.8
Cart Deg MTP z2 (0-5)	0	3.3 ± 0.7	2.9 ± 0.7
Cart Deg MTP z3 (0-5)	0.4 ± 0.5	0.7 ± 0.6	0.1 ± 0.3
3 Zone Sum	0.6 ± 0.5	8.1 ± 1.4	7.1 ± 1.3
Total Cart Deg Score	2.1 ± 1.0	10.8 ± 2.3	11.7 ± 2.6
Cart Matrix Loss Width 0% Depth	0	914.9 ± 255.4	957.4 ± 221.7
Cart Matrix Loss Width 100% Depth	0	52.1 ± 114.9	21.0 ± 68.2
Cart Matrix Loss Width 50% Depth	0	108.4 ± 187.7	25.8 ± 77.8
Total Tibial Cart Degen Width (µm)	0	1364.4 ± 306	1210 ± 243.4
Significant Tibial Cart Degen Width (µm)	0	648.4 ± 274.2	640.7 ± 269.3
Osteophyte Score (0-4)	0	3.3 ± 1.1	2.2 ± 0.8
Osteophyte Width (µm)	0	496.4 ± 116.7	379.7 ± 74.5
Subchondral Bone Score MTP (0-5)	0	2.2 ± 0.9	1.7 ± 0.6
Total Joint Score	2.1 ± 1	16.2 ± 3.2	15.6 ± 3.0

Cartilage attenuation as calculated via EPIC-µCT, increased at 3 weeks in the MMT+vehicle and MMT+MMPi animals compared to the sham controls (Fig. 17), though no difference was observed between the two MMT groups.

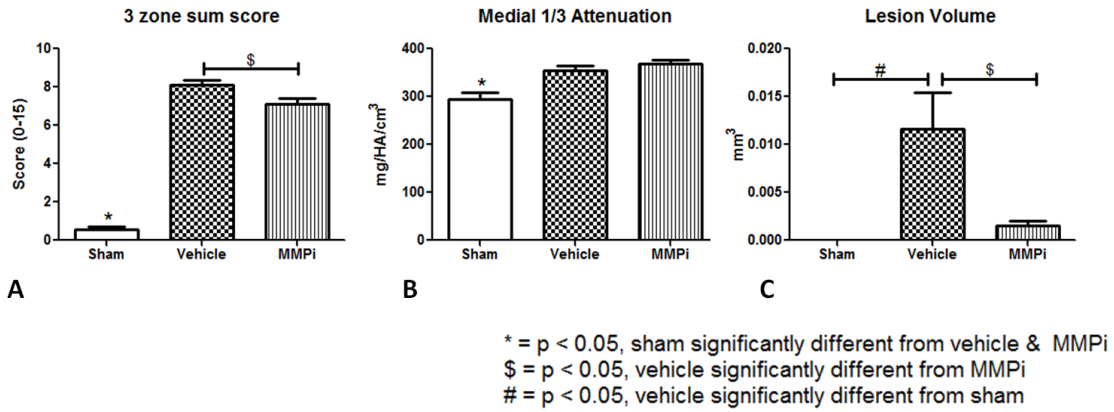

Figure 17. Tibial articular cartilage variables quantified for MMT joints treated with MMPi A. MMPi treatment significantly reduces 3 zone sum score compared to vehicle treated group B. Cartilage attenuation is significantly lower in sham group compared to both vehicle treated and MMPi treated groups C. Lesion volume is significantly reduced in MMPi treated group compared to vehicle treated group. n = 15-21/group
* = p < 0.05, sham significantly different from vehicle &MMPi; $ = p < 0.05, vehicle significantly different from MMPi; # = p < 0.05, vehicle significantly different from sham

EPIC-μCT was also used to measure lesion and erosion incidence, lesion volume, and subchondral bone volume (Table 5). Occurrence of lesions and erosions were not affected by MMPi treatment. However, lesion volume was significantly reduced in the MMT+MMPi group compared to the MMT+vehicle group. The shams showed no lesions on the cartilage.

Table 5. Incidence of Lesions & Erosions in MMPi Study

Incidence of Lesions		
Sham	**Vehicle**	**MMPi**
0*	0.948 ± 0.23	1.048 ± .189
Incidence of Erosions		
Sham	**Vehicle**	**MMPi**
.2 ± .107*	2.474 ± 0.221	2.429 ± 1.028

* = p < 0.05 , sham significantly different from Vehicle & MMPi, n = 15-21/group

Subchondral bone volume was also significantly lower in the MMT+MMPi group compared to the MMT+vehicle group (Fig 18).

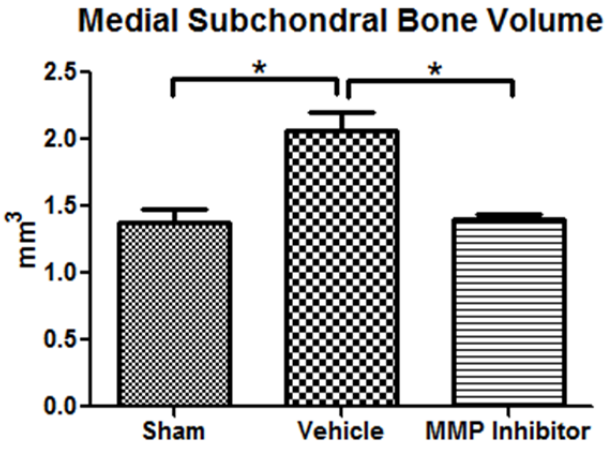

Figure 18. Effect of MMPi on subchondral bone volume. MMPi treatment reduces subchondral bone volume compared to vehicle treated joints. * = $p < 0.05$

A significant decrease in 2D histology OP width was observed in MMPi treated animals compared to vehicle treated animals (Fig. 19). Sham animals did not have width measurements above the 0.2 mm cut off and were scored as zeroes as per the current standard. Quantitative EPIC-µCT similarly showed significantly reduced average 3D thickness, marginal total volume and marginal mineralized volume compared to the vehicle group (Fig. 19). Osteophytes were not detected in shams via histology or EPIC-µCT.

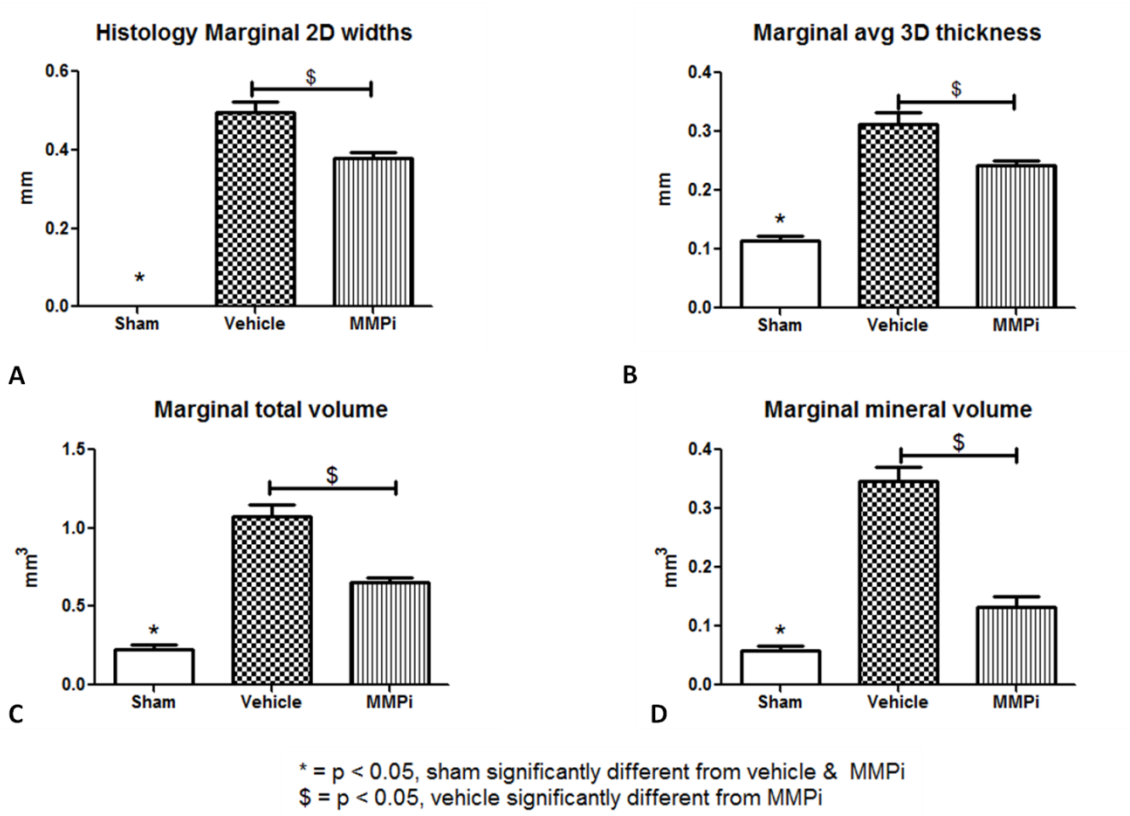

Figure 19. Effect of MMPi on osteophyte development in MMT joints. A: Osteophyte widths as calculated via histo-pathology scoring are significantly lower in MMPi treated group compared to vehicle treated group B-D: Marginal average 3D thickness (B), marginal total volume (C) and marginal mineral volume (D) as calculated via EPIC-μCT are significantly lower in MMPi treated group compared to vehicle treated group. n = 15-21/group

* = p < 0.05, sham significantly different from vehicle &MMPi; $ = p < 0.05, vehicle significantly different from MMPi

Power analysis

A power analysis was performed to measure the minimum number of samples required to detect differences in cartilage degeneration and osteophyte development between the MMPi treated and untreated MMT groups (Table 6). Post-hoc power analysis based on total peripheral volume indicated that a minimum of 7 animals would be needed per group to detect a significant difference at a power > 0.8 and $\alpha = .05$; while histology would require a minimum of 13 samples per group for osteophyte width

(assuming experimental design would be equal between the groups). Other parameters were less sensitive and would require larger sample sizes.

Table 6. Post hoc power analysis

Variable	Power	# of samples needed
EPIC-uCT - Total OP Volume	.8	7
EPIC-uCT – OP width	.8	14 (MMPi) and 12 (Vehicle)
EPIC-uCT – Lesion Volume	.8	22 (MMPi) and 20 (Vehicle)
Histology – OP width	.8	13 (MMPi) and 11 (vehicle)
Histology – 3 zone sum score	.8	25 (MMPi) and 23 (vehicle)
Histology – Total tibial cartilage degeneration width	.8	29 (MMPi) and 27 (vehicle

Discussion

Development of new and improved therapeutics for OA has been limited by techniques which are high in cost and low in throughput. Previously, we have developed EPIC-μCT as an imaging technique that can analyze cartilage quantitatively, efficiently and without destroying the sample (Thote, Lin et al. 2013). In this study we compared quantitative 3D EPIC-μCT results to the gold standard of 2D histopathology in the rat MMT model. We also showed that EPIC-μCT has the sensitivity to evaluate the efficacy of DMOADs in the rat MMT model and is more sensitive than the current gold standard of histopathology.

In this study we showed that EPIC-μCT provides a fully quantitative analytical technique that is non-destructive, quantitative, and has highly sensitive parameters which can be evaluated over the entire region or can be focused on specific regions of interest. Histopathology scoring is semi-quantitative as it subjectively scores 2D sections. Sectioning, imaging and scoring samples is time consuming and the semi-quantitative nature of the technique results in requiring large sample sizes to detect significant differences. Using EPIC-μCT we were able to quantify cartilage attenuation, cartilage volume and thickness, occurrence of lesions and erosions, volume of lesions, osteophyte formation, and subchondral bone thickening.

The 3 zone sum score measurement from histopathology showed a large discrete step increase between shams and the week 1 time point which did not significantly alter over the 3 weeks. In the case of EPIC-μCT a more continuous increase in cartilage attenuation was observed indicating that this parameter is more sensitive to PG changes. The 3 zone sum score is based on the PG loss at a singular location whereas attenuation

data is an average measurement for the entire cartilage within the selected region of interest(Gerwin, Bendele et al. 2010). This data may suggest that the lesion volume measurement may be more similar to the 3 zone sum score than attenuation though lesions are not detected in this model via CT until week 2.

The results of the MMPi treatment showed that MMPi significantly decreased the 3 zone sum score and lesion volume whereas cartilage attenuation was not affected. Though similarities exist between histopathology and EPIC-μCT, this finding calls attention to the fact that the parameters from the two different techniques are measuring different incidences. Additionally, histopathology also scores features such as chondrocyte proliferation, synovial hyperplasia and vascular infiltration which cannot be analyzed via CT(Gerwin, Bendele et al. 2010). However, since EPIC-μCT is non-destructive of the samples, these features can still be analyzed via histology after the samples are scanned.

Osteophytes occur on the joint margins, they are thickening of the marginal tissue observed in human OA as well as in the MMT model. Histopathology scoring of osteophytes involves scoring maximum thickness from three different regions . In this study, we presented a novel method of analyzing both the size and composition of osteophytes using EPIC-μCT. Histopathology findings showed an increasing osteophyte thickness which was also observed in EPIC-μCT data via an increase of 3D thickness and volume. EPIC-μCT also showed mineralization of the osteophyte by two weeks. This mineralization is difficult to view in histology sections as the sections usually need to be decalcified prior to sectioning. Mineralization of the osteophyte is another feature of human OA that similarly develops in the MMT model, though at a highly accelerated

pace. Osteophytes originate from activated periosteum which leads to new cartilaginous outgrowths that eventually mineralizes via endochondral bone formation. A possible mechanism for MMPi effect on OP progression could involve the role that MMP-9 and MMP-13 play in OA. MMP-9 and MMP-13 are highly expressed in osteoclasts and chondrocytes in arthritic cartilage and their inhibition via the MMPi could lead to reduced OP formation as the production of cartilage and bone is limited(Hayami, Pickarski et al. 2004). Osteophyte progression could also be a sensitive parameter in evaluating therapeutic efficacy. In the MMPi treated rats, the most acute effect was observed in the reduction of the mineral volume of osteophyte. This result suggests that the MMPi might be more beneficial towards the later stage of OA progression, at least with regards to the osteophyte.

One of the major limiting factors for screening DMOADs in pre-clinical animal models is the limited sensitivity of outcome techniques. Our post-hoc power analysis results showed that EPIC-μCT could reduce the number of animals required for drug screening. The most sensitive parameter in EPIC-μCT (Total OP volume) showed that only 7 samples per group would be needed whereas the most sensitive histopathology parameter (OP width) showed that at least 13 samples per group would be required. A lower number of animals would have a downstream effect resulting in faster data generation and lower amount of pharmaceutical compound synthesis at the initial stage. Moreover, EPIC-μCT is much faster as analyzing a single sample requires approximately 2.5 hours whereas a full-scale histopathology study can take months to complete, with the decalcification procedure itself taking between 10-14 days. EPIC-μCT parameters could allow for in vivo screening in a rapid, efficient and quantitative manner while allowing

for smaller sample numbers leading to reduction in time needed to identify potential DMOADs which could go through the next testing phase.

CHAPTER 5

THERAPEUTIC EFFECT OF MICRONIZED DEHYDRATED HUMAN AMNION/CHORION MEMBRANE (µ-dHACM) TESTED IN RAT MEDIAL MENISCAL TEAR MODEL USING EPIC-µCT[c]

Abstract

Micronized dehydrated human amnion/chorion membrane (µ-dHACM) is derived from donated human placentae and has anti-inflammatory, low immunogenic and anti-fibrotic properties. This material has been previously used in the clinic in applications such as tendon repair and corneal epithelial defect but has not yet been tested in an OA model. The objective of this study was to quantitatively assess the efficacy of µ-dHACM as a disease modifying intervention in a rat model of OA. It was hypothesized that intra-articular injection of µ-dHACM would attenuate OA progression.Lewis rats underwent medial meniscal transection (MMT) surgery to induce OA. µ-dHACM or saline was injected intra-articularly into both naïve and MMT joints. To simulate clinical OA, rats were injected with µ-dHACM 3 weeks post-surgery as well and analyzed at 6 weeks. Denatured µ-dHACM was tested at the 3 week time point to examine effects of bioactive components. Microstructural changes in the tibial articular cartilage were assessed using EPIC-µCT and the joint was also evaluated histologically. There was no measured

---

[c] Portions of this chapter were adapted from Willett N*, Thote T*, Lin AS, Moran S, Raji Y, Sridaran S, Stevens HY and Guldberg RE. Intra-articular injection of micronized dehydrated human amnion/chorion membrane attenuates osteoarthritis development. Arthritis Research &Therapy16(47). February 2014. Creative Commons Attribution License. (* = Equal contributors)

baseline effect of µ-dHACM on cartilage in naïve animals. µ-dHACM was sequestered in the synovial membrane following intra-articular injection and attenuated cartilage degradation in a rat OA model at 3 weeks and via a delayed injection at 6 weeks. Denaturation of µ-dHACM did not have a chondro-protective effect on the articular cartilage. These data suggest that intra-articular delivery of µ-dHACM may have a therapeutic effect on OA development.

Introduction

Multiple clinical trials have tested a number of potential disease modifying OA drugs (DMOADs), including matrix-metalloproteinase inhibitors (MMPis), cytokine blockers, inhibitors of inducible nitric oxide synthase (iNOS), and doxycycline; however, none have shown a clear therapeutic benefit to date (Martel-Pelletier, Wildi et al. 2012). There are various DMOADs in clinical trials such as rhFGF-18 (Sprimerfin by Merck), a growth factor based therapy, in Phase II which has shown a decrease in cartilage thickness and volume in patients with OA(Hellot, Wirth et al. 2013). Strontium ranelate, in a recently completed a Phase 3 clinical trial showed a significant improvement in joint structure of OA patients (Reginster 2013). Though heavy investment in research continues, OA remains a pervasive and burdensome condition with limited effective clinical options, and there is still a critical need to investigate novel OA therapies.

Testing therapeutics for OA requires selection of a suitable animal model and an efficient and quantitative analysis method. The medial meniscal transection (MMT) rat model is a well-accepted small animal model for evaluating new pharmacologic agents (Gerwin, Bendele et al. 2010). Micro-computed tomography (µCT) imaging can rapidly

and quantitatively evaluate 3D morphologic and degenerative changes in articular cartilage by EPIC-μCT(Palmer, Guldberg et al. 2006).

Locally delivered extracellular matrix proteins are a promising treatment strategy being developed for a wide range of regenerative applications (Niknejad, Peirovi et al. 2008). Dehydrated human amnion/chorion membrane (dHACM) is a tissue derived from donated placentae which possesses anti-inflammatory properties, displays low immunogenicity, and promotes wound healing while inhibiting scar formation (Faulk, Matthews et al. 1980, Akle, Adinolfi et al. 1981, Hao, Ma et al. 2000). There is an established precedence of using this tissue for regenerative applications clinically, ranging from corneal defects to tendon repair (Gruss and Jirsch 1978, He, Li et al. 2002, Mligiliche, Endo et al. 2002, Gajiwala and Gajiwala 2004, Chandra, Maurya et al. 2005, Thatte 2011).

The potential for dHACM to modulate the development of OA has not been previously investigated; however indirect evidence suggests that it may have beneficial effects on cartilage. *In vitro*, dHACM has been shown to maintain chondrocyte phenotype when seeded with chondrocytes (Diaz-Prado, Rendal-Vazquez et al. 2010, I.H.Hussin, Pingquan-Murphy et al. 2011). *In vivo*, chondrocyte seeded dHACM enhanced regeneration of hyaline cartilage in rabbit osteochondral defects after 8 weeks (Jin, Park et al. 2007). One of the limitations of these previous studies has been the use of dHACM in the form of sheets which can only treat large defects and would require an invasive surgery. Micronized dHACM (μ-dHACM) offers a minimally invasive, injectable therapy with a longer shelf life than cellularized constructs. μ-dHACM can be

devitalized while preserving its basement membrane structure and a variety of growth factors including PDGF, FGF and TGF-β (Ji, Xiao et al. 2011).

An injectable formulation of µ-dHACM (EpiFix® Injectable, MiMedx Group, Inc. Marietta, GA) has recently been developed that retains the active factors of the original tissue and allows for minimally invasive local delivery targeted to the disease site. µ-dHACM is developed after the native amnion undergoes the PURION process which maintains bioactive components despite the tissue being devitalized and dehydrated (US Patent 8,357,403– Placenta Tissue Grafts. US Patent 8,372,437-Placenta Tissue Grafts.14. US Patent 8,409,626-Placenta Tissue Grafts). The tissue retains the epithelial and chorion layer after the process. A recent study examined the biological properties of µ-dHACM and in vitro experiments show quantifiable levels of various growth factors, interleukins and TIMPS(Koob, Rennert et al. 2013, Koob, Lim et al. 2014). A subcutaneous in vivo experiment in the same study demonstrated recruitment of mesenchymal progenitor cells to site of implantation as well(Koob, Rennert et al. 2013).

The applicability of this material as a therapeutic for OA has not yet been studied. The objective of this study was to quantitatively assess the efficacy of µ-dHACM as a disease modifying intervention in the rat MMT model and examine the effect of denaturation on the therapeutic effect of µ-dHACM. It was hypothesized that a single intra-articular injection of µ-dHACM would attenuate OA disease progression in the rat MMT model with denaturation of µ-dHACM eliminating any therapeutic benefit observed.

Materials and Methods

Surgical Methods

Weight matched adult male Lewis rats (Charles River, Wilmington, MA) weighing 300-325g, were acclimated for 1 week. For the MMT surgery, the animals were anesthetized with isoflurane, and the skin over the medial aspect of the left femoro-tibial joint was shaved and aseptically prepared. The medial collateral ligament (MCL) was exposed by blunt dissection and transected to reflect the meniscus toward the femur. The joint space was visualized, and a full thickness cut was made through the meniscus at its narrowest point (Janusz, Bendele et al. 2002).The skin was closed with 4.0 Vicryl sutures and then stapled using wound clips. For the 3 week study, 24 hours post MMT surgery, either µ-dHACM (AmnioFix® Injectable, MiMedx Group Inc. Marietta GA) or saline was injected intra-articularly into the stifle joint of the left leg (n=5 per group, per time point). µ-dHACM was sourced from two different donors processed in two different batches. µ-dHACM was resuspended according to the product insert and injected into the articular joint space using a 25 gauge needle. Animals were euthanized at 3 days or 3 weeks post-surgery. Naïve animals did not undergo any surgical procedure and were injected with µ-dHACM or saline. For the six week study,µ-dHACM was injected either 24 hours post-surgery (single injection), 3 weeks post-surgery (delayed injection) or at both 24 hours and 3 weeks post-surgery (multiple injection) into the left leg. Sham surgery was performed in rats as well where the MCL was transected but the joint was sutured without transecting the meniscus (n = 6-8 per group). MMT surgery with saline injection served as a control group. Animals were euthanized 6 weeks post-surgery. For the denatured dHACM study,either µ-dHACM, denatured µ-dHACM or saline was

injected intra-articularly in the left knee 24 hours post-surgery. Sham surgeries were also performed as controls (n = 8 per group). Animals were euthanized 3 weeks post-surgery. The Georgia Institute of Technology Institutional Animal Care and Use Committee approved experimental procedures for these in vivo studies (IACUC protocol #A09007 and IACUC protocol #A10218). The experimental design is listed in the table below (Table 7):

Table 7. Experimental Design

Study 1 – 3 week µ-dHACM study					
Groups (n = 5)	Naïve + Saline	Naïve + µ-dHACM	MMT + Saline	MMT + µ-dHACM	
Study 2 – 6 week µ-dHACM study					
Groups (n = 6-8)	Sham	MMT + Saline (Saline)	MMT + µ-dHACM @ 24 hrs (Single)	MMT + µ-dHACM @ 3 weeks (Delayed)	MMT + µ-dHACM @ 24hrs + 3 weeks (Multiple)
Study 3 – 3 week denatured µ-dHACM study					
Groups (n = 7-8)	Sham	MMT + Saline	MMT + µ-dHACM	MMT + Denatured µ-dHACM	

µ-dHACM was manufactured using the proprietary Purion® process and is compliant with the American Association of Tissue Banks regulations for donor tissues (MiMedx Group, Inc. Marietta, GA). The process produces a dehydrated, devitalized amnion and chorion tissue graft which is then micronized, sterilized and can be suspended in saline (US Patent 8,357,403– Placenta Tissue Grafts; US Patent 8,372,437-Placenta Tissue Grafts; US Patent 8,409,626-Placenta Tissue Grafts).µ-dHACM was denatured by boiling the saline suspended µ-dHACM for 60 minutes.

Synovial Fluid Analysis

Rats were euthanized via CO_2 inhalation at 3 days or 21 days post-surgery for both the naïve group and MMT surgery group for the 3 week study. Synovial fluid was collected by first injecting 100µl of saline intra-articularly using a 30 gauge insulin syringe, followed by aspirating approximately 50-100µl of the synovial fluid and saline using the same syringe. Synovial fluid was analyzed using the Quantibody® Rat Inflammation Array 1, a multiplex ELISA kit that quantitatively measured 10 rat inflammatory factors - IFNγ, IL-1α, IL-1β, IL-2, IL-4, IL-6, IL-10, IL-13, MCP-1, TNFα (RayBiotech, Norcross, GA).

EPIC-µCT Analysis of Articular Cartilage

Articular cartilage structure and composition were quantitatively evaluated in the tibial plateau as described in our previous study (Thote, Lin et al. 2013). Scanco evaluation software was used to assess 3D morphological parameters and local attenuation. Dissected tibia were immersion fixed in 10% neutral buffered formalin for 48 hours then stored in 70% ethanol until ready for scanning. Immediately prior to scanning, tibiae were immersed in 2ml of 30% Hexabrix™ 320 contrast agent (Covidien, Hazelwood, MO) and 70% PBS at 37°C for 30 minutes (Palmer, Guldberg et al. 2006, Xie, Lin et al. 2009). Samples were then scanned using a µCT 40 (Scanco Medical, Brüttisellen, Switzerland) at 45 kVp, 177 µA, 200 ms integration time, and a voxel size of 16 µm (Xie, Lin et al. 2009). Raw data were automatically reconstructed to 2D grayscale tomograms. These were rotated to sagittal sections, and the cartilage was

contoured and thresholded with global segmentation parameters (Gauss sigma - 1.2, support - 2, threshold - 175-225). Direct distance transformation algorithms were used to quantify 3D morphology (Hildebrand and Ruegsegger 1997, Laib, Barou et al. 2000, Xie, Lin et al. 2009). The subsequently generated 3D images were delineated into three volumes of interest (VOIs). For the MMT model, images were evaluated for: (1) Full articular cartilage in the proximal tibia including medial and lateral aspects, (2) Medial 1/3 of the medial tibial plateau and (3) Focal lesions on the medial plateau only. Outcome measures included average articular cartilage thickness, volume and attenuation. Cartilage attenuation is a quantitative parameter that is inversely proportional to sulfated glycosaminoglycan (sGAG) content (Palmer, Guldberg et al. 2006). Degraded cartilage contains lower sGAG content and therefore higher contrast agent content and higher attenuation values (Xie, Lin et al. 2009). Two outcome measures were defined for evaluation of focal defects: erosion (defect depth extending to less than 50% of cartilage thickness) and lesion (defect depth extending to more than 50% of cartilage thickness) (Pritzker and Aigner 2010). To define VOIs of focal lesions, manual contouring was performed in the isolated lesion area to account for the curvature of the surrounding cartilage tissue and exclude the subchondral bone and surrounding air. Within this VOI, segmented cartilage volume was subtracted from the total volume evaluated to compute lesion volume. For the 6 week study, osteophytes were also evaluated. Surface roughness and exposed bone area were calculated using a custom MATLAB script using images rendered by the CT software.

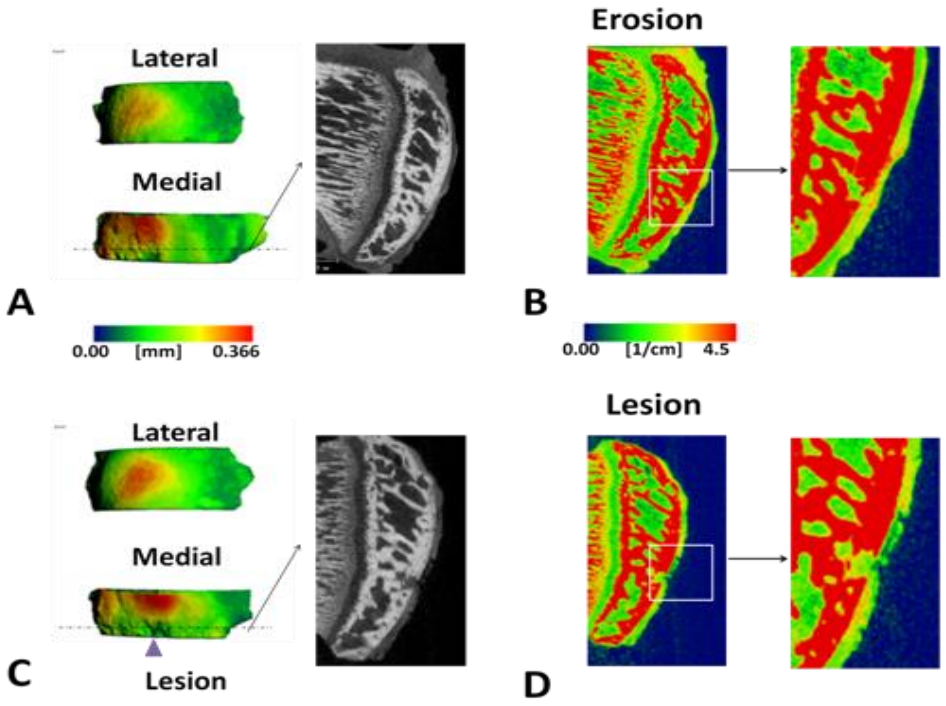

Figure 20.EPIC-µCT images indicating focal defects in MMT ratsA. Representative image isolating erosion in MMT joint B. Attenuation map indicating erosion on the MMT joint (Inset shows zoomed in view of erosion) C. Representative image isolating lesion in MMT joint D. Attenuation map indicating erosion on the MMT joint (Inset shows zoomed in view of erosion)

Histology

For the 3 day time point, the entire limb was harvested with knee joint intact, fixed in 10% neutral buffered formalin for 3-4 days, transferred to 70% ethanol, and stored at 4°C. For the 21 day and 6 week time point, the tibiae and femora were harvested separately, dissected free of surrounding tissues, fixed in 10% neutral buffer formalin for 3-4 days, transferred to 70% ethanol, and stored at 4°C. For femoral dissections, care was taken to preserve the synovium, meniscus, and femoro-meniscal connective tissue. Following EPIC-µCT scanning, tibiae and femora were decalcified in Cal-Ex II (Fisher Scientific, Waltham, MA) for 14 days. Dehydrated samples were routinely processed into paraffin embedded blocks. For comparison with EPIC-µCT images, sagittal sections were

cut at 5µm thickness. Sections were stained for sGAGs with a 0.5% Safranin-O (Saf-O) solution and a 0.2% aqueous solution of FastGreen as a counter-stain or with hematoxylin and eosin (H&E).

Histological assessment of µ-dHACM and denatured µ-dHACM was performed via embedding the samples in histogel (Wong, Vosburgh et al. 2012). Briefly, µ-dHACM was mixed with histogel in an approximate 1:3 V/V ratio. This mixture was pipetted into a standard cryo cassette and flash frozen. The resulting block was routinely cryo-sectioned and stained with H&E.

In vitro study

Extracts for cell culture were acquired by incubatingµ-dHACM or denatured µ-dHACM in DMEM without 10%calf serum at a concentration of 20mg of tissue per ml of medium for 24 hours. The tissuewas removed by centrifugation and the extract was sterilefiltered.

Adult human dermal fibroblasts (HDFa, Life Technologies Corp., Grand Island, NY) were plated on 96-wellplates for 24 hours in Dulbecco's modified Eagle's medium (DMEM) containing 10% calf serum (GIBCO, Life Technologies Corp.).After 24 hours, the medium was aspirated from the wells and replaced with one of the following: basal media (DMEM lacking serum - control), complete media (DMEM plus 10% calf serum positive control) or DMEM containing extracts of dHACM at 10, 5 and 1mg/ml. After 72 hours, the plate was washed to remove unattached cells and a CyQuant assay (MolecularProbes CyQuant, Life Technologies C7026) was performed to quantify the number of cells as per manufacturer's instructions (Koob, Rennert et al. 2013).

Statistical analysis

All quantitative data were expressed as mean ± standard error. Joint parameters between groups were evaluated using a one factor (left vs. right) ANOVA with Tukey's test for post-hoc analysis. Joint parameters within the same group were compared between experimental and control knees using paired t-tests. Statistical significance was set at $p < 0.05$. All data were analyzed using GraphPad Prism software version 5.0 (GraphPad Software, Inc., La Jolla, CA).

Results

Short Term 3 Week Study

µ-dHACM Injected into Naïve Joints

µ-dHACM was injected into naïve joints to assess the inflammatory response at 3 and 21 days. Histology three days post-injection showed µ-dHACM particles incorporated into the adjacent synovial tissue (Figure 21). The material appeared as variably-sized fragments of multi-layered eosinophilic, fibrillar material. µ-dHACM fragments were surrounded by moderate inflammatory infiltrate consisting of macrophages, lymphocytes, and plasma cells indicating an inflammatory response to the xenogeneic material. No fragments were observed in control samples injected with saline, and these samples exhibited minimal hemorrhage or inflammatory cell presence in the synovial membrane.

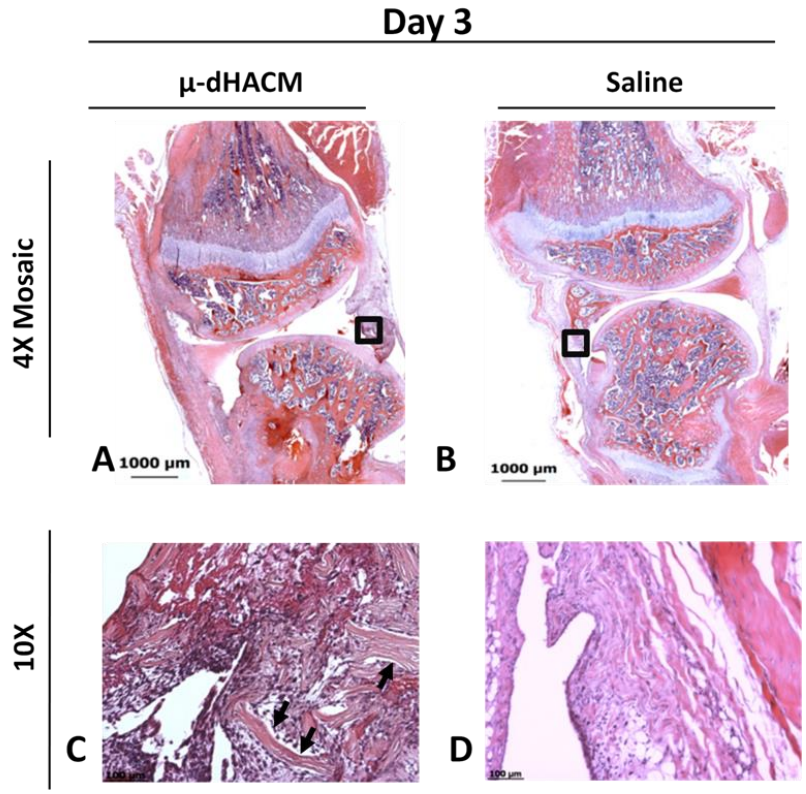

Figure 21. Histological assessment of µ-dHACM injected in naïve rats at Day 3. A-D: Representative histology images of µ-dHACM treated naïve joints and saline treated. C-D are zoomed in versions of regions of interest (black box) defined in A-B respectively. µ-dHACM visible at 3 days as fibrillar/eosinophilic material, indicated by black arrows

At 21 days post-surgery, histological staining of µ-dHACM treated stifle joints showed the continued presence of µ-dHACM in the synovium along with inflammatory cells. At 21 days, a distribution of smaller sized dHACM particles appeared compared to the 3 day time point and a similar foreign body response was observed surrounding the µ-dHACM fragments at both time points (Figure 22).

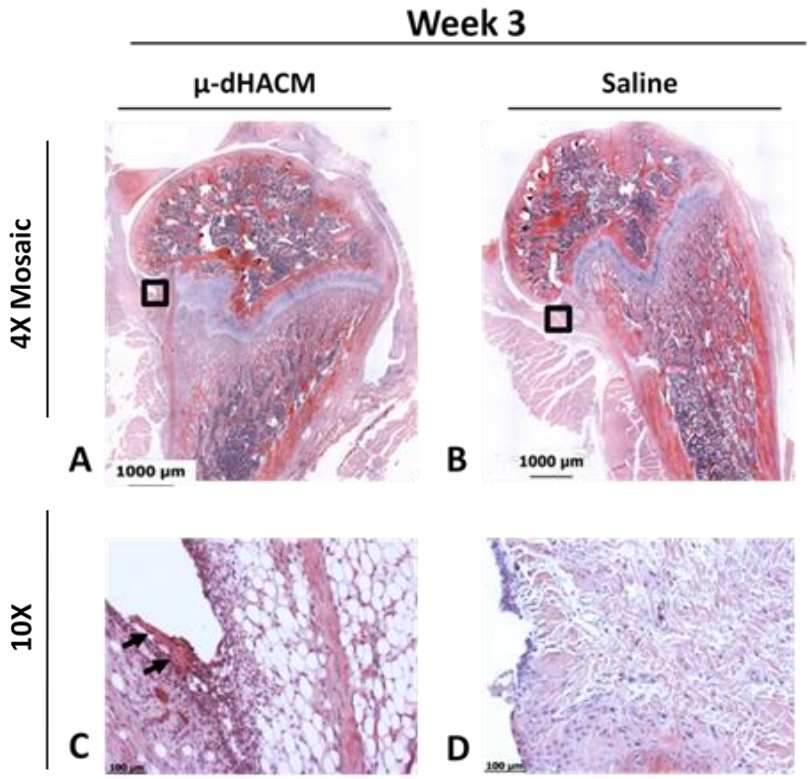

Figure 11. Histological assessment of µ-dHACM injected in naïve rats at Week 3. A-D: Representative images of µ-dHACM treated MMT joints and saline treated naïve. C-D are zoomed in versions of regions of interest (black box) defined in A-B respectively. µ-dHACM fragments visible at day week 3 as indicated by black arrows (C).

Synovial fluid showed a significant increase in Monocyte Chemoattractant Protein-1 (MCP-1) concentration in µ-dHACM treated joints compared to control joints at 3 days but no difference was observed at 21 days. MCP-1 levels significantly decreased from day 3 to day 21 in both treated and untreated groups (Figure 23).

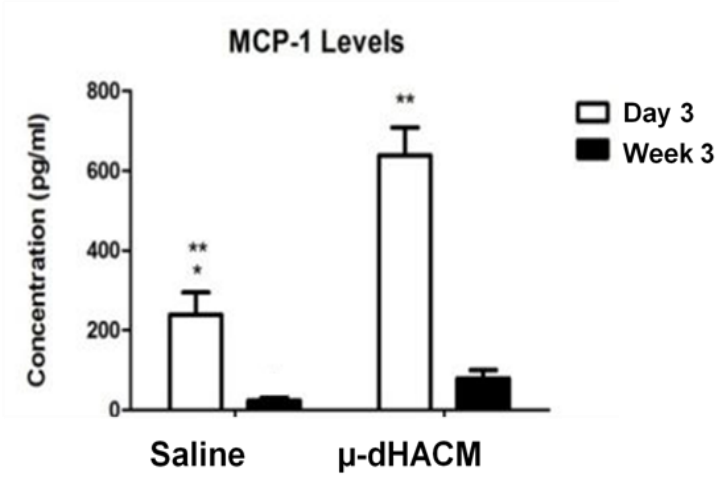

Figure 23.MCP-1 levels in µ-dHACM treated and saline injected naïve rats. MCP-1 levels were significantly higher at 3 days in both saline and µ-dHACM injected groups compared to 21 days. MCP-1 level at 3 days was significantly higher in the µ-dHACM injected joints compared to saline treated joints. ** $p < 0.05$ for MCP-1 levels at 3 and 21 days for both groups.* $p<0.05$ for MCP-1 levels at day 3 in saline injected and µ-dHACM injected. n = 5.

The othercytokines tested did not show any significant differences or were below the limit of detection (Table 8). Numerical values for all cytokines are presented in the following table.

Table 8. Cytokine ELISA data for naïve joints. Data represented as Mean ± std. dev. - indicates cytokine content lower than limit of detection

Cytokines	Naïve joints (pg/ml)			
	Day 3		Day 21	
	Saline	µdHACM	Saline	µdHACM
IFNγ	-	-	-	-
IL-1a	-	-	-	-
IL-1b	46.26 ± 20.42	58.35 ± 27.10	-	-
IL-2	-	-	-	153.85 ± 113.00
IL-4	-	-	-	-
IL-6	60.91 ± 38.54	195.87 ± 214.80	503.21 ± 178.94	253.12 ± 181.61
IL-10	-	-	-	-
IL-13	-	-	61.94 ± 58.28	-
MCP-1	239.06 ± 125.48	638.16 ± 156.80	24.34 ± 16.19	79.84 ± 46.35
TNFα	-	-	-	-

Cartilage structure and composition were assessed at 21 days using EPIC-µCT. Representative 3D reconstructions of the cartilage with thickness heat maps appeared normal in structure in naïve animals treated with µ-dHACM or saline (Figure 24). Quantitative assessments of cartilage volume and thickness indicated no differences between saline and µ-dHACM treated joints (Figure 24). Similarly, cartilage attenuation showed no significant difference between saline and µ-dHACM treated joints, indicating no differences in PG content (Figure 24). No lesions or erosions were observed in saline or µ-dHACM injected naïve joints.

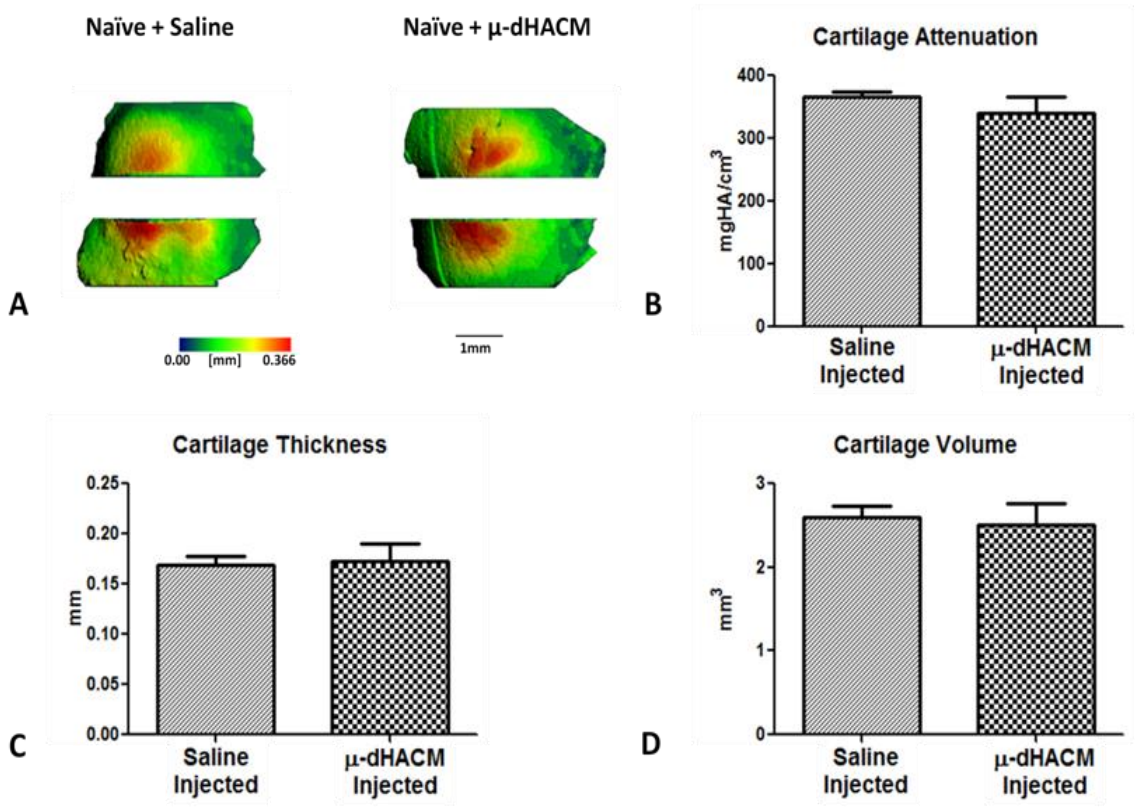

Figure 24. Tibial articular cartilage variables quantified for µ-dHACM in naïve joints. A. Representative EPIC-µCT tibial articular cartilage thickness maps for µ-dHACM and saline injected samples in naïve joints. B. Average cartilage attenuation C. Average cartilage thickness D. Average cartilage volume measure at 21 days. No differences in cartilage parameters were observed between µ-dHACM and saline injected groups. n = 5.

µ-dHACM Injected into MMT Joints

MMT joints were injected with µ-dHACM or saline, and the effects on the joint and synovium were assessed at 3 and 21 days. Histological analysis showed µ-dHACM incorporated into the synovium at both time points. As observed in naïve joints, the amnion fragments were surrounded by moderate inflammatory infiltrate and appeared reduced in size at 21 days. No fragments were visible in saline treated MMT animals at either 3 or 21 days (Figure 25).

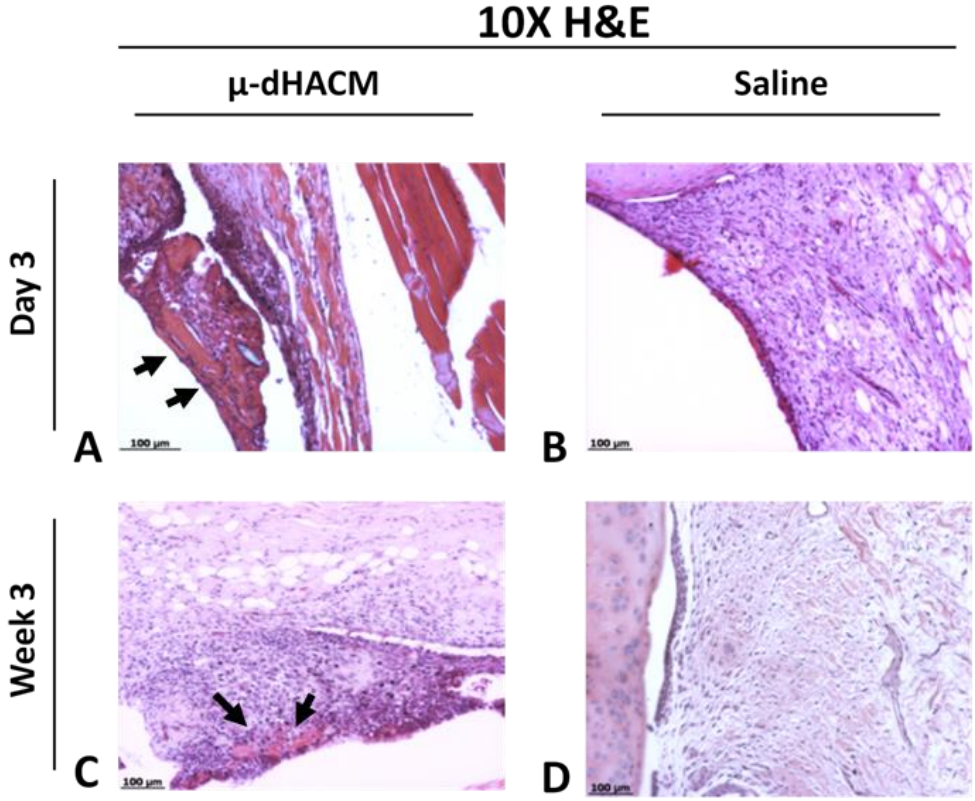

Figure 25. Histological assessment of µ-dHACM injected in MMT rats. A-D: Representative H&E stained histology images of µ-dHACM treated MMT joints and saline treated MMT joints. µ-dHACM visible at 3 days and 3 weeks as fibrillar/eosinophilic material as indicated by black arrows (A & C).Hypercellularity observed in area around µ-dHACM fragments.

In the saline treated MMT animals at 21 days, lesions and areas of erosion were evident along with diminished Saf-O staining of the tibial surface suggesting loss of PG content. In contrast, histological analysis of dHACM-treated joints showed a smooth cartilage surface with no lesions and strong Saf-O staining (Figure 26). Histological observations did not indicate any differences in cartilage morphology between the two groups at 3 days.

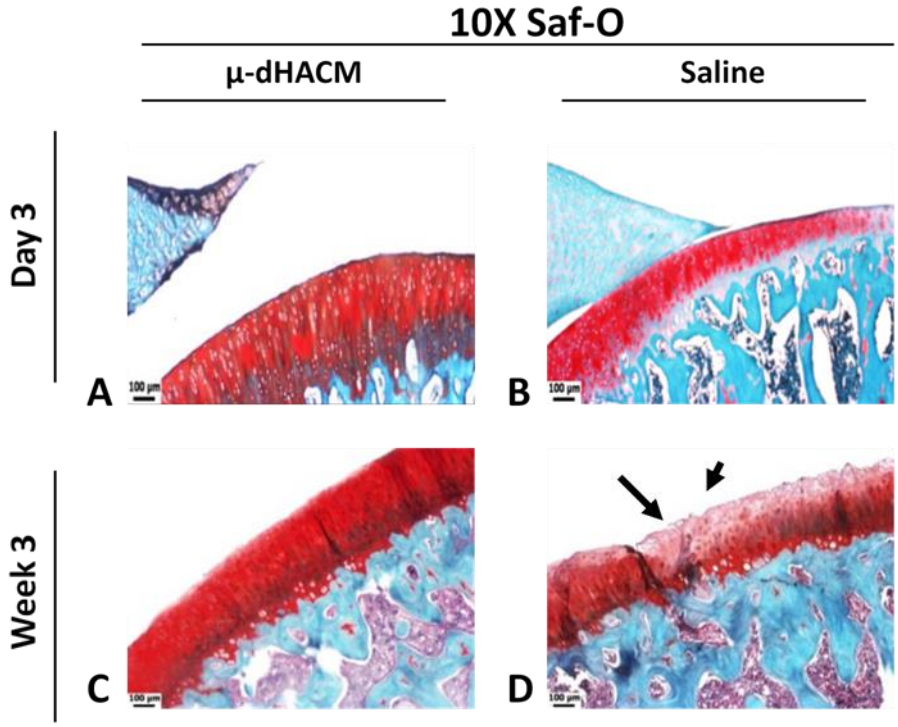

Figure 26. Histological assessment of tibial articular cartilage in µ-dHACM injectedMMT rats. A-D: Representative Saf-O stained histology images of µ-dHACM treated MMT joints and saline treated MMT joints. µ-dHACM treatment protected tibial articular cartilage from damage. Saline injected joints show decrease in PG content at Week 3 and surface damage (indicated by black arrows)

Synovial fluid analysis did not show significant differences between cytokine levels and most cytokines were below the limit of detection (Table 9). Values are presented in the following table.

Table 9. Cytokine ELISA data for MMT joints. Data represented as Mean ± std. dev. - indicates cytokine content lower than limit of detection

Cytokines	MMT joints(pg/ml)			
	Day 3		Day 21	
	Saline	µdHACM	Saline	µdHACM
IFNγ	-	-	-	-
IL-1a	-	-	-	-
IL-1b	-	-	-	-
IL-2	-	-	-	-
IL-4	-	-	-	-
IL-6	-	-	-	-
IL-10	76.19 ± 27.66	69.13 ± 81.83	-	-
IL-13	-	-	-	-
MCP-1	331.31 ± 260.01	444.86 ± 200.23	102.46 ± 42.10	132.09 ± 113.40
TNFα	137.44 ± 113.30	25.83 ± 44.74	117.11 ± 108.90	95.65 ± 76.00

EPIC-µCT was used to characterize cartilage and focal defects at 21 days. Representative planes and 2D EPIC-µCT attenuation heat maps of the tibial section from µ-dHACM treated MMT joints and saline injected MMT joints are presented (Figure 27). Qualitatively, MMT animals with saline injections displayed noticeable cartilage focal lesions and erosion sites. In contrast, cartilage surfaces in µ-dHACM treated joints appeared more consistently uniform, and no lesions were observed.

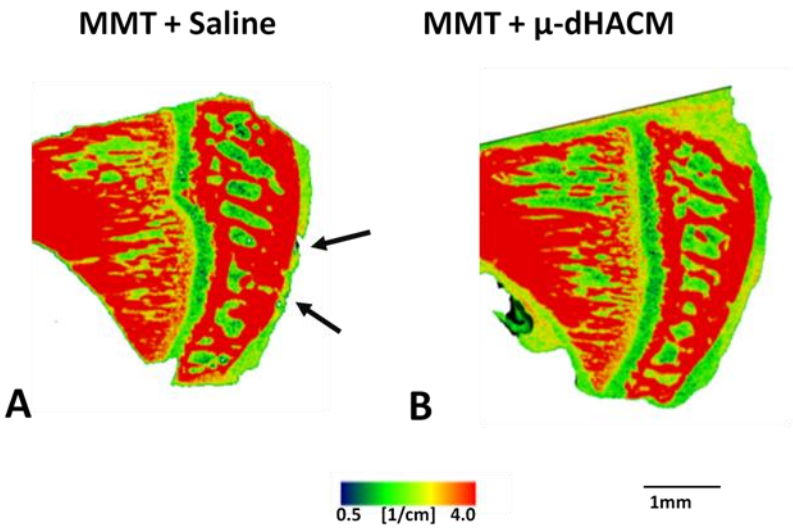

Figure 27.EPIC-µCT pseudocolor attenuation map. Sagittal tibial section for a saline injected (A) and µ-dHACM injected (B) MMT joint. Red = higher attenuation values (lower PG content), green = lower attenuation values (higher PG content). Black arrows indicate focal defects. The µ-dHACM treated joints did not display lesions on the tibial articular cartilage surface.

Quantitative EPIC-µCT at 21 days post-surgery showed that µ-dHACM treated joints had lower cartilage attenuation, indicating higher PG content, in the medial 1/3 of the tibial plateau compared to saline injected MMT joints. There was no significant difference between average attenuation values between naïve joints and µ-dHACM-treated MMT joints, suggesting the treatment maintained PG content comparable to intact joints (Figure 28). MMT joints injected with saline had an average incidence of 2.8 ± 0.2 erosion and 2.4 ± 0.4 lesion sites per medial tibial plateau with an average lesion volume of .00725 ± .005 mm^3. µ-dHACM treated MMT joints displayed significantly fewer erosion sites (1.2 ± .374) and no lesions (Figure 28).

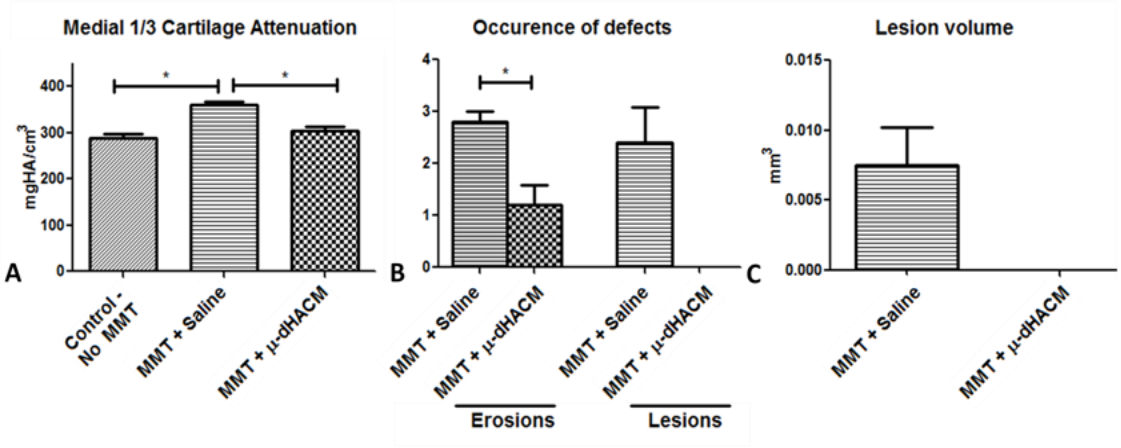

Figure 28. Tibial articular cartilage variables quantified for µ-dHACM in MMT joints. A. Average cartilage attenuation was significantly decreased in µ-dHACM treated MMT joints compared to saline injected MMT joints for the medial 1/3 tibial plateau. B. Average number of erosions was significantly decreased in µ-dHACMtreated MMT joints compared to saline injected MMT joints. No lesions were observed in the µ-dHACM treated MMT joints. C. Average focal lesion volume in saline injected MMT joints.* $p < 0.05$ & $n = 5$.

Medial 1/3 cartilage volume was also analyzed. A significant increase in cartilage thickness was observed in both saline treated and µ-dHACM treated samples compared to contralateral controls (Fig 29). There was also a significant increase in thickness between the µ-dHACM treated and saline treated samples.

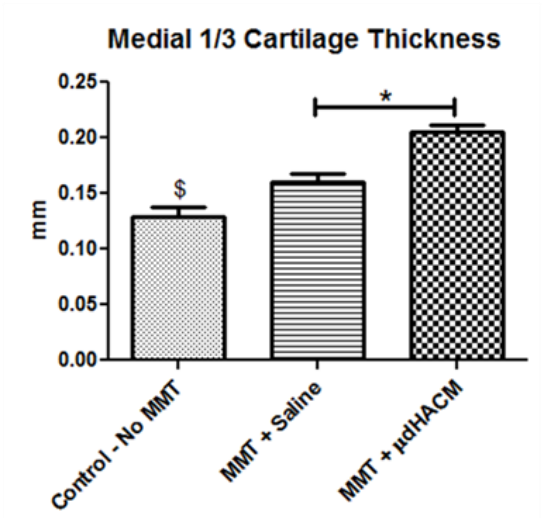

Figure 29. Effect of µ-dHACM on cartilage thickness. Cartilage thickness significantly increased in µ-dHACM treated MMT joints and saline injected MMT joints compared to contralateral control. Cartilage thickness for µ-dHACM treated MMT joints was also significantly higher than saline injected MMT joints. $ = $p < 0.05$ compared to saline and µ-dHACM treated MMT joints. * $p < 0.05$ & n =5.

Longer Term 6 Week Study

EPIC-µCT was used to generate 2D EPIC-µCT attenuation heat maps of the tibial section from the experimental groups (Figure 30). Qualitatively, MMT animals with saline injections and single injections displayed higher attenuation (in red) compared to the sham, delayed and multiple injection group.

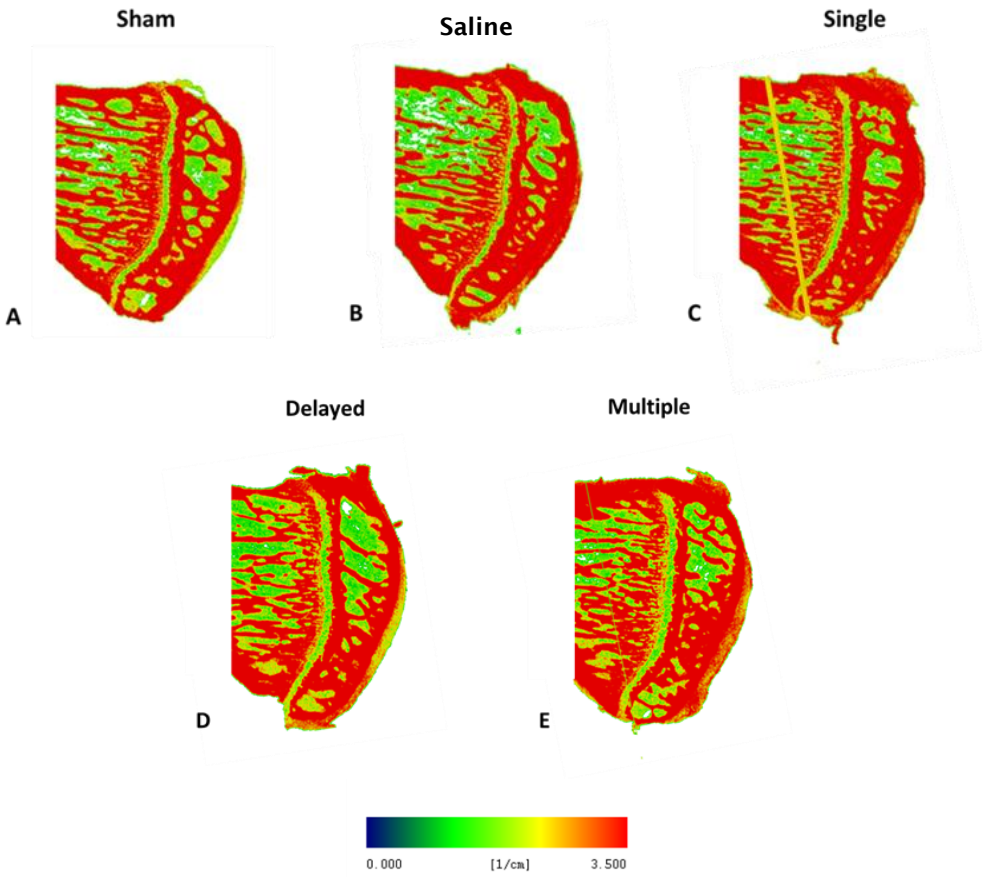

Figure 30. Qualitative EPICµCT pseudocolor attenuation maps. µ-dHACM on cartilage thickness.MMT (B) and Single Injection (C) samples showed higher attenuation compared to sham(A), delayed (D) and multiple injections (E). Red = higher attenuation values (lower PG content), green = lower attenuation values (higher PG content).

The medial 1/3 region of the medial tibial plateau was evaluated for cartilage attenuation, subchondral bone volume and cartilage volume (Fig 31). Cartilage attenuation was significantly higher in the saline and single injection group compared to sham, delayed and multiple injection group. Subchondral bone volume was significantly higher in the saline and single injection group compared to the delayed injection group. The sham group showed a lower subchondral bone volume compared to saline, single and multiple injection groups. No significant differences in cartilage volume were observed.

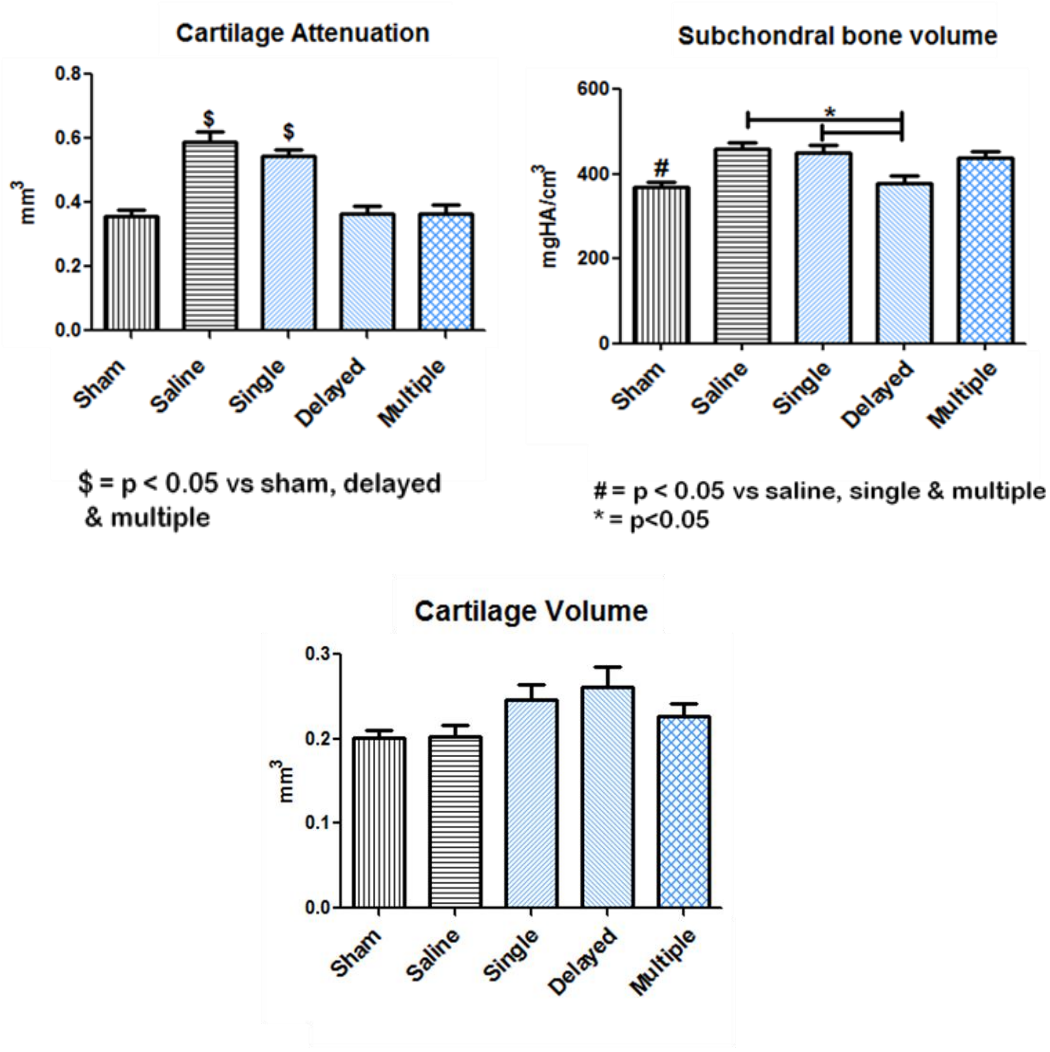

Figure 31. Medial 1/3 tibial articular cartilage variables quantified for µ-dHACM 6 week study. A. Cartilage attenuation significantly increased saline and single injection group compared to sham, delayed and multiple injection group. B. Subchondral bone volume was significantly higher in the saline and single injection group compared to the delayed injection group and lower in sham compared to saline, single and multiple injection group. C. No differences were observed in cartilage volume

The entire medial tibial plateau was evaluated for osteophytes. Three parameters were measured – marginal total volume, marginal mineral volume and marginal cartilaginous volume (Fig 32). Saline and single injection groups had significantly higher marginal total & cartilaginous volume compared to sham and delayed injection groups.

Marginal mineral volume was also higher in saline and single injection groups compared to sham.

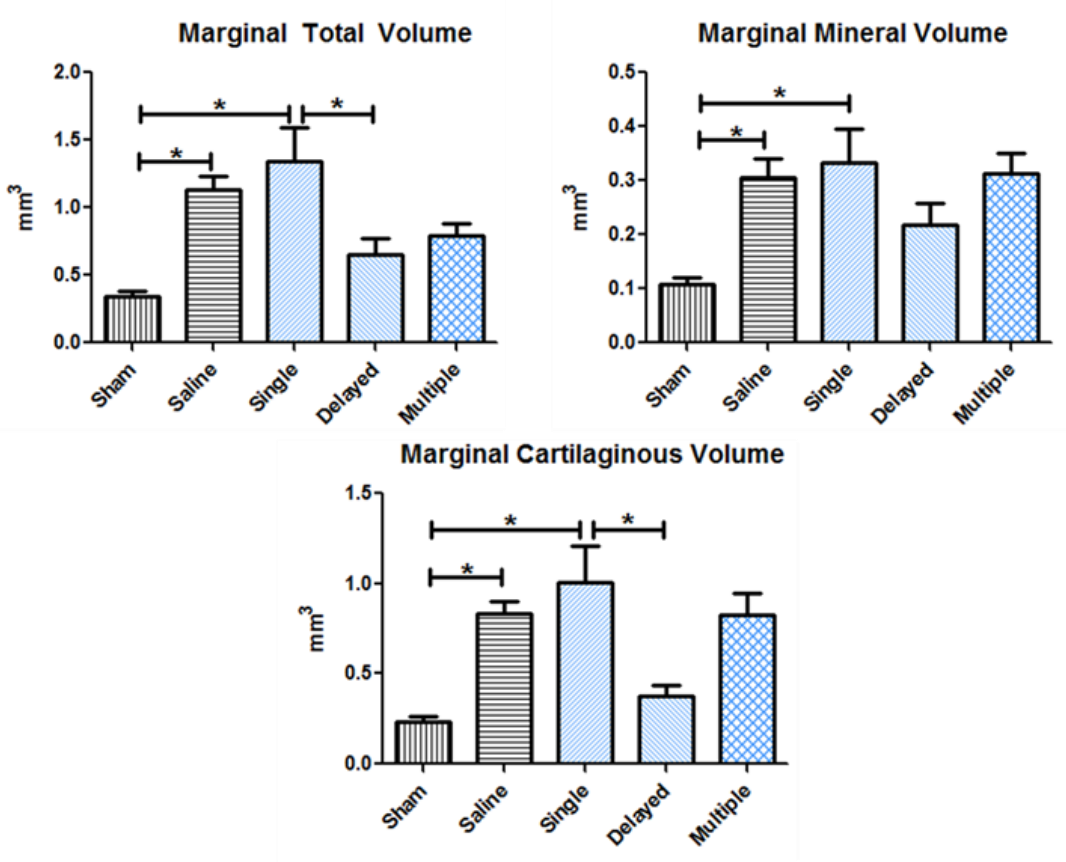

Figure 32. Osteophyte progression quantified for µ-dHACM 6 week study. A. Marginal total volume significantly increased in saline and single injection group compared to sham and delayed injection group. B. Marginal mineral volume significantly increased in saline and single injection group compared to shams. C. Marginal cartilaginous volume significantly increased in saline and single injection group compared to sham and delayed injection group. (* = $p < 0.05$)

Surface roughness and exposed bone area was analyzed for the medial and medial 1/3 tibial plateau (Fig 33). No significant differences were observed in medial surface roughness. Medial 1/3 surface roughness was significantly lower in sham and delayed injection groups compared to saline, single and multiple injection group.

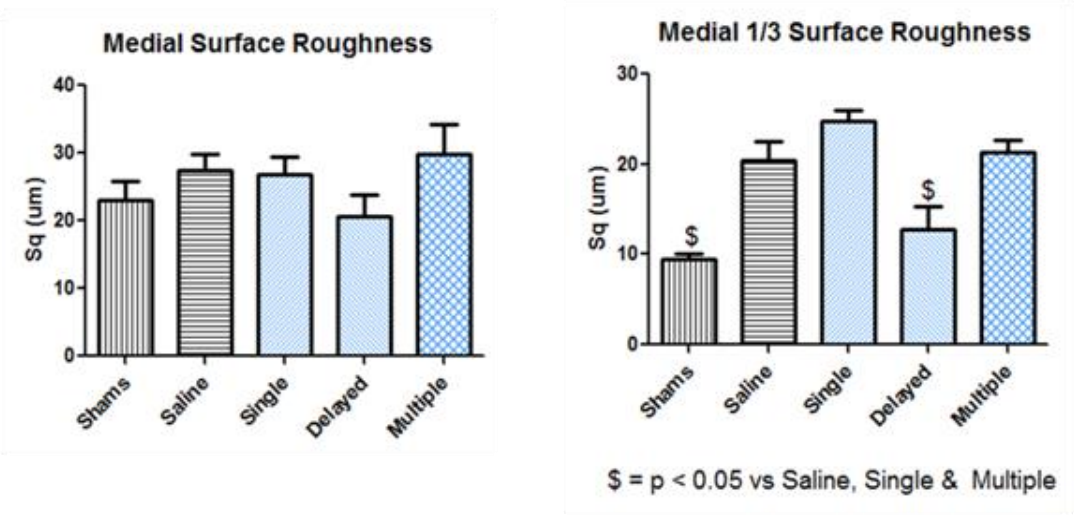

Figure 33. Quantification of surface roughness. A. No differences observed in medial surface roughness. B. Medial 1/3 surface roughness was significantly lower in sham and delayed injection groups compared to saline, single and multiple injection group

Medial exposed bone was significantly higher in saline and multiple injection group compared to sham and delayed groups (Fig 34). Medial 1/3 exposed bone was also significantly higher in saline and multiple injection group compared to sham and delayed groups. Average exposed bone value for contralateral controls for medial exposed bone was .044 ± 0.023 and for medial 1/3 exposed bone was 0.025 ± 0.021.

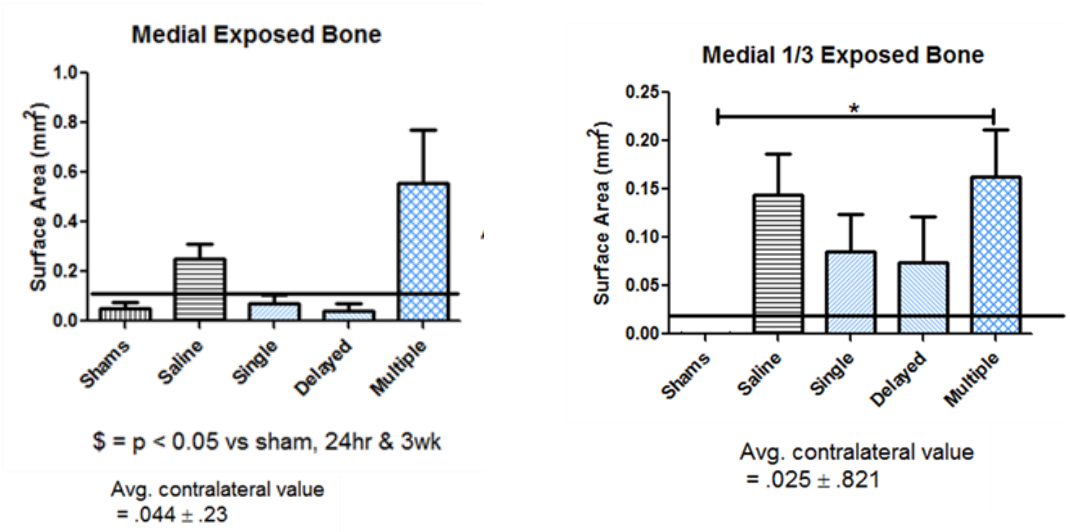

Figure 34. Quantification of exposed bone. A. No differences observed in medial surface roughness. B. Medial 1/3 surface roughness was significantly lower in sham and delayed injection groups compared to saline, single and multiple injection group

Histology images of coronal sections display cartilage damage in saline, single and multiple injection groups (Fig 35). Smooth cartilage surface is observed in the sham surgery group indicated by red staining of PGs on the cartilage surface. Chondrocytes appear in a loop structure in the delayed injection group.

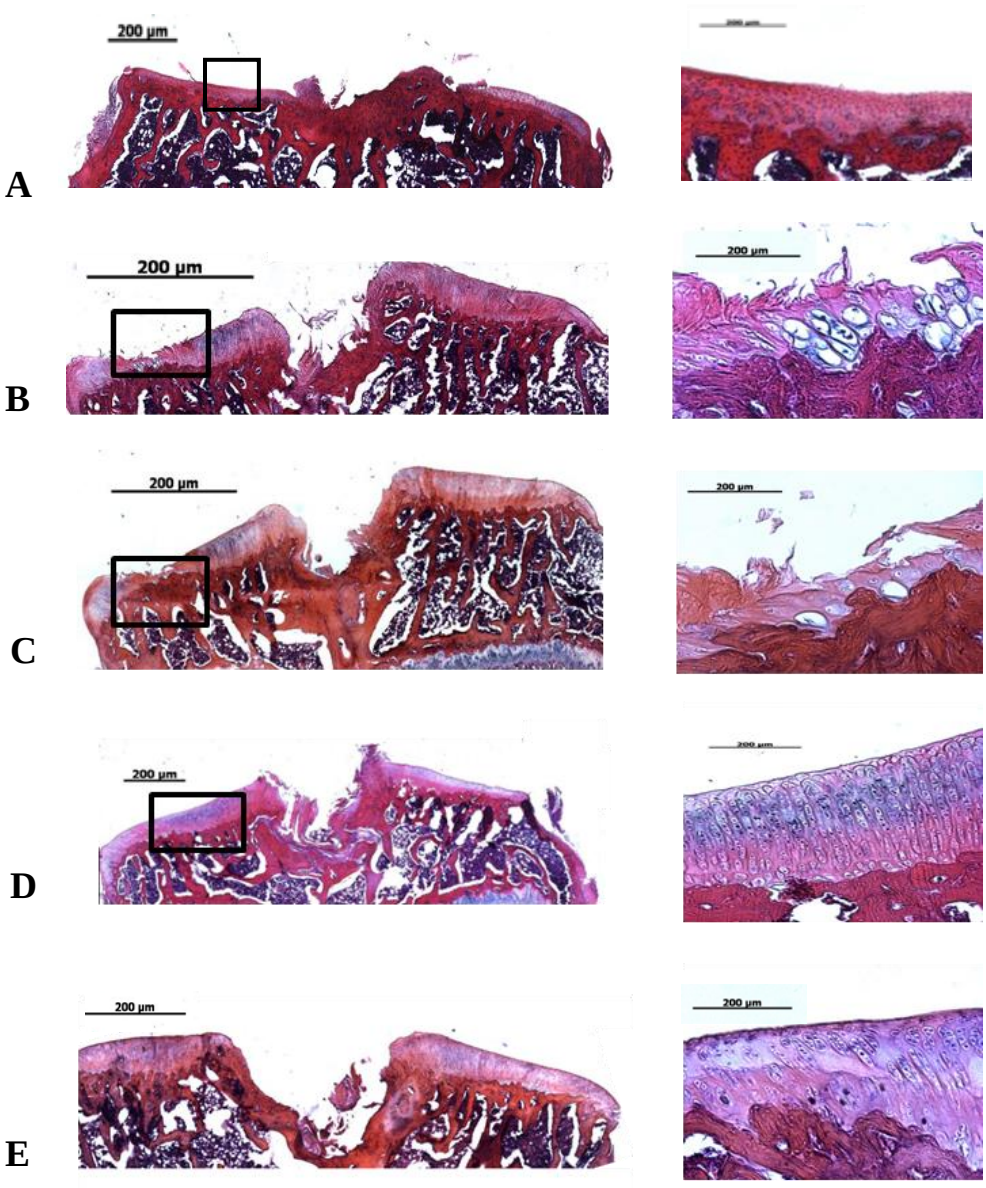

Figure 35. Histological assessment of tibia in µ-dHACM 6 week study. Representative H&E stained coronal tibial sections for sham (A), saline (B), single (C), delayed (D) and multiple (E) injections. A. Sham joints show no cartilage damage. B – C: Cartilage damage observed on surface, zoomed in image shows fibrillation of cartilage degradation. Zoomed in image shows fibrillation of surface group. D: Delayed injection shows protective effect and no surface damage is observed. Inset shows chondrocytes in a looped structure. E. Multiple injections shows moderate inhibition of cartilage damage but not as extensive as D.

Denatured µ-dHACM Study

µ-dHACM was denatured via heat treatment and histology was performed on histogel embedded µ-dHACM samples (Fig 36). µ-dHACM showed linear, fibrillar structure whereas denatured µ-dHACM appeared to be smaller. Webbing like structure was also observed in denatured µ-dHACM.

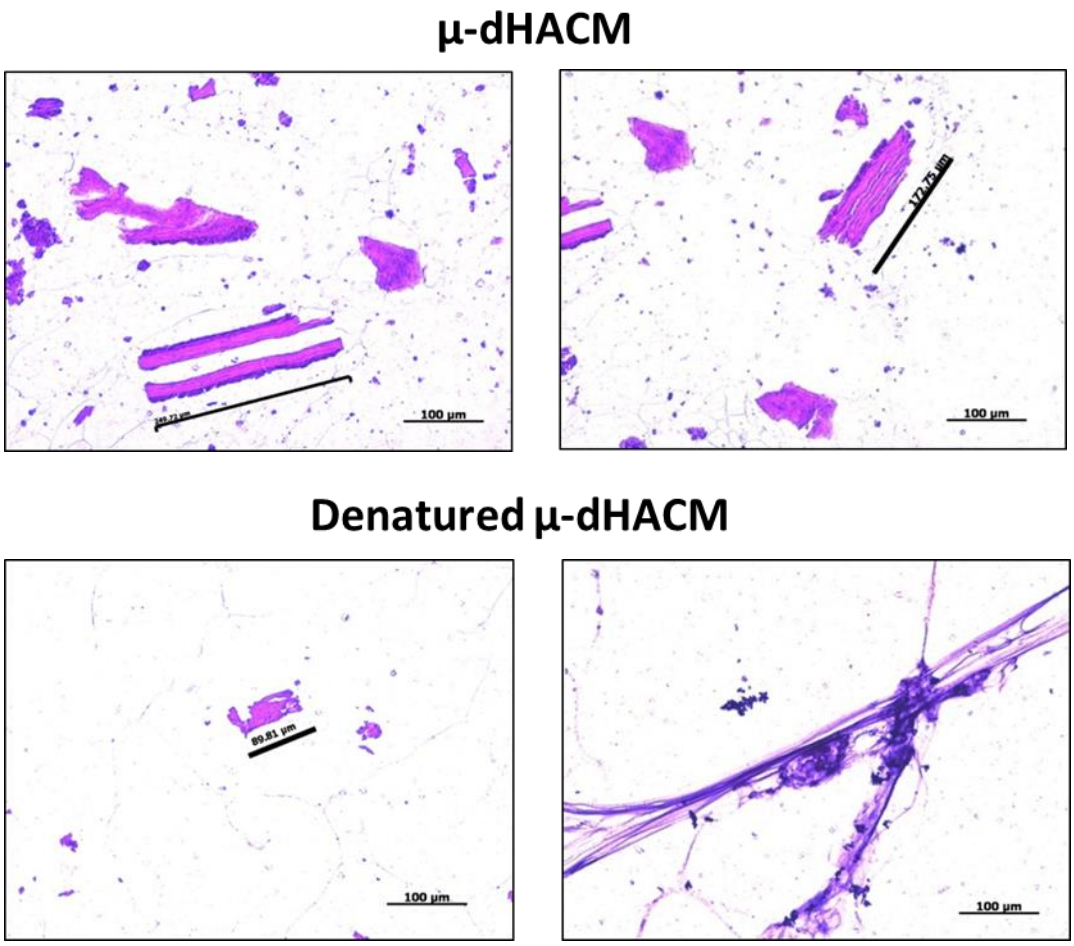

Figure 36.H&E stained µ-dHACM. Top panel shows µ-dHACM in linear, fibrillar structure. Bottom panel shows denatured µ-dHACM that appears to be in smaller fragments. Webbing like structure also observed in denatured µ-dHACM.

In-vitro cell culture human fibroblasts did not show a change in cell number via a CyQuant assay in response to denatured µ-dHACM (Fig 37). Cell number was significantly lower in both µ-dHACM and denatured µ-dHACM treated cultures compared to complete media.

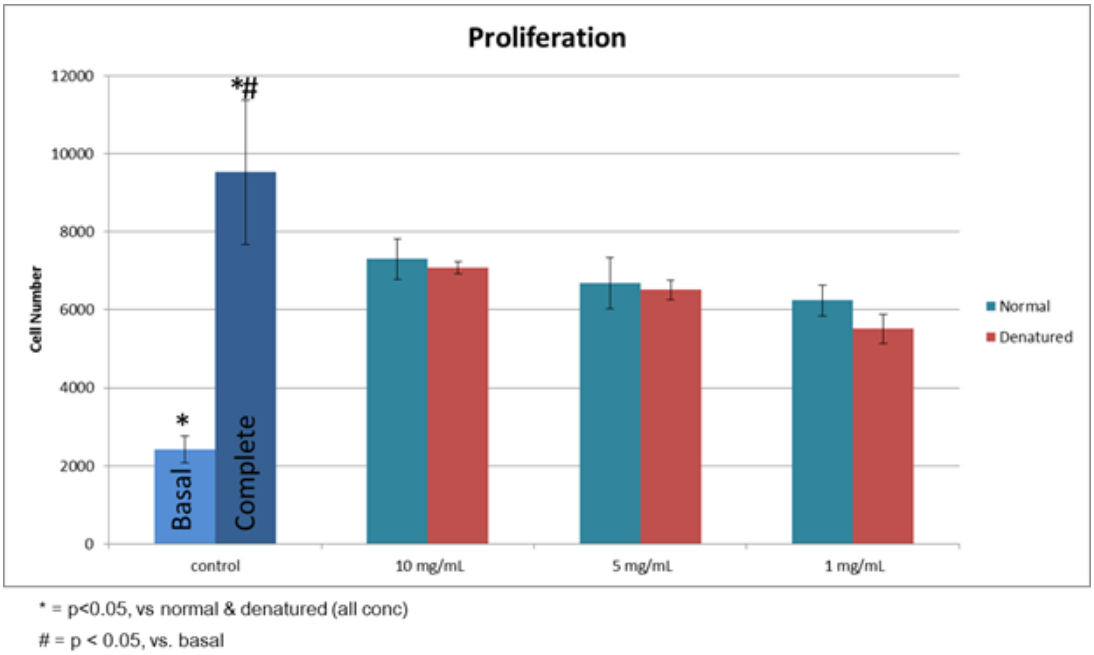

Figure 37. In vitro cell culture data. Denaturation of µ-dHACM did not have an effect on cell number compared to normal µ-dHACM. Complete media treated cells were significantly higher in cell number compared to all other groups.

The medial 1/3 region of the medial tibial plateau was evaluated for cartilage volume, thickness and attenuation subchondral bone volume and cartilage volume (Fig 38). Cartilage volume was significantly lower in sham compared to other three groups. Cartilage thickness was significantly lower in sham compared to other three groups as well but a significant increase in cartilage thickness was observed in the denatured µ-dHACM group compared to µ-dHACM. Cartilage attenuation significantly increased in saline and denatured µ-dHACM compared to sham.

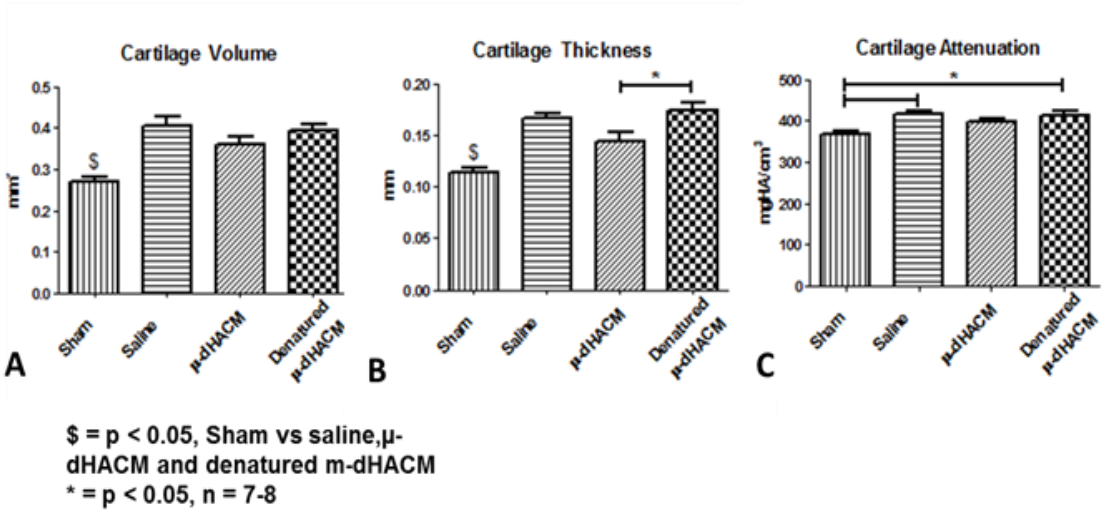

Figure 38. Medial 1/3 tibial articular cartilage variables quantified for µ-dHACM 6 week study. A. Cartilage volume was significantly lower in sham compared to other three groups. B. Cartilage thickness was significantly lower in sham compared to other three groups. A significant increase in cartilage thickness was observed in the denaturedµ-dHACM group compared to µ-dHACM. C. Cartilage attenuation significantly increased in saline and denatured µ-dHACM compared to sham compared to saline, single and multiple injection group.

Lesion volume calculations showed no lesions in the sham group. Lesion volume was also significantly lower in the µ-dHACM group compared to saline and denatured µ-dHACM group (Fig 39).

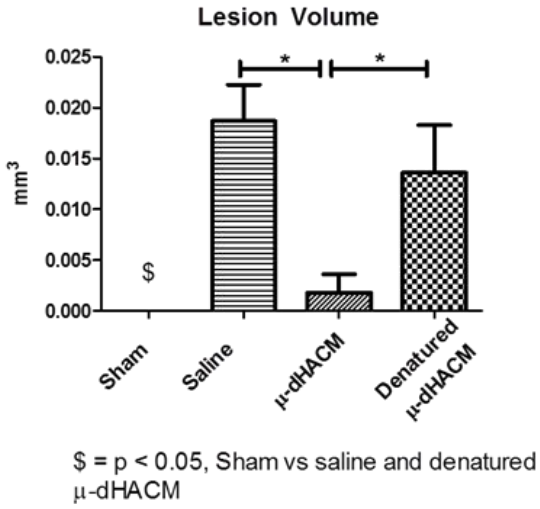

Figure 39. Quantification of lesion volume. Lesion volume was significantly lower in sham compared to the other groups. Lesion volume was significantly reduced in µ-dHACM injected group compared to saline and denatured µ-dHACM groups.

Histology images of the synovium surrounding the femur show retention of both µ-dHACM and denatured µ-dHACM in the synovium (Fig 40). The materialis fragmented and surrounding by infiltrating cells.

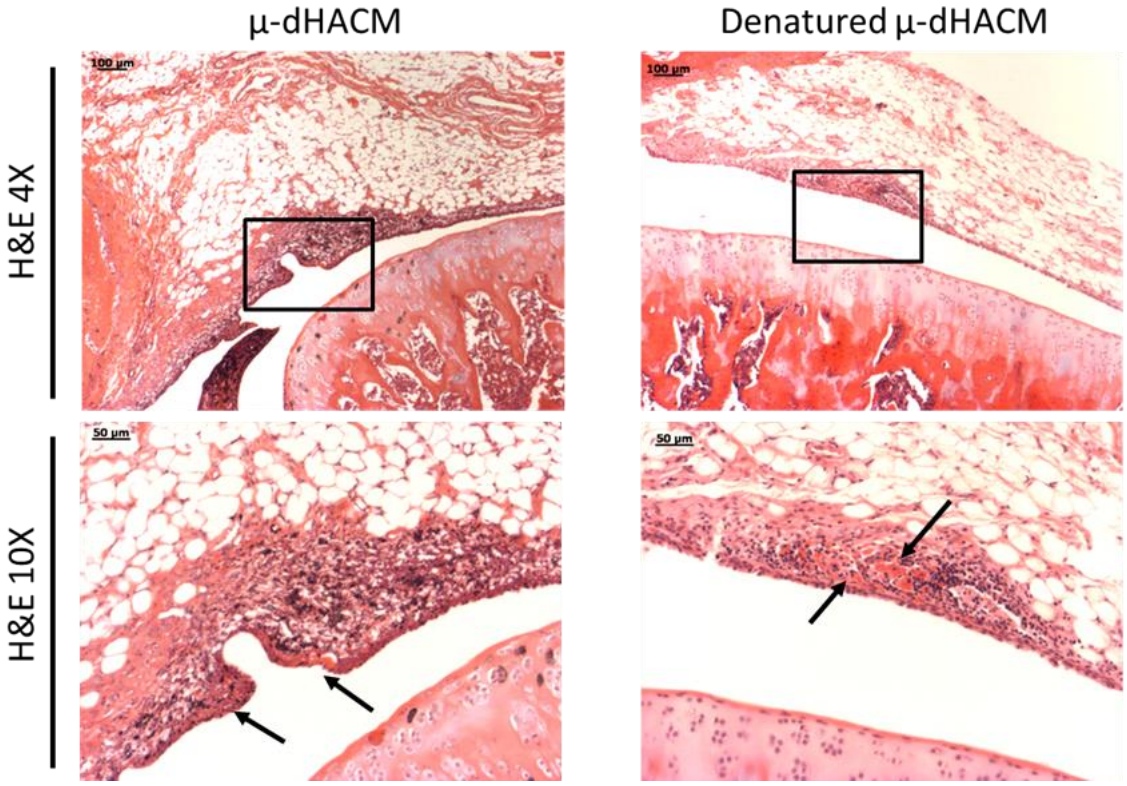

Figure 40. Histological assessment of µ-dHACM and denatured µ-dHACM injected in MMT rats. Fragments of material are visible in both groups as indicated by black arrows.

Discussion

There is an unmet medical need for OA therapeutics as no DMOADs have been approved for clinical use. Extracellular matrices such as dHACM are a promising therapeutic strategy due to their mix of extracellular matrix proteins, growth factors, and anti-inflammatory factors (Ahmed and Burke 1983). Human dHACM allografts also have an established precedence in clinical applications ranging from corneal defects to tendon repair (He, Li et al. 2002, Chandra, Maurya et al. 2005). The objective of this study was to quantitatively assess the efficacy of µ-dHACM (EpiFix® Injectable) as a disease modifying intervention in a rat model of OA.

EPIC-μCT image analysis provided 3D, non-destructive and quantitative evaluation of changes in articular cartilage composition and morphology. The EPIC-μCT data showed a significant reduction in cartilage damage in the form of higher PG levels (lower average attenuation), fewer incidences of erosions and no lesions in the MMT joints treated with μ-dHACM. We also performed histology in this study to compare to our EPIC-μCT results by embedding and processing samples in the sagittal plane. This is the first study to demonstrate the protective effect of a single intra-articular injection of μ-dHACM in the rat MMT OA model.

μ-dHACM had not previously been injected into the joint space; therefore biocompatibility and inflammatory responses were evaluated. Histological analysis indicated moderate local hypercellularity at 3 days and which persisted at 21 days. This response was localized to regions surrounding the μ-dHACM particles and was not present throughout the synovial membrane. This agreed with synovial fluid analyses, which demonstrated an increase in MCP-1 for animals treated with μ-dHACM at 3 days which was then reduced by 21 days. This increase in MCP-1 in response to μ-dHACM was not observed in the MMT/saline animals. This could be due to the fact that the MMT surgery itself caused inflammation and masked the upregulation of MCP-1 caused by μ-dHACM treatment. While MCP-1 can activate and recruit monocytes during inflammation, this pro-inflammatory state may even support a healing response depending on the types of monocytes/macrophages recruited (Mosser and Edwards 2008, Ding, Sun et al. 2009). We did not observe an upregulation in other pro-inflammatory cytokines. The initial analysis of the inflammatory response has some limitations as levels of most cytokines were below the limit of detection by the ELISA multiplex array.

This is likely a technical limitation due to the challenge of harvesting rat synovial fluid, sensitivity of the synovial fluid assay and the limited volume of fluid present in the joint cavity. Alternative methods to explore in the future for synovial fluid analysis include using filter paper absorbent to extract synovial fluid from the joint space and using a more sensitive ELISA such as magnetic beads based multiplex assays. Another reason for these aberrations could be due to fact that µ-dHACM is a xenograft that is being injected in the rat joint. Although we observed a mild to moderate mononuclear inflammation, we did not identify granulocytes, which would indicate a chronic inflammatory response.

Our 6 week study showed some interesting results. This was the first study treating a pre-arthritic joint with µ-dHACM. Interestingly, multiple injections did not seem to have any added benefit compared to a single delayed injection (3 weeks post-surgery). This could be due to animal variability or due to the fact that the animals had to be anesthetized and injected twice, with the injection itself causing some trauma to the joint. A single injection 24 hours post-surgery did not have a lasting benefit up to 6 weeks. This could attributed to the clearance of particles from the joint space as histology at 6 weeks did not show the presence of µ-dHACM in the synovium (Data not shown). Based on previous data and other studies, it is known that lesions are formed on the cartilage surface by 3 weeks in the MMT model. However, no lesions were observed at 6 weeks in the delayed injection group. Histological analysis does depict a more densely packed columnar structure with a bluish tinge in the delayed injection group compared to the sham. The structure of the chondrocytes with its slightly elongated and flattened nuclei indicates towards a mix of fibrocartilage with normal hyaline cartilage(Ross and Pawlina 2011). Studies are ongoing currently to take down animals 1, 3 and 7 days post

delayed injection to examine where the µ-dHACM particles are located and if the lesions are getting filled with a mix of fibrocartilage.

Denaturation of µ-dHACM eliminated its therapeutic effect in vivo. However, in vitro denaturation did not affect cell number. For a more complete picture, additional assays to measure cell activity would be needed. A functional assay, such as a cell migration assay can help understand if there are bioactive factors still present or not after denaturation that influence cell behavior. Denaturation did change the gross morphology of µ-dHACM as observed via histology. The tissue was smaller and appeared to create web like structures. Despite the fragments being smaller, the denatured µ-dHACM was still retained in the synovium up to 21 days. Since a therapeutic effect was not observed but µ-dHACM was retained in the synovium, it indicates that there are components which were deactivated by denaturation and normally do contribute towards a chondro-protective effect. Further studies are needed to characterize and compare the bioactive components in normal and denatured µ-dHACM.

There are several possible mechanisms by which dHACM may modulate the progression of OA. A recent study used ELISA assays to analyze growth factor levels present in µ-dHACM and showed quantifiable levels of PDGF-AA, PDGF-BB, TGFα, TGFβ, basic fibroblast growth factor (bFGF), epidermal growth factor (eGF), placental growth factor (PLGF), granulocyte colony stimulating growth factor, IL-4, IL-6,IL-8, IL-10 and TIMP 1,2 & 4. The PURION process allowed µ-dHACM to retain its biological activity which may play a role in its effect on attenuation of OA in the rat MMT model. dHACM has been shown to suppress the expression of potent pro-inflammatory cytokines, such as IL-1α and IL-1β, and also to decrease MMP levels through expression

of natural MMP inhibitors present in the membrane (Kim, Kim et al. 2000, Solomon, Rosenblatt et al. 2001). dHACM also contains IL-1Ra, a receptor antagonist for IL-1, a pro-inflammatory cytokine that has been shown to be upregulated in OA (Hao, Ma et al. 2000). Two low molecular mass elastase inhibitors – secretory leukocyte proteinase inhibitor (SLPI) and elafin – are present in the dHACM, both of which exhibit anti-inflammatory properties (Niknejad, Peirovi et al. 2008). Hyaluronic acid is also present and acts as a ligand for the CD44 receptor which is expressed on inflammatory cells and plays a role in adhesion capabilities of immune cells (Niknejad, Peirovi et al. 2008). In addition to anti-inflammatory molecules, devitalized µ-dHACM particles have been shown to retain a variety of bioactive substances including multiple growth factors such as PDGF and FGF (Ji, Xiao et al. 2011). PDGF and FGF-18 have previously been implicated in chondrocyte growth (Liu, Lavine et al. 2007). All of these potential mechanisms, including maintenance of cartilage homeostasis and reduction of inflammation and MMP expression, may be active contributing factors to the observed protective effect of µ-dHACM. dHACM also retains natural structural components such as collagens (types I, III, IV, V, VI), fibrinogen, laminin, nidogen and PGs. While these components clearly are important for the regulation and maintenance of normal chondrocyte metabolism, whether the extracellular matrix composition of dHACM directly affects OA is unclear (Jin, Park et al. 2007). However, retention of the active regulatory components may be influenced by the size and composition of the dHACM particles.

While the mode of action of a disease modifying therapy is a key component to the efficacy, local retention of the factor is also thought to be critical. Retention is

particularly challenging when considering small molecule DMOADs. The particle size of the drug or carrier is critical since particles less than 6 microns are quickly filtered through intercellular gaps or phagocytosed by macrophages (Edwards 2011). Clinical studies measuring residence time of various NSAIDs delivered intra-articularly found the half-life to range from 1.1 to 5.2 hours (Owen, Francis et al. 1994). Alternatively, larger particles likely illicit an immune response or may cause physical damage to the articular surface (Martel-Pelletier, Wildi et al. 2012). In this study, the µ-dHACM particles sequestered in the synovial membrane at three days were large enough to prevent rapid clearance. Recent research has focused on extending the residence time of drugs in the joint cavity via the use of biomaterials including PLGA, albumin and bio-polymer based carriers. In pre-clinical models, drug release from PLGA particles has been reported to last up to 14 days, but once released, the drugs were rapidly cleared (Butoescu, Jordan et al. 2009). Although further studies are needed to elucidate release kinetics and assess whether extended residence time translates to increased duration of therapeutic activity, µ-dHACM presents a potential advantage over other intra-articular therapeutics due to its retention through 21 days in the synovium, though release kinetics of any active factors would also play a role. µ-dHACM thus has the potential to require less-frequent injections to treat OA.

In conclusion, this is the first study demonstrating reduction in cartilage degeneration in a small animal OA model via a single intra-articular injection of an ECM based treatment derived from amniotic membrane. EPIC-µCT, used as an analytical tool, showed, by way of several quantitative metrics, a cartilage-protective role for µ-dHACM. µ-dHACM is a minimally manipulated and marketed allograft material which has been

shown to be clinically effective in a variety of applications (Sharma, Maria et al. 2011, Forbes and Fetterolf 2012)and now through this study, µ-dHACM is presented as a potential disease modifying OA therapy.

CHAPTER 6

SUMMARY AND FUTURE DIRECTIONS

Overall Summary

Developing and testing new DMOADs remains a pressing clinical need. This research would require improved diagnostic techniques and suitable outcome measures in pre-clinical animal models to enhance the drug development process. A variety of new therapeutics are being tested in pre-clinical models; however, this testing is time consuming, semi-quantitative and expensive. The lack of an objective, quantitative technique to analyze articular cartilage has limited the utility of testing different therapeutics in an efficient, standard manner. EPIC-µCT is a unique and powerful tool with the ability to rapidly and quantitatively analyze articular cartilage in OA models.

Articular cartilage cannot be visualized via normal imaging methods due to its composition and analyzing the effects of a therapeutic on cartilage in a pre-clinical rat OA model via traditional imaging techniques is a challenge. Accordingly, the overall objective of this proposal was to examine two distinct treatment strategies for OA in a rat joint degeneration model using EPIC-µCT. The central hypothesis of this work was that EPIC-µCT could be used to establish quantitative outcome measures which would be sensitive to detect effects of therapeutics in the rat OA model.

To test our hypothesis, OA was induced surgically in the rat and two different therapies were tested in the model. First, we characterized two models of joint degeneration using EPIC-µCT in the rat – the MIA model and the MMT model (Aim I, Chapter 3). Our results indicated that the MIA model, even a low dose, causes global articular cartilage damage whereas the MMT model leads to focal areas of damage which

can be quantified via EPIC-μCT. We were able to define ROIs for the MMT model and establish outcome measures such as lesion volume and attenuation. Our results coupled with the fact that the MMT model is the most commonly used model for testing DMOADs, led us to selecting the MMT model for future experiments. Following this, we analyzed the sensitivity of the EPIC-μCT technique by testing a small molecule drug, an MMPi, in the MMT model (Aim II, Chapter 4). In this study, we analyzed earlier time points and were successfully able to detect changes in the articular cartilage as early as two weeks. Results of a power analysis showed that EPIC-μCT was more sensitive than histopathology based on certain parameters. We established multiple quantitative outcome measures using EPIC-μCT- cartilage thickness/volume/attenuation, subchondral bone volume, osteophyte thickness/volume and lesion/erosion incidence and lesion volume. Finally, building on these two studies we finally tested a novel ECM based therapeutic (μ-dHACM) in the rat OA model with EPIC-μCT as our diagnostic tool (Aim III; Chapter 5). The results demonstrated reduction in joint degeneration in response to a single intra-articular injection of μ-dHACM. More interestingly, μ-dHACM also slowed down the progression of OA in a pre-arthritic joint when examined at a longer time point. Denaturation of μ-dHACM led to loss of a chondro-protective effect. Overall, this thesis presents original research on using EPIC-μCT as a diagnostic tool for analyzing articular cartilage in combination with presenting a novel ECM based therapeutic that can slow down OA progression.

Articular Cartilage Analysis in the MMT Model

Aim I focused on characterizing the MMT model using EPIC-µCT. To our knowledge, this is the first instance of using contrast based imaging to evaluate this model and determine quantitative parameters. Our working hypothesis was that EPIC-µCT could quantitatively detect degenerative cartilage changes in the MMT model. To test this hypothesis, we induced joint degeneration surgically in the MMT model and defined localized regions of interest to facilitate detection of cartilage changes and compared the results to contralateral joints. We followed this study with Aim II, where we analyzed the effects of a small molecule based MMPi on the articular cartilage to determine the sensitivity of the EPIC-µCT technique and compared it to traditional histopathology results.

Our results from Aim I for the MMT model contradicted some of the previously published results in literature. An increase in cartilage volume and thickness was observed in the MMT joints compared to contralateral controls. This was interesting as the expected and most commonly observed result observed via histology is thinning of the articular cartilage, a hallmark of OA. This "thickening" effect of the cartilage in an arthritic joint was detected by EPIC-µCT. There are a couple of reasons why it has not been observed commonly in the past. First, histology processing involves dehydrating samples. Since cartilage is mostly water, this thickening effect would be difficult to detect. Second, histology measurements are 2D and are based on only a few slices per sample to get representative values. EPIC-µCT, however, provides a complete 3D analysis and the sample is not dehydrated. We believe that the cartilage thickening effect observed was in response to the MMT surgery, where the PG network is loosening and

will eventually lead to cartilage degeneration. Our 6 week data in Aim III, did show large areas of surface damage and a lower degree of cartilage thickening compared to our 3 week study. Another factor that could be contributing the increase in cartilage thickness is marginal osteophyte growth.

Osteophytes are another characteristic of OA, which we evaluated in Aim II. The EPIC-μCT analysis was performed on sagittal sections as our volume of interest was the medial tibial and medial 1/3 of the medial tibial plateau. Osteophytes grow on the periphery of the cartilage and can be observed on coronal slices. Delineating the cartilage in the sagittal sections could have included portions of the osteophyte on the margins which could also lead to an increase in the value of cartilage thickness/volume measurements. One of the most interesting results with regards to OP was the visible progression of mineralization. Mineralization in OP, particularly at early time points such as 2 weeks is difficult to detect via histology due to decalcification of samples. In human OA, as the disease progresses, the OP gets mineralized eventually showing up on x-rays as bone spurs. The MMT model, while does show OP progression does not show bone spurs at least at a 6 week time point.

The MMT model though widely used does also have certain limitations. One, the model presents a continued destabilization of the joint which is challenging for a therapeutic to overcome. Longer term studies in this model, even the 6 week time point (Aim III) showed extensive cartilage damage. Since the meniscus can never be repaired, the continuous loading of the joint would lead to cartilage damage which even an effective therapy cannot reverse. In humans, in case of a meniscus tear or similar injury, the joint is usually stabilized externally and less weight is put on the joint. In rats, the

continuous movement can make it difficult to necessarily observe a significant therapeutic benefit. A recent study showed that the transection of the meniscus also does not lead to a functional deficit as measured by gait analysis until 8 weeks(Allen, Mata et al. 2012). With OA, there isn't a strongly coupled structural-function relationship as often there are patients whose x-rays show no anomalies but suffer from pain and there are cases with patients with bone spurs only having mild pain. The lack of an earlier functional response in this model renders it unsuitable for analyzing pain. Using both the MIA and MMT model to evaluate a therapeutic could be useful to examine a pain response and disease modifying response, respectively. EPIC-μCT can still be used as a diagnostic tool for articular cartilage analysis with additional measures such as histology for cellular behavior and gait analysis for functional assays.

EPIC-μCT provides various parameters that can be evaluated in response to a therapeutic though certain limitations exist. EPIC-μCT scans are at a 16μm voxel size which is not high enough to examine cellular morphology or microscopic changes. Histology can provide additional parameters including cellularity. There may be surface damage lower than 16um which cannot be analyzed by EPIC-μCT. Real-time longitudinal analysis via contrast based imaging is an area that is being explored by various groups but the resolution and segmentation remains a challenge. Piscaer et al. performed in vivo EPIC-μCT arthrography in a high dose MIA model and were able to show changes in cartilage volume and attenuation(Piscaer, Waarsing et al. 2008). However, equilibrium of the contrast agent was not achieved and it was not possible to have a standard threshold measure to discriminate between the cartilage and underlying calcified cartilage bone layer (Piscaer, Waarsing et al. 2008). Being able to analyze the

cartilage longitudinally will significantly reduce number of animals required and help understand real time effects of various therapeutics.

This work has advanced our knowledge about the MMT model and the suitability of EPIC-µCT as an imaging technique. Ongoing work in the lab includes shorter time points for the MMT surgery and utilizing MATLAB to write custom programs to perform surface analysis in addition to EPIC-µCT outcomes. Future work involves translating the MMT model to a larger animal (sheep) and developing suitable EPIC-µCT imaging methods to analyze the cartilage. We are also trying to optimize the technique using a uCT50 scanner of 8µm resolution to analyze murine cartilage. This will open up the area to test therapeutics in transgenic mice as well as use knock-out OA models for analysis.

The use of EPIC-µCT in this thesis has been limited to articular cartilage analysis in the MMT model. The technique can be extrapolated to other applications as well including but not limited to osteochondritis dissecans(OCD), intervertebral disc disorders, micro-fractures and cartilage explant models. This would require optimizing the technique for the particular application in terms of equilibration times, concentration of contrast agent, selecting suitable VOIs but it is a possibility. Current work in the lab includes developing an OCD model in the rats and using EPIC-µCT to analyze it. With suitable outcome measures, EPIC-µCT provides a new platform for cartilage analysis in a rapid, quantitative and efficient manner.

Mode of Delivery

In this study we used two modes of drug delivery - oral delivery of MMPi and intra-articular delivery of µ-dHACM. Oral delivery allows for controlling the dose and

having a formulation that can be ingested. Intra-articular delivery allows for localized injection but is limited by half-life and retention rates in the joint space.

The current line of treatment, NSAIDs and COX-2 inhibitors are mostly delivered orally. However, this has led to side effects including GI ulcers and bleeding (Janssen, Mihov et al. 2014). Several MMPi's have been tested in clinical trials but none have been successful yet due to lack of efficacy and unfavorable risk-benefit profile (Fingleton 2007). There is also the challenge of bio-availability via oral or systemic delivery (Janssen, Mihov et al. 2014). Assessment of therapeutic index for MMPi's which is the ratio of dose required for efficacy vs. toxicology is challenging and systemic delivery necessitates the use of a larger dose (Peterson 2006). This has led to research for alternate methods to deliver therapeutics. Intra-articular (IA) drug delivery is clinically used for compounds such as hyaluronan. This mode is limited due to its invasiveness and a maximum of four injections/year are allowed (Hinton, Moody et al. 2002). Half-life of compounds in the knee joint and rapid clearance rates are limiting factors for this.

In our study, 30mg/kg of MMPi was delivered orally every day which showed a therapeutic benefit in-vivo. In the case of μ-dHACM, a single IA injection at 80mg/ml suspended in 50μl saline, showed a therapeutic benefit as well. Though the same drug was not used in both the experiments and a direct comparison is not possible, the fact that a lower amount of therapeutic was needed intra-articularly is not surprising.

Oral/systemic delivery requires a greater dose leading to higher risk of side-effects. IA delivery allows for localized injection where the effects of the drug are mostly restricted to the joint space. A key factor for suitable IA delivery is size which affects

retention rate. The presence of synovial fluid in the joint leads to clearance of particles from the joint space if they are too small. If the particles are too large, that can cause irritation in the joint and lead to inflammation (Gerwin, Hops et al. 2006). µ-dHACM was retained in the synovium and this could be due the fact that it possesses fragments of natural ECM in its matrix.

Choosing a mode of delivery is dependent on the structure and mechanism of action of the therapeutic. The MMPi treatment is a small molecule which could not be retained in the joint without a suitable delivery vehicle whereas µ-dHACM is an ECM based therapeutic that could not be ingested orally. Longer term effects and toxicology studies for both the MMPi and µ-dHACM can help understand if the selected mode is optimal and what parameters might need to be modulated for effective delivery.

Therapeutic Effect of µ-dHACM

The search for effective DMOADs is a very active area of research. There are at least 12 DMOADs that are in human clinical trials currently, most of them delivered orally (Hunter 2011). Fibroblast growth factor 18 (FGF-18) demonstrated cartilage repair in the rat MMT model and is currently in clinical trials as well (Beenken and Mohammadi 2009). We took an ECM based therapeutic approach in the form of u-dHACM to test its effect on the articular cartilage as listed in Aim III. Our working hypothesis was that intra-articular delivery of µ-dHACM (EpiFix™ Injectable) will ameliorate the progression and extent of joint degeneration in the rat MMT model and based on our results from Aim II, EPIC-µCT would be able to assess changes in the articular cartilage in response to µ-dHACM. We tested this hypothesis by injectingµ-

dHACM in MMT rats 24 hours post-surgery and analyzing cartilage at 3 weeks. We also examined longer term effects at 6 weeks, delivering µ-dHACM 24 hours and/or 3 weeks post-surgery. Finally, we denatured µ-dHACM to see if denaturation of the matrix leads to a loss of therapeutic benefit.

Our data showed some very promising results of µ-dHACM as a DMOAD in this pre-clinical study. In the 3 week study, a single intra-articular injection of µ-dHACM led to inhibition of lesion formation in the treatment group. In the MMT model, if the surgery is performed correctly, all joints develop lesions by 3 weeks which has been observed in multiple studies(Bendele 2002, Moore, Bendele et al. 2005, Gerwin, Hops et al. 2006, Gerwin, Bendele et al. 2010). The inhibition of these lesions was a very potent effect of µ-dHACM, that too with just a single injection. Histology showed retention of µ-dHACM fragments in the synovium up to 3 weeks post injection suggesting that this presence might be important for a therapeutic response. Injecting µ-dHACM 24 hours post-surgery can help delay the onset of OA as indicated in the 3 week study. This could be useful in situations of post-traumatic OA. Individuals with joint injuries such as ACL transection, meniscal tear are more prone to OA. Post-traumatic OA is prevalent in the military population with joints suffering from war injuries leading to 60% rate of OA and with a 100% rate of OA following knee injury (Rivera, Wenke et al. 2012). Exploring the applicability of pre-treatment withµ-dHACM to delay the onset of post-traumatic OA is another area of interest.

Based on our 3 week study results, we wanted to test what would happen at a later time point of 6 weeks in case of a single injection (24 hours post-surgery), delayed injection (3 weeks post-surgery) and multiple injection (24 hours and 3 weeks post-

surgery). Our 6 week results were surprising, as the delayed injection group showed the greatest therapeutic benefit whereas the multiple injection did not perform any better than the delayed. The single injection did not have any therapeutic benefit at 6 weeks. It is important to note that the MMT model is an aggressive model, and the ability of µ-dHACM to show a chondro-protective effect at 6 weeks was very promising. The lack of a benefit of multiple injections was unexpected though. One reason could be animal variability or the invasiveness of the injection since the animals had to be anesthetized twice and injected into joint space. Histology at 6 weeks did not show retention of µ-dHACM in the joint space. This could be due to the aggressive nature of the MMT model and increased clearance rates through the joint as the disease progresses. As the disease caused more degradation at 6 weeks, we had to include new parameters for EPIC-µCT analysis. Lesion volume calculations were not possible as extensive degradation was observed in the saline injected MMT joints making it difficult to delineate suitable contours. Hence, exposed bone area was calculated using a custom MATLAB program. The reasoning behind conducting a 6 week study, though the standard is 3 weeks in the field, was to simulate human OA. In the clinic, patients start taking therapeutics after pain and damage has already started(Hunter, Guermazi et al. 2013). The delayed injection simulates treatment of a pre-arthritic joint as by 3 weeks cartilage damage is already observed in the MMT model.

µ-dHACM presents itself as a potential DMOAD candidate but the mechanism behind its working is still unclear. In this thesis, the focus was to test EPIC-µCT as a diagnostic tool for articular cartilage analysis. We used it to examine the effects of µ-dHACM and saw promising results. Denaturing µ-dHACM was the first step to examine

the role that growth factors and cytokines might play. Denaturation of µ-dHACM was performed via heat treatment and histology results indicate changes in the µ-dHACM structure. Though the results did show that denatured µ-dHACM did not have a therapeutic benefit similar to µ-dHACM, it is difficult to conclude if this was due to change in structure or depletion of GFs. In vitro results were inconclusive as well since cell proliferation was not affected by the denaturation process. In this study, only one in vitro assay was performed which does have limitations. For a more complete picture on the role of GFs and cytokines, additional assays to measure GFs in extract and cell culture would be needed. A functional assay, such as a cell migration assay can help understand if there are bioactive factors still present or not after denaturation. Further work is needed to tease out the role that GFs might play.

There are multiple lines of future work involved with µ-dHACM. One includes performing a time course experiment to determine how long µ-dHACM is retained in the synovium and examining if there is a correlation between retention period and therapeutic benefit. We are currently performing additional histology on the delayed injection study, by taking down animals 1, 3 or 7 days post injection (where the injection is 3 weeks post-surgery). This would help understand if µ-dHACM is being retained in the joint space and if it is filling up the pre-existing lesions that develop at 6 weeks. Our lab has also performed experiments with different formulations of µ-dHACM, where one formulation removes the epithelial layer during the production process (Unpublished data). This can shed light on the role of the epithelial layer with its different constituents on the chondro-protective effect. We have also looked at different size formulations including super-micronized µ-dHACM to see if the size of the original particles affects the articular

cartilage (Unpublished data). To understand the mechanism of µ-dHACM, in vitro assays would be essential. Contrary to our expectations, denaturation did not provide concrete conclusions towards the role of GFs. Inhibition of GFs implicated in OA and present in µ-dHACM (ex: PDGF, FGF, EGF) via small molecules with appropriate controls in vitro could be a first step. This could be translated in vivo by injecting µ-dHACM pre-incubated with these inhibitors. Another step could be decellularizing µ-dHACM followed by testing it in vitro and in vivo. The PURION® process devitalizes the amnion matrix but does not actively decellularize the material. A study by Bhatia et al. demonstrated elimination of growth factors and cytokines after decellularization of human amniotic membrane(Bhatia, Pereira et al. 2007). Another study showed a significant decrease in collagen, GAG, elastin, DNA and matrix hydroxyproline upon decellularization as well (Wilshaw, Kearney et al. 2006). Comparing and characterizing denatured, decellularized µ-dHACM and normal µ-dHACM and its responses in vivo could help understand the therapeutic effect observed. Additionally, the outcome measures so far have focused on articular cartilage. Analyzing the inflammatory and immune response would also be important in the future. One limitation is that µ-dHACM is human derived material which would always elicit some form of inflammatory/immune response in the rat model. Also, the MMT model causes inflammation as well and sham surgeries would be required as a control to compare responses in various groups. Another avenue to explore would be testing µ-dHACM in the MIA model to evaluate effects on pain. There are plans to translate this work to a larger animal model, in the sheep, in collaboration with San Antonia Military Medical Center (SAMMC).

There is no published work from other groups on the utility of µ-dHACM as a DMOAD. This is a clear area for future investigation in light of the results observed in the rat MMT model. As with in vivo models, it is important to understand the limitations of the selected model. OA in rats translates to a functional deficit much later than large animal models. Additional outcome measures other than EPIC-µCT need to be considered now that µ-dHACM has passed the initial screening process of having a positive effect on the articular cartilage. By designing suitable experiments with appropriate controls, we can advance our understanding of µ-dHACM and the role it plays on articular cartilage. This can open the area towards exploring ECM based therapies for OA, stepping away from the traditional small molecule inhibitor drugs.

CONCLUSIONS

In conclusion, the results demonstrate the utility of EPIC-μCT as an innovative tool to quantitatively analyze articular cartilage in a pre-clinical OA model. Multiple 3D parameters were established that can quantify localized damage in the MMT model and used as outcome measures to test therapeutic efficacy. The ability of this technique to screen DMOADs was demonstrated by testing an MMPi and discerning its therapeutic effects on articular cartilage. A novel ECM based material - μ-dHACM is also presented as a potential DMOAD in this thesis. This is the first instance that shows an ECM based therapeutic ameliorating OA progression via a single intra-articular injection. Moreover, a delayed injection slowed the rate of disease progression in a pre-arthritic joint which has not been observed previously. Taken together, the results suggest that EPIC-μCT can be successfully used to screen for DMOADs and μ-dHACM is one such screened therapeutic that can potentially be translated to larger animal models.

APPENDIX A

EFFECT OF PREGNANCY ON PROGRESSION OF JOINT DEGENERATION IN A RAT MODEL[d]

Introduction

OA is a progressive joint disease characterized by loss of cartilage, sclerosis of subchondral bone, formation of osteophyte and inflammation of synovial membrane due to imbalance in production and degradation of the cartilage extracellular matrix (Goldring and Goldring 2007).

Multiple factors have been proposed to be involved in the initiation and progression of OA, such as injury, age, gene, sex and obesity (Goldring and Goldring 2007). Local factors, such as the curvature and lubrication of articular cartilage, load bearing, alignment of low limb, have been well studied, while systemic factors have yet to be well investigated due to their complexity. Systemic factors such as age, gene and gender have been proposed to regulate ageing and rejuvenate blood and other tissues(Mayack, Shadrach et al. 2010). These factors have been proposed to be implicated in OA. Genetic factors are influenced by gene. The candidate genes associated to OA are variant between men and women (Valdes, Loughlin et al. 2007). The incidence of OA disease peaks with the age being > 30 in men and > 50 in women (Claassen, Schicht et al. 2011).Menopause in women has also been co-related with a higher incidence of OA prevalence (Claassen, Schicht et al. 2011). It is associated with significant systemic

[d] Portions of this chapter were adapted from Zhang K*, Thote T*, Leng H, Guldberg RE, Ge Z. Effects of Pregnancy on Progression of Osteoarthritis Induced by Monosodium Iodoacetate in Rats. JMBE33(5): 449-454. 2013. (* Co-first authors)

physiologic changes, such as regulation of immune response and changes in hormones (estrogens, progesterone, prolactin, and androgens).

Pregnancy is involved in significant change of hormones, metabolism, and gene expression. Pregnancy has also been reported to suppress expression of both synthetic and degradative genes, including type II collagen, biglycan, TGF-β, collagenase, TIMP-1, IL-1β, TNF-α, iNOS and COX-2 (Hellio Le Graverand, Reno et al. 1998, Hellio Le Graverand, Reno et al. 2000). Based from these studies, it is reasonable to hypothesize that pregnancy, as well as subsequent physiological changes may affect the progression of OA.

OA can be induced through various methods such as via surgery, chemical injection, mechanical overuse or through spontaneous genetic OA models. Injection of monosodium iodoacetate presents a method of chemical induction of OA that is well characterized and has been extensively used in relation to examining joint pain in rats(Guzman, Evans et al. 2003). In the current study, OA was induced in Wistar rats using a low dose of MIA based on previous studies (Janusz 2001). EPIC-μCT was used as a quantitative method to analyze cartilage morphology and structure (Xie, Lin et al. 2012).

Methods

Animal Experiment

All animal experiments were operated in Animal Center of Peking University, which has been approved by the Association for Assessment and Accreditation of Laboratory Animal Care (AALAC). Twenty female Wistar rats aged 12 weeks weighting 280-300g were divided into four groups, and five adult male rats were used to mate with

female rats. All the animals were housed in sterile animal rooms with controlled temperature and humidity. The animals were divided into four groups: A – Pregnancy + MIA, B – Only MIA in naïve rats, C – Only pregnancy and D – Saline injections in naïve rats. MIA (I2512, Sigma-Aldrich, St. Louis, MO) injection was injected into the intra-articular joint space of the female rats on the day of detection of vaginal plug. The rat knee joint was injected with 0.3 mg MIA in 50µL saline with a 27 gauge needle after pregnancy was confirmed. Group B received the same dose of MIA. Group C (only pregnancy) and group D (sham group) received saline injections. All the rats were euthanized on day 18 via CO_2 inhalation.

Macroscopic score

Rat limbs were harvested after sacrificing the rats and the left legs were fixed in 10% neutral buffered formalin for 48 h. The rat joint was dissected and surrounding tissue was excised. Images were taken using a digital camera (DSC-H10, Sony) and these macroscopic images were evaluated by two people in a blinded evaluation. The cartilage was assessed using a scoring system with a range of 0–4. Increasing score represented increasing severity of OA (0 represented normal appearance; 1 represented slight yellowish discoloration in the surface; 2 represented little erosions in load-bearing zone; 3 represented large erosions extending to the subchondral bone; and 4 represented large erosions with subchondral bone exposure (Janusz 2001). The scores were added and the mean was calculated for different groups.

µCT

EPIC-µCT was performed as listed in Aim I. Briefly, the proximal end of each tibia was immersed in 2ml of 30% Hexabrix 320 contrast agent (Covidien, Hazelwood, MO) and 70% ion-free PBS at 37ºC for 30 minutes, an incubation period known to result in equilibration of the agent (Palmer, Guldberg et al. 2006, Xie, Lin et al. 2009). Proximal tibiae were blotted dry and scanned using a µCT 40 (Scanco Medical, Brüttisellen, Switzerland)at 45 kVp, 177 µA, 200 ms integration time, and a voxel size of 16 µm (Xie, Lin et al. 2009). Scanco evaluation software was used to assess 3D morphology and composition. Raw scan data were automatically reconstructed to 2D grayscale tomograms.

GAG Quantification

For quantification of the GAG content, fresh tibial cartilage from the right knees of the rat joints was harvested using a scalpel, weighed and flash freezed using liquid nitrogen. The lyophilized sample was digested with 0.5 mg/mL proteinase K (P2308, Sigma) in 100 mM K_2HPO_4 at pH 8.0 in 56°C overnight. The digested sample was added to 1, 9-dimethylmethylene blue solution (DMMB, 341088, Sigma-Aldrich, St. Louis, MO), shaken for 30 min, and then centrifuged at 10,000g to separate the precipitate. The precipitate was dissolved with a dissociation reagent and the absorbance was measured at a wavelength of 656 nm in a microplate reader (680, Bio-rad, Japan). The standard of GAG content was constructed using chondroitin sulfate (C4384, Sigma-Aldrich (Shanghai) Trading Co.,Ltd). The GAG content of each group was normalized by its weight.

Statistical analysis

All the data are presented as mean ± SD. SPSS V13.0 (SPSS Inc., IL, USA) was used to analyze the data, and one-way analysis of variance (ANOVA, LSD) was utilized to compare the pregnancy + MIA, MIA, pregnancy and sham groups. The statistical significance was set at a 95% confidence interval ($p<0.05$).

Results

Macroscopic score

There were no signs of infection in all experimental animals during the entire experiment. The tibial plateaus were smooth without any observable damage in the rats from group A (Figure 1A), group B (Figure 1B), group C (Figure 1C) and group D (Figure 1D). No chondral erosions were observed and neither did erosions appear in the load-bearing areas. No statistical significance could be detected in group A, B, C and D based on macroscopic scoring.

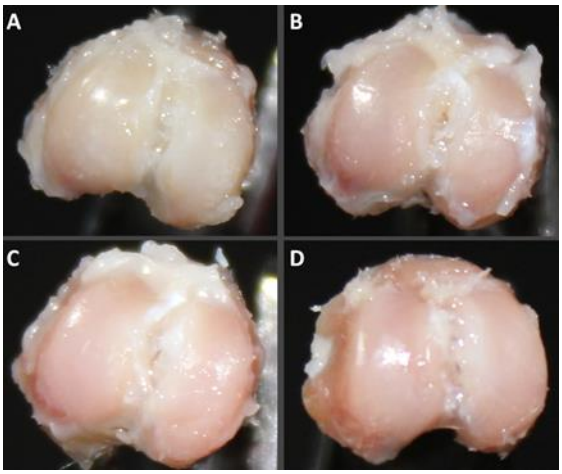

Figure A.1. Macroscopic image of tibial cartilage in (A) Pregnancy+MIA; (B) MIA; (C) Pregnancy; (D) Sham groups.

µCT

EPIC-µCT was used to measure cartilage attenuation and volume. No significant difference was observed in cartilage volume between groups. Cartilage attenuation was significantly higher in Pregnancy + MIA and MIA groups compared to Pregnancy and Sham groups(Figure A.2).

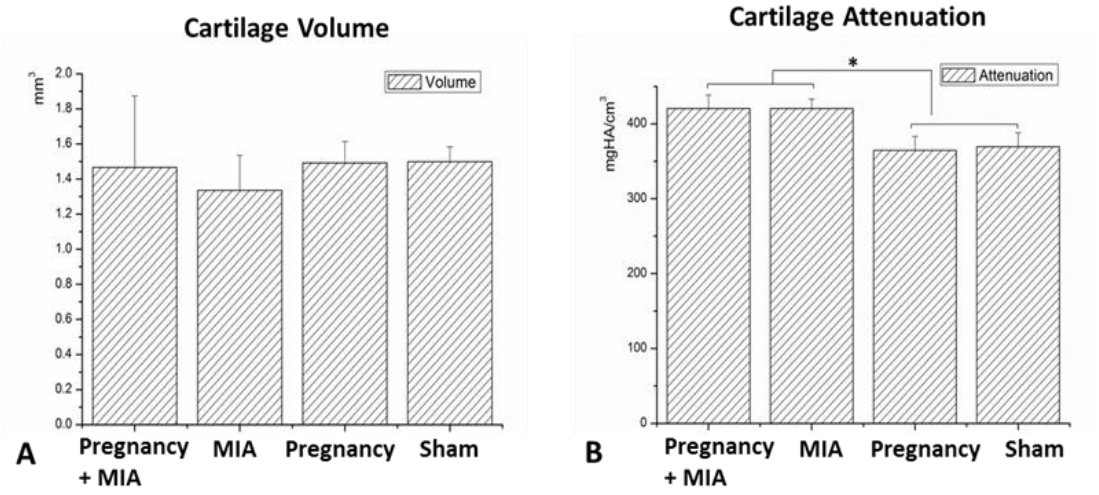

Figure A.2. EPIC-µCT measurements of articular cartilage. A. Cartilage volume was not significantly different between groups. B. Cartilage attenuation was significantly higher in Pregnancy + MIA and MIA groups compared to Pregnancy and Sham groups
* = $p < 0.05$, n = 5

GAG Quantification

MIA induced low GAG content of cartilagein rat OA model.GAG amount was significantly higher in Pregnancy and Sham groups compared to Pregnancy + MIA and MIA groups(Figure A.3.).

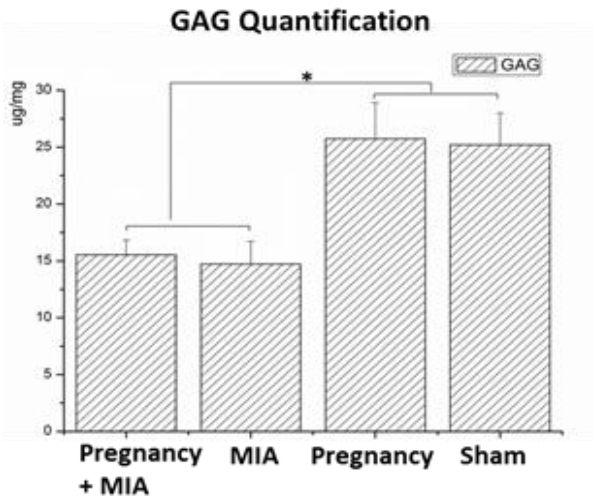

Figure A.3. GAG quantification of articular cartilage. GAG content was significantly lower in Pregnancy + MIA and MIA groups compared to Pregnancy and Sham groups
* = $p < 0.05$, n = 5

Discussion

Pregnancy is a complex physiological process accompanied with changes in the hormonal level. It has been implicated in playing a role in the regenerative capacity of certain tissues and cells. In this study, the focus was to examine the effect of pregnancy on the progression of OA.

Multiple factors are involved in the initiation and progression of OA, and estrogen is one of these. Estrogen receptors have been found in cartilage, immortalized chondrocyte cell lines and in primary chondrocytes (Claassen, Schicht et al. 2011). This suggests that cartilage is a potential target for estrogen. However, the relationship between estrogen and OA remains inconsistent. Some studies found that there was no direct relationship between estrogen and OA. Estrogen treatment did not have an effect on the severity of OA in ovariectomized animals and deletion of estrogen receptors did not cause overt cartilage damage (Ham, Oegema et al. 2004, Ma, Blanchet et al. 2007,

Sniekers, van Osch et al. 2009). On the other hand, some results indicated that estrogen had protective effects on OA. OA was elevated with estrogen deficiency and estrogen therapy preserved cartilage(Tanko, Sondergaard et al. 2008, Roman-Blas, Castaneda et al. 2009).Contrarily, some results suggest that estrogen has negative effects on OA. Estrogen treatment caused synovial estrogen and estradiol receptor bindings to be increased, which induced cartilage degeneration and cell death, leading to the development of knee OA (Silberbe.R 1971, Tsai, Liu et al. 1992). As the relationship between estrogen and OA is still unclear, a definitive conclusion to this subject remains to be stated.

As estrogen is a pregnancy associated hormone and elevated during the process in mammals, pregnancy may be related with metabolism of cartilage and OA. The gene expression of normal articular cartilage can be influenced by pregnancy. Gene expression of type II collagen, biglycan, collagenase, TIMP-1, IL-1β, TNF-α, TGF-β, iNOS and COX-2 has been reported to be suppressed in pregnant rabbits Although pregnancy could improve the regenerative capacity of some tissues, the relationship between pregnancy and OA cartilage has not been explored in vivo.

Various animal models have been established to mimic human OA and study the pathology of the disease, including surgical/physical, chemical and spontaneous models. Considering the gestation period of rats of around 20 days, MIA was chosen as the method to induce OA due to its rapid effect(Janusz 2001). MIA induces OA through restraining glycolysis of the chondrocytes by inhibiting of glyceraldehyde-3-phosphate dehydrogenase. It is different from the natural OA process, as inflammatory mediators such as interleukin-1β(IL-1β) and tumor necrosis factor (TNF)-α are increasing. It is

important to be noted that the animal model cannot represent all aspects of human OA(Goldring 2012). As we focused on the morphology of arthritic cartilage, MIA induced OA model was chosen as it is efficient and reproducible. We used a low dose MIA model to be able to elucidate the changes in the pregnant rat. Using a low dose, prevented severe articular damage from taking place but did result in lower PG content.

In our results, the attenuation of cartilage as detected by EPIC-μCT was higher in MIA groups compared to non-MIA groups. This indicated lower PG levels in MIA groups, which is a characteristic of OA. However, there was no significant effect of pregnancy on attenuation, volume, thickness and GAG content between the pregnant and non-pregnant groups.

In this study, as no significant effects were found, it is difficult to speculate on long term effects of pregnancy and OA. One of the reasons for no changes could be due to the short gestation period of rats compared to other mammals. It was possible that if an animal with longer gestation was analyzed, significant changes could be observed. However, with our data we were unable to prove that pregnancy had any effect on OA cartilage. Though no changes were observed, EPIC-μCT provided a successful method to analyze articular cartilage in the MIA model. In order to study the comprehensive effect of pregnancy on the cartilage, more parameters such as gene expression, protein levels and analysis of synovial fluid are needed.

APPENDIX B

PROTOCOLS

B.1 Medial Meniscal Tear Surgery

Procedure

1. All personnel should wear scrubs, masks, head caps, and booties to ensure sterile environment.
2. Surgeons and sterile assistants should scrub in.
3. After scrubbing in, sterile personnel should assemble surgery tables making care to ensure a sterile surgical field. Non-sterile personnel assist in opening packaging.
4. Position glass bead sterilizer and turn on.
5. Position the circulating water bed and turn on to pre-warm for surgery. Cover with a sterile drape.
6. Animal prep can begin when surgeons are adequately close to operating. Care should be taken to minimize the time that animals are anesthetized.
7. Transfer a properly prepared rat to the surgery table. Insert the rat's nose into the nose cone, and straighten the tail so that it is not in contact with the feet of the animal.
8. Non-sterile personnel should hold each foot/toes with forceps to allow sterile personnel to wrap the feet with ioban.
9. Cut a hole in a sterile drape and position over the rat such that only the leg and surgical site are exposed.
10. Have sterile assist orient the leg to have the medial joint space facing the surgeon

11. Feel for the joint space using either hemostat or fingers. This can be done by flexing the knee
12. Make a skin incision using the scalpel with the joint space as the mid-point
13. Perform blunt dissection to reach the MCL
14. Slide the micro-dissections forceps under the MCL to grip the MCL in the forceps teeth (make sure to not cause any trauma with forceps)
15. Transect the MCL with microdissection scissors (long tip) above the joint space
16. Peel and cut away tissue attaching MCL to the underlying bone to reveal the meniscus
17. Use cotton swabs to stem the bleeding to observe clearly
18. Have sterile assist “pop” the knee by bending the knee lightly so as to cause the meniscus to separate from the joint
19. Once, the connection point of meniscus to bone is observed, carefully cut the attaching tissue to create space.
20. Grip the meniscus using the forceps, switch the forceps to the left hand and then use the microdissection scissors (short-tip) to transect the meniscus at its narrowest
21. Check if the meniscus is completely transected using the forceps to hold one of the cut ends
22. Once transected, suture the muscle. Staple the incision using wound clips and follow post-op procedure

B.2 Intra-articular Injections

Procedure

1. Anesthetize the rat and prepare for injection by preparing the rat knee with aseptic technique
2. Prepare solution for injection (26.5 gauge needle on 1ml luer lock syringe)
3. Use tape cut at .7mm width to stick to the bottom of the needle to ensure that the needle is not inserted too deep into the joint space
4. Have assistant bend the knee with one finger beneath the knee pushing up, so as to open the joint space
5. Feel for the joint space by flexing the knee
6. Gently insert needle in the selected location through the patella, feeling for any barriers
7. If it hits bone, remove immediately and reposition
8. If needle is inserted correctly, there will be a little resistance at the beginning which will give way indicating needle insertion in the joint space
9. Once needle is in the joint space, have the assist release the tension in the joint by just loosely bending the knee
10. Gently inject solution and remove the needle slowly. Palpitate the joint to make sure the fluid is distributed in the joint space

REFERENCES

Ahmed, A. M. and D. L. Burke (1983). "In-vitro measurement of static pressure distribution in synovial joints--Part I: Tibial surface of the knee." J Biomech Eng**105**(3): 216-225.

Aigner, T. and J. Dudhia (2003). "Genomics of osteoarthritis." Curr Opin Rheumatol**15**(5): 634-640.

Aigner, T. and J. Stove (2003). "Collagens--major component of the physiological cartilage matrix, major target of cartilage degeneration, major tool in cartilage repair." Adv Drug Deliv Rev**55**(12): 1569-1593.

Akle, C. A., M. Adinolfi, K. I. Welsh, S. Leibowitz and I. McColl (1981). "Immunogenicity of human amniotic epithelial cells after transplantation into volunteers." Lancet**2**(8254): 1003-1005.

Allen, K. D., B. A. Mata, M. A. Gabr, J. L. Huebner, S. B. Adams, Jr., V. B. Kraus, D. O. Schmitt and L. A. Setton (2012). "Kinematic and dynamic gait compensations resulting from knee instability in a rat model of osteoarthritis." Arthritis Res Ther**14**(2): R78.

Arokoski, J. P., J. S. Jurvelin, U. Vaatainen and H. J. Helminen (2000). "Normal and pathological adaptations of articular cartilage to joint loading." Scand J Med Sci Sports**10**(4): 186-198.

Athanasiou, K. A., A. R. Shah, R. J. Hernandez and R. G. LeBaron (2001). "Basic science of articular cartilage repair." Clinics in Sports Medicine**20**(2): 223-+.

Ayral, X. (2001). "Injections in the treatment of osteoarthritis." Best Pract Res Clin Rheumatol**15**(4): 609-626.

Bader, D. L. and G. E. Kempson (1994). "The short-term compressive properties of adult human articular cartilage." Biomed Mater Eng**4**(3): 245-256.

Bansal, P. N., N. S. Joshi, V. Entezari, B. C. Malone, R. C. Stewart, B. D. Snyder and M. W. Grinstaff (2011). "Cationic contrast agents improve quantification of glycosaminoglycan (GAG) content by contrast enhanced CT imaging of cartilage." J Orthop Res**29**(5): 704-709.

Bar-Yehuda, S., L. Rath-Wolfson, L. Del Valle, A. Ochaion, S. Cohen, R. Patoka, G. Zozulya, F. Barer, E. Atar, S. Pina-Oviedo, G. Perez-Liz, D. Castel and P. Fishman (2009). "Induction of an antiinflammatory effect and prevention of cartilage damage in rat knee osteoarthritis by CF101 treatment." Arthritis Rheum**60**(10): 3061-3071.

Baragi, V. M., G. Becher, A. M. Bendele, R. Biesinger, H. Bluhm, J. Boer, H. Deng, R. Dodd, M. Essers, T. Feuerstein, B. M. Gallagher, Jr., C. Gege, M. Hochgurtel, M. Hofmann, A. Jaworski, L. Jin, A. Kiely, B. Korniski, H. Kroth, D. Nix, B. Nolte, D. Piecha, T. S. Powers, F. Richter, M. Schneider, C. Steeneck, I. Sucholeiki, A. Taveras, A. Timmermann, J. Van Veldhuizen, J. Weik, X. Wu and B. Xia (2009). "A new class of potent matrix metalloproteinase 13 inhibitors for potential treatment of osteoarthritis: Evidence of histologic and clinical efficacy without musculoskeletal toxicity in rat models." Arthritis Rheum**60**(7): 2008-2018.

Barve, R. A., J. C. Minnerly, D. J. Weiss, D. M. Meyer, D. J. Aguiar, P. M. Sullivan, S. L. Weinrich and R. D. Head (2007). "Transcriptional profiling and pathway analysis of monosodium iodoacetate-induced experimental osteoarthritis in rats: relevance to human disease." Osteoarthritis Cartilage**15**(10): 1190-1198.

Beenken, A. and M. Mohammadi (2009). "The FGF family: biology, pathophysiology and therapy." Nat Rev Drug Discov**8**(3): 235-253.

Bendele, A., J. McComb, T. Gould, T. McAbee, G. Sennello, E. Chlipala and M. Guy (1999). "Animal models of arthritis: relevance to human disease." Toxicol Pathol**27**(1): 134-142.

Bendele, A. M. (2001). "Animal models of osteoarthritis." J Musculoskelet Neuronal Interact**1**(4): 363-376.

Bendele, A. M. (2002). "Animal models of osteoarthritis in an era of molecular biology." J Musculoskelet Neuronal Interact**2**(6): 501-503.

Bhatia, M., M. Pereira, H. Rana, B. Stout-, C. Lewis, S. Abramson, K. Labazzo, C. Ray, Q. Liu, W. Hogartner and R. Hariri (2007). "The mechanism of cell interaction and response on decellularized human amniotic membrane: Implications in wound healing." Wounds-a Compendium of Clinical Research and Practice**19**(8): 207-217.

Bitton, R. (2009). "The economic burden of osteoarthritis." Am J Manag Care**15**(8 Suppl): S230-235.

Blaney Davidson, E. N., E. L. Vitters, H. M. van Beuningen, F. A. van de Loo, W. B. van den Berg and P. M. van der Kraan (2007). "Resemblance of osteophytes in experimental osteoarthritis to transforming growth factor beta-induced osteophytes: limited role of bone morphogenetic protein in early osteoarthritic osteophyte formation." Arthritis Rheum**56**(12): 4065-4073.

Borah, B., T. E. Dufresne, P. A. Chmielewski, T. D. Johnson, A. Chines and M. D. Manhart (2004). "Risedronate preserves bone architecture in postmenopausal women with osteoporosis as measured by three-dimensional microcomputed tomography." Bone**34**(4): 736-746.

Bove, S. E., S. L. Calcaterra, R. M. Brooker, C. M. Huber, R. E. Guzman, P. L. Juneau, D. J. Schrier and K. S. Kilgore (2003). "Weight bearing as a measure of disease progression and efficacy of anti-inflammatory compounds in a model of monosodium iodoacetate-induced osteoarthritis." Osteoarthritis Cartilage**11**(11): 821-830.

Bove, S. E., K. D. Laemont, R. M. Brooker, M. N. Osborn, B. M. Sanchez, R. E. Guzman, K. E. Hook, P. L. Juneau, J. R. Connor and K. S. Kilgore (2006). "Surgically induced osteoarthritis in the rat results in the development of both osteoarthritis-like joint pain and secondary hyperalgesia." Osteoarthritis Cartilage**14**(10): 1041-1048.

Buckwalter, J. A. and T. D. Brown (2004). "Joint injury, repair, and remodeling: roles in post-traumatic osteoarthritis." Clin Orthop Relat Res(423): 7-16.

Buckwalter, J. A. and D. R. Lappin (2000). "The disproportionate impact of chronic arthralgia and arthritis among women." Clin Orthop Relat Res(372): 159-168.

Buckwalter, J. A. and J. A. Martin (2006). "Osteoarthritis." Adv Drug Deliv Rev**58**(2): 150-167.

Buckwalter, J. A., C. Saltzman and T. Brown (2004). "The impact of osteoarthritis: implications for research." Clin Orthop Relat Res(427 Suppl): S6-15.

Burrage, P. S. and C. E. Brinckerhoff (2007). "Molecular targets in osteoarthritis: metalloproteinases and their inhibitors." Curr Drug Targets**8**(2): 293-303.

Butoescu, N., O. Jordan and E. Doelker (2009). "Intra-articular drug delivery systems for the treatment of rheumatic diseases: a review of the factors influencing their performance." Eur J Pharm Biopharm**73**(2): 205-218.

Calvo, E., I. Palacios, E. Delgado, J. Ruiz-Cabello, P. Hernandez, O. Sanchez-Pernaute, J. Egido and G. Herrero-Beaumont (2001). "High-resolution MRI detects cartilage swelling at the early stages of experimental osteoarthritis." Osteoarthritis Cartilage**9**(5): 463-472.

Chandra, A., O. P. Maurya, B. Reddy, G. Kumar, K. Pandey and G. Bhaduri (2005). "Amniotic membrane transplantation in ocular surface disorders." J Indian Med Assoc**103**(7): 364-366, 368.

Chiang, H. and C. C. Jiang (2009). "Repair of articular cartilage defects: review and perspectives." J Formos Med Assoc**108**(2): 87-101.

Cicuttini, F. M. and T. D. Spector (1996). "The genetics of osteoarthritis." J Clin Pathol**49**(8): 617-618.

Cimmino, M. A. and M. Parodi (2005). "Risk factors for osteoarthritis." Semin Arthritis Rheum**34**(6 Suppl 2): 29-34.

Claassen, H., M. Schicht, J. Brandt, K. Reuse, R. Schädlich, M. B. Goldring, S. S. Guddat, A. Thate and F. Paulsen (2011). "C-28/I2 and T/C-28a2 chondrocytes as well as human primary articular chondrocytes express sex hormone and insulin receptors—Useful cells in study of cartilage metabolism." Annals of Anatomy - Anatomischer Anzeiger**193**(1): 23-29.

Claassen, H., M. Schicht and F. Paulsen (2011). "Impact of sex hormones, insulin, growth factors and peptides on cartilage health and disease." Progress in Histochemistry and Cytochemistry**45**(4): 239-293.

Clouet, J., C. Vinatier, C. Merceron, M. Pot-vaucel, Y. Maugars, P. Weiss, G. Grimandi and J. Guicheux (2009). "From osteoarthritis treatments to future regenerative therapies for cartilage." Drug Discov Today**14**(19-20): 913-925.

Combe, R., S. Bramwell and M. J. Field (2004). "The monosodium iodoacetate model of osteoarthritis: a model of chronic nociceptive pain in rats?" Neurosci Lett**370**(2-3): 236-240.

Cotofana, S., R. Buck, W. Wirth, F. Roemer, J. Duryea, M. Nevitt and F. Eckstein (2012). "Cartilage thickening in early radiographic human knee osteoarthritis - within-person, between-knee comparison." Arthritis Care Res (Hoboken).

Crepaldi, G. and L. Punzi (2003). "Aging and osteoarthritis." Aging Clin Exp Res**15**(5): 355-358.

Cutler, D. M. and K. Ghosh (2012). "The potential for cost savings through bundled episode payments." N Engl J Med**366**(12): 1075-1077.

Diaz-Prado, S., M. E. Rendal-Vazquez, E. Muinos-Lopez, T. Hermida-Gomez, M. Rodriguez-Cabarcos, I. Fuentes-Boquete, F. J. de Toro and F. J. Blanco (2010). "Potential use of the human amniotic membrane as a scaffold in human articular cartilage repair." Cell Tissue Bank**11**(2): 183-195.

Dieppe, P. A. and L. S. Lohmander (2005). "Pathogenesis and management of pain in osteoarthritis." Lancet**365**(9463): 965-973.

Dillon, C. F., E. K. Rasch, Q. Gu and R. Hirsch (2006). "Prevalence of knee osteoarthritis in the United States: arthritis data from the Third National Health and Nutrition Examination Survey 1991-94." J Rheumatol**33**(11): 2271-2279.

Ding, T., J. Sun and P. Zhang (2009). "Study on MCP-1 related to inflammation induced by biomaterials." Biomed Mater**4**(3): 035005.

Edwards, S. H. (2011). "Intra-articular drug delivery: the challenge to extend drug residence time within the joint." Vet J**190**(1): 15-21.

Eyre, D. R. (2004). "Collagens and cartilage matrix homeostasis." Clin Orthop Relat Res(427 Suppl): S118-122.

Eyre, D. R., M. A. Weis and J. J. Wu (2006). "Articular cartilage collagen: an irreplaceable framework?" Eur Cell Mater**12**: 57-63.

Faulk, W. P., R. Matthews, P. J. Stevens, J. P. Bennett, H. Burgos and B. L. Hsi (1980). "Human amnion as an adjunct in wound healing." Lancet**1**(8179): 1156-1158.

Felson, D. T. (2004). "An update on the pathogenesis and epidemiology of osteoarthritis." Radiol Clin North Am**42**(1): 1-9, v.

Felson, D. T., A. Naimark, J. Anderson, L. Kazis, W. Castelli and R. F. Meenan (1987). "The prevalence of knee osteoarthritis in the elderly. The Framingham Osteoarthritis Study." Arthritis Rheum**30**(8): 914-918.

Fernihough, J., C. Gentry, M. Malcangio, A. Fox, J. Rediske, T. Pellas, B. Kidd, S. Bevan and J. Winter (2004). "Pain related behaviour in two models of osteoarthritis in the rat knee." Pain**112**(1-2): 83-93.

Fingleton, B. (2007). "Matrix metalloproteinases as valid clinical targets." Curr Pharm Des**13**(3): 333-346.

Fitzpatrick, L. R., C. Green, L. W. Maines and C. D. Smith (2011). "Experimental osteoarthritis in rats is attenuated by ABC294640, a selective inhibitor of sphingosine kinase-2." Pharmacology**87**(3-4): 135-143.

Flannery, C. R., R. Zollner, C. Corcoran, A. R. Jones, A. Root, M. A. Rivera-Bermudez, T. Blanchet, J. P. Gleghorn, L. J. Bonassar, A. M. Bendele, E. A. Morris and S. S. Glasson (2009). "Prevention of cartilage degeneration in a rat model of osteoarthritis by intraarticular treatment with recombinant lubricin." Arthritis Rheum**60**(3): 840-847.

Forbes, J. and D. E. Fetterolf (2012). "Dehydrated amniotic membrane allografts for the treatment of chronic wounds: a case series." J Wound Care**21**(6): 290, 292, 294-296.

Forster, H. and J. Fisher (1996). "The influence of loading time and lubricant on the friction of articular cartilage." Proc Inst Mech Eng H**210**(2): 109-119.

Fortin, P. R., J. R. Penrod, A. E. Clarke, Y. St-Pierre, L. Joseph, P. Belisle, M. H. Liang, D. Ferland, C. B. Phillips, N. Mahomed, M. Tanzer, C. Sledge, A. H. Fossel and J. N. Katz (2002). "Timing of total joint replacement affects clinical outcomes among patients with osteoarthritis of the hip or knee." Arthritis Rheum**46**(12): 3327-3330.

Gajiwala, K. and A. L. Gajiwala (2004). "Evaluation of lyophilised, gamma-irradiated amnion as a biological dressing." Cell Tissue Bank**5**(2): 73-80.

Gelber, A. C., M. C. Hochberg, L. A. Mead, N. Y. Wang, F. M. Wigley and M. J. Klag (2000). "Joint injury in young adults and risk for subsequent knee and hip osteoarthritis." Ann Intern Med**133**(5): 321-328.

Gerwin, N., A. M. Bendele, S. Glasson and C. S. Carlson (2010). "The OARSI histopathology initiative - recommendations for histological assessments of osteoarthritis in the rat." Osteoarthritis Cartilage**18 Suppl 3**: S24-34.

Gerwin, N., C. Hops and A. Lucke (2006). "Intraarticular drug delivery in osteoarthritis." Adv Drug Deliv Rev**58**(2): 226-242.

Goldring, M. B. (2012). "Do mouse models reflect the diversity of osteoarthritis in humans?" Arthritis & Rheumatism**64**(10): 3072-3075.

Goldring, M. B. and S. R. Goldring (2007). "Osteoarthritis." J Cell Physiol**213**(3): 626-634.

Grogan, S. P., S. Miyaki, H. Asahara, D. D. D'Lima and M. K. Lotz (2009). "Mesenchymal progenitor cell markers in human articular cartilage: normal distribution and changes in osteoarthritis." Arthritis Res Ther**11**(3): R85.

Gruss, J. S. and D. W. Jirsch (1978). "Human amniotic membrane: a versatile wound dressing." Can Med Assoc J**118**(10): 1237-1246.

Guingamp, C., P. Gegout-Pottie, L. Philippe, B. Terlain, P. Netter and P. Gillet (1997). "Mono-iodoacetate-induced experimental osteoarthritis: a dose-response study of loss of mobility, morphology, and biochemistry." Arthritis Rheum**40**(9): 1670-1679.

Guzman, R. E., M. G. Evans, S. Bove, B. Morenko and K. Kilgore (2003). "Mono-Iodoacetate-Induced Histologic Changes in Subchondral Bone and Articular Cartilage of Rat Femorotibial Joints: An Animal Model of Osteoarthritis." Toxicologic Pathology**31**(6): 619-624.

Ham, K. D., T. R. Oegema, R. F. Loeser and C. S. Carlson (2004). "Effects of long-term estrogen replacement therapy on articular cartilage IGFBP-2, IGFBP-3, collagen and proteoglycan levels in ovariectomized cynomolgus monkeys." Osteoarthritis and Cartilage**12**(2): 160-168.

Hao, Y., D. H. Ma, D. G. Hwang, W. S. Kim and F. Zhang (2000). "Identification of antiangiogenic and antiinflammatory proteins in human amniotic membrane." Cornea**19**(3): 348-352.

Hayami, T., M. Pickarski, G. A. Wesolowski, J. McLane, A. Bone, J. Destefano, G. A. Rodan and T. Duong le (2004). "The role of subchondral bone remodeling in osteoarthritis: reduction of cartilage degeneration and prevention of osteophyte formation by alendronate in the rat anterior cruciate ligament transection model." Arthritis Rheum**50**(4): 1193-1206.

He, Q., Q. Li, B. Chen and Z. Wang (2002). "Repair of flexor tendon defects of rabbit with tissue engineering method." Chin J Traumatol**5**(4): 200-208.

Hellio Le Graverand, M. P., C. Reno and D. A. Hart (1998). "Influence of pregnancy on gene expression in rabbit articular cartilage." Osteoarthritis and cartilage / OARS, Osteoarthritis Research Society**6**(5): 341-350.

Hellio Le Graverand, M. P., C. Reno and D. A. Hart (2000). "Heterogenous response of knee cartilage to pregnancy in the rabbit: assessment of specific mRNA levels." Osteoarthritis and cartilage / OARS, Osteoarthritis Research Society**8**(1): 53-62.

Hellot, S., W. Wirth, A. Guermazi, C. Pena Rossi and F. Eckstein (2013). "Location-independant analysis of intraarticular sprifermin effects on cartilage structure using ordered values." Osteoarthritis and Cartilage**21, Supplement**(0): S32-S33.

Herzog, W. and S. Federico (2006). "Considerations on joint and articular cartilage mechanics." Biomech Model Mechanobiol**5**(2-3): 64-81.

Hildebrand, T. and P. Ruegsegger (1997). "Quantification of Bone Microarchitecture with the Structure Model Index." Comput Methods Biomech Biomed Engin**1**(1): 15-23.

Hinton, R., R. L. Moody, A. W. Davis and S. F. Thomas (2002). "Osteoarthritis: diagnosis and therapeutic considerations." Am Fam Physician**65**(5): 841-848.

Huber, M., S. Trattnig and F. Lintner (2000). "Anatomy, biochemistry, and physiology of articular cartilage." Invest Radiol**35**(10): 573-580.

Hunter, D. J. (2011). "Pharmacologic therapy for osteoarthritis--the era of disease modification." Nat Rev Rheumatol**7**(1): 13-22.

Hunter, D. J., A. Guermazi, F. Roemer, Y. Zhang and T. Neogi (2013). "Structural correlates of pain in joints with osteoarthritis." Osteoarthritis Cartilage**21**(9): 1170-1178.

Hunziker, E. B. (2002). "Articular cartilage repair: basic science and clinical progress. A review of the current status and prospects." Osteoarthritis Cartilage**10**(6): 432-463.

I.H.Hussin, B. Pingquan-Murphy and S. Z. Osman (2011). The Fabrication of Human Amniotic Membrane Based Hydrogel for Cartilage Tissue Engineering Applications: A Preliminary Study. IFMBE.

Iagnocco, A. (2010). "Imaging the joint in osteoarthritis: a place for ultrasound?" Best Pract Res Clin Rheumatol**24**(1): 27-38.

Janssen, M., G. Mihov, T. Welting, J. Thies and P. Emans (2014). "Drugs and Polymers for Delivery Systems in OA Joints: Clinical Needs and Opportunities." Polymers**6**(3): 799-819.

Janusz, M. (2001). "Moderation of iodoacetate-induced experimental osteoarthritis in rats by matrix metalloproteinase inhibitors." Osteoarthritis and Cartilage**9**(8): 751-760.

Janusz, M. J., A. M. Bendele, K. K. Brown, Y. O. Taiwo, L. Hsieh and S. A. Heitmeyer (2002). "Induction of osteoarthritis in the rat by surgical tear of the meniscus: Inhibition of joint damage by a matrix metalloproteinase inhibitor." Osteoarthritis Cartilage**10**(10): 785-791.

Ji, S. Z., S. C. Xiao, P. F. Luo, G. F. Huang, G. Y. Wang, S. H. Zhu, M. J. Wu and Z. F. Xia (2011). "An epidermal stem cells niche microenvironment created by engineered human amniotic membrane." Biomaterials**32**(31): 7801-7811.

Jin, C. Z., S. R. Park, B. H. Choi, K. Y. Lee, C. K. Kang and B. H. Min (2007). "Human amniotic membrane as a delivery matrix for articular cartilage repair." Tissue Eng**13**(4): 693-702.

Jordan, J. M., C. G. Helmick, J. B. Renner, G. Luta, A. D. Dragomir, J. Woodard, F. Fang, T. A. Schwartz, A. E. Nelson, L. M. Abbate, L. F. Callahan, W. D. Kalsbeek and M. C. Hochberg (2009). "Prevalence of hip symptoms and radiographic and symptomatic hip osteoarthritis in African Americans and Caucasians: the Johnston County Osteoarthritis Project." J Rheumatol**36**(4): 809-815.

Kalbhen, D. A. (1987). "Chemical model of osteoarthritis--a pharmacological evaluation." J Rheumatol**14 Spec No**: 130-131.

Karsdal, M. A., I. Byrjalsen, K. Henriksen, B. J. Riis, E. M. Lau, M. Arnold and C. Christiansen (2010). "The effect of oral salmon calcitonin delivered with 5-CNAC on bone and cartilage degradation in osteoarthritic patients: a 14-day randomized study." Osteoarthritis Cartilage**18**(2): 150-159.

Kawai, M., U. I. Modder, S. Khosla and C. J. Rosen (2011). "Emerging therapeutic opportunities for skeletal restoration." Nat Rev Drug Discov**10**(2): 141-156.

Kim, H. A. and F. J. Blanco (2007). "Cell death and apoptosis in osteoarthritic cartilage." Curr Drug Targets**8**(2): 333-345.

Kim, J. S., J. C. Kim, B. K. Na, J. M. Jeong and C. Y. Song (2000). "Amniotic membrane patching promotes healing and inhibits proteinase activity on wound healing following acute corneal alkali burn." Exp Eye Res**70**(3): 329-337.

Kleerekoper, M. (2006). "Osteoporosis prevention and therapy: preserving and building strength through bone quality." Osteoporos Int**17**(12): 1707-1715.

Kobayashi, K., R. Imaizumi, H. Sumichika, H. Tanaka, M. Goda, A. Fukunari and H. Komatsu (2003). "Sodium iodoacetate-induced experimental osteoarthritis and associated pain model in rats." J Vet Med Sci**65**(11): 1195-1199.

Koob, T. J., J. J. Lim, M. Massee, N. Zabek and G. Denoziere (2014). "Properties of dehydrated human amnion/chorion composite grafts: Implications for wound repair and soft tissue regeneration." J Biomed Mater Res B Appl Biomater.

Koob, T. J., R. Rennert, N. Zabek, M. Massee, J. J. Lim, J. S. Temenoff, W. W. Li and G. Gurtner (2013). "Biological properties of dehydrated human amnion/chorion composite graft: implications for chronic wound healing." Int Wound J**10**(5): 493-500.

Laib, A., O. Barou, L. Vico, M. H. Lafage-Proust, C. Alexandre and P. Rugsegger (2000). "3D micro-computed tomography of trabecular and cortical bone architecture with application to a rat model of immobilisation osteoporosis." Med Biol Eng Comput**38**(3): 326-332.

Lawrence, R. C., D. T. Felson, C. G. Helmick, L. M. Arnold, H. Choi, R. A. Deyo, S. Gabriel, R. Hirsch, M. C. Hochberg, G. G. Hunder, J. M. Jordan, J. N. Katz, H. M. Kremers and F. Wolfe (2008). "Estimates of the prevalence of arthritis and other rheumatic conditions in the United States. Part II." Arthritis Rheum**58**(1): 26-35.

Leigh, J. P., W. Seavey and B. Leistikow (2001). "Estimating the costs of job related arthritis." J Rheumatol**28**(7): 1647-1654.

Little, C. B. and M. M. Smith (2008). "Animal Models of Osteoarthritis." Current Rheumatology Reviews**4**(3): 175-182.

Liu, Z., K. J. Lavine, I. H. Hung and D. M. Ornitz (2007). "FGF18 is required for early chondrocyte proliferation, hypertrophy and vascular invasion of the growth plate." Dev Biol**302**(1): 80-91.

Loeser, R. F., S. R. Goldring, C. R. Scanzello and M. B. Goldring (2012). "Osteoarthritis: a disease of the joint as an organ." Arthritis Rheum**64**(6): 1697-1707.

Loeser, R. F., Jr. (2004). "Aging cartilage and osteoarthritis--what's the link?" Sci Aging Knowledge Environ**2004**(29): pe31.

Ma, H. L., T. J. Blanchet, D. Peluso, B. Hopkins, E. A. Morris and S. S. Glasson (2007). "Osteoarthritis severity is sex dependent in a surgical mouse model." Osteoarthritis and Cartilage**15**(6): 695-700.

Mapp, P. I., D. A. Walsh, J. Bowyer and R. A. Maciewicz (2010). "Effects of a metalloproteinase inhibitor on osteochondral angiogenesis, chondropathy and pain behavior in a rat model of osteoarthritis." Osteoarthritis Cartilage**18**(4): 593-600.

Martel-Pelletier, J., L. M. Wildi and J. P. Pelletier (2012). "Future therapeutics for osteoarthritis." Bone**51**(2): 297-311.

Mayack, S. R., J. L. Shadrach, F. S. Kim and A. J. Wagers (2010). "Systemic signals regulate ageing and rejuvenation of blood stem cell niches (Retraction of vol 463, pg 495, 2010)." Nature**467**(7317): 872-872.

Mligiliche, N., K. Endo, K. Okamoto, E. Fujimoto and C. Ide (2002). "Extracellular matrix of human amnion manufactured into tubes as conduits for peripheral nerve regeneration." J Biomed Mater Res**63**(5): 591-600.

Moore, E. E., A. M. Bendele, D. L. Thompson, A. Littau, K. S. Waggie, B. Reardon and J. L. Ellsworth (2005). "Fibroblast growth factor-18 stimulates chondrogenesis and cartilage repair in a rat model of injury-induced osteoarthritis." Osteoarthritis Cartilage**13**(7): 623-631.

Mosser, D. M. and J. P. Edwards (2008). "Exploring the full spectrum of macrophage activation." Nat Rev Immunol**8**(12): 958-969.

Muir H, C. S. (1987). Pathological and biochemical changes in cartilage and other tissues of the canine knee resulting from induced joint instability. Joint loading: biology and health of articular structures. Bristol, Wright**:** 47-63.

NIH (2008). Treatment for patients with osteoarthritis (OA).

NIH (2010). AS902330 in cartilage injury repair (CIR).

NIH (2010). Dose finding study of bone morphogenetic protein 7 (BMP-7) in subjects with osteoarthritis (OA) of the knee.

NIH (2012). Efficacy and safety of oral salmon calcitonin in patients with knee osteoarthritis (OA 2 study).

Niknejad, H., H. Peirovi, M. Jorjani, A. Ahmadiani, J. Ghanavi and A. M. Seifalian (2008). "Properties of the amniotic membrane for potential use in tissue engineering." Eur Cell Mater**15**: 88-99.

O'Neal, J. M., T. Diab, M. R. Allen, B. Vidakovic, D. B. Burr and R. E. Guldberg (2010). "One year of alendronate treatment lowers microstructural stresses associated with trabecular microdamage initiation." Bone**47(**2): 241-247.

Oeppen, R. S., S. A. Connolly, J. T. Bencardino and D. Jaramillo (2004). "Acute injury of the articular cartilage and subchondral bone: a common but unrecognized lesion in the immature knee." AJR Am J Roentgenol**182**(1): 111-117.

Owen, S. G., H. W. Francis and M. S. Roberts (1994). "Disappearance kinetics of solutes from synovial fluid after intra-articular injection." Br J Clin Pharmacol**38**(4): 349-355.

Palmer, A. W., R. E. Guldberg and M. E. Levenston (2006). "Analysis of cartilage matrix fixed charge density and three-dimensional morphology via contrast-enhanced microcomputed tomography." Proc Natl Acad Sci U S A**103**(51): 19255-19260.

Peach, C. A., A. J. Carr and J. Loughlin (2005). "Recent advances in the genetic investigation of osteoarthritis." Trends Mol Med**11**(4): 186-191.

Peterson, J. T. (2006). "The importance of estimating the therapeutic index in the development of matrix metalloproteinase inhibitors." Cardiovasc Res**69**(3): 677-687.

Petit-Zeman, S. (2004). "Characteristics of COX2 inhibitors questioned." Nat Rev Drug Discov**3**(9): 726-727.

Pinals, R. S. (1996). "Mechanisms of joint destruction, pain and disability in osteoarthritis." Drugs**52 Suppl 3**: 14-20.

Piscaer, T. M., J. H. Waarsing, N. Kops, P. Pavljasevic, J. A. Verhaar, G. J. van Osch and H. Weinans (2008). "In vivo imaging of cartilage degeneration using microCT-arthrography." Osteoarthritis Cartilage**16**(9): 1011-1017.

Pritzker, K. P. and T. Aigner (2010). "Terminology of osteoarthritis cartilage and bone histopathology - a proposal for a consensus." Osteoarthritis Cartilage**18 Suppl 3**: S7-9.

Reginster, J. Y. (2013). "Efficacy and safety of strontium ranelate in the treatment of knee osteoarthritis: results of a double-blind randomised, placebo-controlled trial." Ann Rheum Dis.

Rieppo, J., M. M. Hyttinen, E. Halmesmaki, H. Ruotsalainen, A. Vasara, I. Kiviranta, J. S. Jurvelin and H. J. Helminen (2009). "Changes in spatial collagen content and collagen network architecture in porcine articular cartilage during growth and maturation." Osteoarthritis Cartilage**17**(4): 448-455.

Rivera, J. C., J. C. Wenke, J. A. Buckwalter, J. R. Ficke and A. E. Johnson (2012). "Posttraumatic osteoarthritis caused by battlefield injuries: the primary source of disability in warriors." J Am Acad Orthop Surg**20 Suppl 1**: S64-69.

Roemer, F. W., M. D. Crema, S. Trattnig and A. Guermazi (2011). "Advances in imaging of osteoarthritis and cartilage." Radiology**260**(2): 332-354.

Roman-Blas, J. A., S. Castaneda, R. Largo and G. Herrero-Beaumont (2009). "Osteoarthritis associated with estrogen deficiency." Arthritis Research & Therapy**11**(5).

Roos, H., M. Lauren, T. Adalberth, E. M. Roos, K. Jonsson and L. S. Lohmander (1998). "Knee osteoarthritis after meniscectomy: prevalence of radiographic changes after twenty-one years, compared with matched controls." Arthritis Rheum**41**(4): 687-693.

Ross, M. H. and W. Pawlina (2011). Histology : a text and atlas : with correlated cell and molecular biology. Philadelphia, Wolters Kluwer/Lippincott Williams & Wilkins Health.

Schouten, H. C. (1992). "The importance of cytogenetic and molecular biologic abnormalities in understanding the pathogenesis of malignant diseases: an overview." Neth J Med**40**(3-4): 203-208.

Sharma, L., C. Lou, S. Cahue and D. D. Dunlop (2000). "The mechanism of the effect of obesity in knee osteoarthritis: the mediating role of malalignment." Arthritis Rheum**43**(3): 568-575.

Sharma, Y., A. Maria and P. Kaur (2011). "Effectiveness of human amnion as a graft material in lower anterior ridge vestibuloplasty: a clinical study." J Maxillofac Oral Surg**10**(4): 283-287.

Silberbe.R (1971). "STIMULATION OF ARTICULAR CARTILAGE OF YOUNG ADULT MICE BY HORMONES." Pathologia Et Microbiologia**37**(1): 23-&.

Smith, M. M., C. B. Little, K. Rodgers and P. Ghosh (1997). "Animal models used for the evaluation of anti-osteoarthritis drugs." Pathol Biol (Paris)**45**(4): 313-320.

Sniekers, Y. H., G. van Osch, A. G. H. Ederveen, J. Inzunza, J. A. Gustafsson, J. van Leeuwen and H. Weinans (2009). "Development of osteoarthritic features in estrogen receptor knockout mice." Osteoarthritis and Cartilage**17**(10): 1356-1361.

Solomon, A., M. Rosenblatt, D. Monroy, Z. Ji, S. C. Pflugfelder and S. C. Tseng (2001). "Suppression of interleukin 1alpha and interleukin 1beta in human limbal epithelial cells cultured on the amniotic membrane stromal matrix." Br J Ophthalmol**85**(4): 444-449.

Spector, T. D., F. Cicuttini, J. Baker, J. Loughlin and D. Hart (1996). "Genetic influences on osteoarthritis in women: a twin study." BMJ**312**(7036): 940-943.

Tanko, L. B., B. C. Sondergaard, S. Oestergaard, M. A. Karsdal and C. Christiansen (2008). "An update review of cellular mechanisms conferring the indirect and direct effects of estrogen on articular cartilage." Climacteric**11**(1): 4-16.

Thatte, S. (2011). "Amniotic membrane transplantation: An option for ocular surface disorders." Oman J Ophthalmol**4**(2): 67-72.

Thote, T., A. S. Lin, Y. Raji, S. Moran, H. Y. Stevens, M. Hart, R. V. Kamath, R. E. Guldberg and N. J. Willett (2013). "Localized 3D analysis of cartilage composition and morphology in small animal models of joint degeneration." Osteoarthritis Cartilage**21**(8): 1132-1141.

Topol, E. J. (2004). "Failing the public health--rofecoxib, Merck, and the FDA." N Engl J Med**351**(17): 1707-1709.

Tsai, C. L., T. K. Liu and T. J. Chen (1992). "ESTROGEN AND OSTEOARTHRITIS - A STUDY OF SYNOVIAL ESTRADIOL AND ESTRADIOL-RECEPTOR BINDING IN HUMAN OSTEOARTHRITIC KNEES." Biochemical and Biophysical Research Communications**183**(3): 1287-1291.

Upadhyay, J., S. J. Baker, R. Rajagovindan, M. Hart, P. Chandran, B. A. Hooker, S. Cassar, J. P. Mikusa, A. Tovcimak, M. J. Wald, S. K. Joshi, A. Bannon, J. K. Medema, J. Beaver, P. Honore, R. V. Kamath, G. B. Fox and M. Day (2013). "Pharmacological modulation of brain activity in a preclinical model of osteoarthritis." Neuroimage**64**: 341-355.

Valdes, A. M., J. Loughlin, M. V. Oene, K. Chapman, G. L. Surdulescu, M. Doherty and T. D. Spector (2007). "Sex and ethnic differences in the association ofASPN,CALM1,COL2A1,COMP, andFRZB with genetic susceptibility to osteoarthritis of the knee." Arthritis & Rheumatism**56**(1): 137-146.

Vane, J. R., Y. S. Bakhle and R. M. Botting (1998). "Cyclooxygenases 1 and 2." Annu Rev Pharmacol Toxicol**38**: 97-120.

Wancket, L. M., V. Baragi, S. Bove, K. Kilgore, P. J. Korytko and R. E. Guzman (2005). "Anatomical localization of cartilage degradation markers in a surgically induced rat osteoarthritis model." Toxicol Pathol**33**(4): 484-489.

Warner, T. D., F. Giuliano, I. Vojnovic, A. Bukasa, J. A. Mitchell and J. R. Vane (1999). "Nonsteroid drug selectivities for cyclo-oxygenase-1 rather than cyclo-oxygenase-2 are associated with human gastrointestinal toxicity: a full in vitro analysis." Proc Natl Acad Sci U S A**96**(13): 7563-7568.

Wei, T., N. H. Kulkarni, Q. Q. Zeng, L. M. Helvering, X. Lin, F. Lawrence, L. Hale, M. G. Chambers, C. Lin, A. Harvey, Y. L. Ma, R. L. Cain, J. Oskins, M. A. Carozza, D. D. Edmondson, T. Hu, R. R. Miles, T. P. Ryan, J. E. Onyia and P. G. Mitchell (2010). "Analysis of early changes in the articular cartilage transcriptisome in the rat meniscal tear model of osteoarthritis: pathway comparisons with the rat anterior cruciate

transection model and with human osteoarthritic cartilage." Osteoarthritis Cartilage**18**(7): 992-1000.

White, A. G., H. G. Birnbaum, C. Janagap, S. Buteau and J. Schein (2008). "Direct and indirect costs of pain therapy for osteoarthritis in an insured population in the United States." J Occup Environ Med**50**(9): 998-1005.

Wieland, H. A., M. Michaelis, B. J. Kirschbaum and K. A. Rudolphi (2005). "Osteoarthritis - an untreatable disease?" Nat Rev Drug Discov**4**(4): 331-344.

Wilshaw, S. P., J. N. Kearney, J. Fisher and E. Ingham (2006). "Production of an acellular amniotic membrane matrix for use in tissue engineering." Tissue Engineering**12**(8): 2117-2129.

Winalski, C. S. and P. Rajiah (2011). "The evolution of articular cartilage imaging and its impact on clinical practice." Skeletal Radiol**40**(9): 1197-1222.

Wong, C., E. Vosburgh, A. J. Levine, L. Cong and E. Y. Xu (2012). "Human neuroendocrine tumor cell lines as a three-dimensional model for the study of human neuroendocrine tumor therapy." J Vis Exp(66): e4218.

Xie, L., A. S. Lin, K. Kundu, M. E. Levenston, N. Murthy and R. E. Guldberg (2012). "Quantitative imaging of cartilage and bone morphology, reactive oxygen species, and vascularization in a rodent model of osteoarthritis." Arthritis Rheum.

Xie, L., A. S. Lin, M. E. Levenston and R. E. Guldberg (2009). "Quantitative assessment of articular cartilage morphology via EPIC-microCT." Osteoarthritis Cartilage**17**(3): 313-320.

Xie, L. Q., A. S. P. Lin, K. Kundu, M. E. Levenston, N. Murthy and R. E. Guldberg (2012). "Quantitative imaging of cartilage and bone morphology, reactive oxygen species, and vascularization in a rodent model of osteoarthritis." Arthritis and Rheumatism**64**(6): 1899-1908.

Yelin, E., L. Murphy, M. G. Cisternas, A. J. Foreman, D. J. Pasta and C. G. Helmick (2007). "Medical care expenditures and earnings losses among persons with arthritis and other rheumatic conditions in 2003, and comparisons with 1997." Arthritis Rheum**56**(5): 1397-1407.

Zhang, Y. and J. M. Jordan (2010). "Epidemiology of osteoarthritis." Clin Geriatr Med**26**(3): 355-369.

Zhang, Y., J. Niu, M. Kelly-Hayes, C. E. Chaisson, P. Aliabadi and D. T. Felson (2002). "Prevalence of symptomatic hand osteoarthritis and its impact on functional status among the elderly: The Framingham Study." Am J Epidemiol**156**(11): 1021-1027.